Modeling Engine Oil Vaporization and Transport of the Oil Vapor in the Piston Ring Pack of Internal Combustion Engines

by

Yeunwoo Cho

B.S., School of Electrical Engineering
Seoul National University, Korea, 2001

Submitted to the Department of Mechanical Engineering
in Partial Fulfillment of the Requirements for the Degree of
Master of Science in Mechanical Engineering

at the

Massachusetts Institute of Technology

September 2004

Signature of Author_____
Department of Mechanical Engineering
August 6, 2004

Certified by_____
Tian Tian
Lecturer, Department of Mechanical Engineering
Thesis supervisor

Accepted by_____
Ain A. Sonin
Chairman, Department Committee on Graduate Students
Department of Mechanical Engineering

(This page was intentionally left blank)

Modeling Engine Oil Vaporization and Transport of the Oil Vapor in the Piston Ring Pack of Internal Combustion Engines

by

Yeunwoo Cho

Submitted to the Department of Mechanical Engineering
on August 6, 2004 in Partial Fulfillment of the
Requirements for the Degree of Master of Science in
Mechanical Engineering

ABSTRACT

A model was developed to study engine oil vaporization and oil vapor transport in the piston ring pack of internal combustion engines. With the assumption that the multi-grade oil can be modeled as a compound of several distinct paraffin hydrocarbons, a set of equations governing the oil vapor density variations were derived by applying the mass conservation law to the amount of oil vaporized from the piston and the amount of oil vapor transported within the piston ring pack.

The model was applied to a heavy-duty diesel engine. First, the case with the maximum oil supply to all the piston regions was studied and the results showed that, under this condition, the oil consumption from vaporization alone was far greater than the typical oil consumption value measured in the engine. Then, to show the contribution of oil vaporization to oil consumption and the dependence of vaporization on oil supply to different regions, different lubrication conditions for the high temperature regions of the piston were studied.

Finally, a liquid oil transport model was integrated with this oil vaporization model in order to investigate the change of oil composition on the crown land with each engine cycle and the contribution of liquid-phase oil and vapor-phase oil to the total oil consumption under a fixed liquid oil supply rate to the crown land.

Thesis Supervisor: Dr. Tian Tian
Title: Lecturer of Mechanical Engineering

(This page was intentionally left blank)

Acknowledgements

First and foremost, I would like to thank my advisor, Dr. Tian Tian for his contribution to this work. His technical insight and expertise have led me on the right path while doing my research at MIT. What I learned under his guidance will play an important role in whatever professional area where I will participate hereafter.

This work was sponsored by the MIT lubrication consortium in internal combustion engines. Current members include Dana Corp., Mahle GmbH, Renault SA, PSA Peugeot Citroen, and AB Volvo. I would like to thank all of the above consortium members for their support.

I would like to express my special thanks to Mr. Bengt Olsson at Volvo for supplying engine test data. I also would like to thank Dr. Ertan Yilmaz at GE for his technical advice regarding this work and for supplying engine oil data.

I would like to thank several people in the Sloan Automotive Laboratory for their help regarding my work and thesis. First, I would like to thank Dr. Victor W. Wong for his useful advice regarding the work. Next, I would like to thank Grant Smedley for his continuous and useful help with this work and Fiona McClure for her thorough and sharp review of my thesis. In addition, I would like to thank Kevin Lang and Vince Constanzo for their exhaustive review of my thesis. I also would like to thank Gerardo Jose Cordova Lao and Joseph Acar for their final and keen review of this work.

I also would like to thank following people in the lab for their camaraderie: Liang Liu, Mohammad Rasuli, Jungik Kim, Jinchul Hong, Dongkun Lee, Yong Li, Oscar Lopez, Yuetao Zhang, Alexis Rozantes.

Outside the lab, I would like to thank Leslie Reagan for her help and guidance in life at MIT and I also would like to thank my new friends at MIT for their support.

Outside the U.S., I would like to thank my old friends in my country, Korea for their constant presence.

Last but not least, I would like to thank my family for their endless support and encouragement through my life and specially, during the stay at MIT.

(This page was intentionally left blank)

Table of Contents

(This page was intentionally left blank)

List of Figures

List of Tables

(This page was intentionally left blank)

1. Introduction

1.1. Problems Relating to Engine Oil Vaporization

High piston temperatures during the operation of internal combustion engine cause engine oil vaporization, which is a potentially important source of engine oil consumption. The phenomenon of vaporization of engine oil causes unnecessary consumption of engine oil, which is unsatisfactory to customers. The vaporized oil is transported by the gas flow within the piston ring pack (**Figure 1-1**).

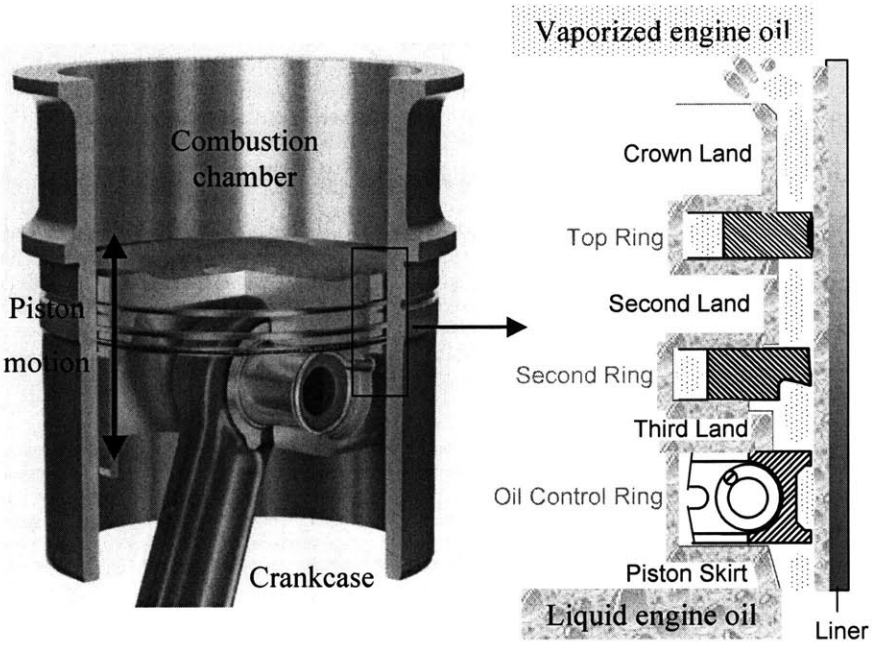

Figure 1-1. Piston ring pack system in the internal combustion engine

The gas flow in the piston ring pack from the combustion chamber is mainly towards the crankcase (blowby) and sometimes in the reverse direction, i.e., towards combustion chamber (reverse blowby). The transported oil vapor due to this gas flow that arrives near the crown land and the top ring groove has a high probability of entering the combustion chamber. If the transported oil reaches via the crankcase, it will also tend to enter the combustion chamber through the PCV (Positive Crankcase Ventilation) system. Once oil

vapor enters the combustion chamber, it will escape from the combustion chamber through the exhaust valve. Oil vapors then block the early part of the after-treatment device, such as catalytic converter, and also have an adverse effect on the efficiency of the catalytic converter due to chemical poisoning. Sometimes these oil vapors may also cause a malfunction of the oxygen sensor which is the part of the engine management system (EMS) [1]. These technical problems are directly related to emission problems. In addition, when either partially burned or unburned oil vapor exits the combustion chamber, and arrives outside the vehicle, this directly causes serious particulate problem.

As vaporization of oil occurs, the remaining oil on the piston will experience oxidation by hot combustion gas or by the condensation of degraded oil vapor [2]. As a result, the remaining oil can be either transported back to the crankcase after being potentially degraded from composition change and chemical reaction with the hot blowby gas/degraded oil vapor, or becomes carbon deposit on the piston lands and grooves. Oil degradation affects the performance of the engine oil and, in turn, is directly related to the oil exchange period. This is the major concern of customers/manufacturers, particularly in Europe. Carbon deposit can cause technical problems with engine operation by causing immobility of piston rings.

The main source of the catalytic converter blocking is metallic elements from engine oil additives since most of the hydrocarbon components will eventually vaporize. Catalytic converter poisoning and oxygen sensor malfunction are caused by phosphorus compounds in the engine oil additive, e.g., ZDDP (zinc-dialkyl-dithio-phosphates) poisoning. The particulate matter (PM) problem is caused by hydrocarbon components from the base stock in the engine oil [1]. The contribution of hydrocarbon components to the PM was confirmed from the experimental measurement of trace metal composition, particularly Ca (Calcium), in the engine oil [3]. The carbon deposit problem is the result of reactive hydrocarbon substance known as deposit precursor [1].

All these problems are related to the engine oil vaporization. The catalytic converter blocking, catalytic converter poisoning, oxygen sensor malfunction, and PM problem are

directly related to the engine oil vaporization, i.e., additive vaporization or base stock hydrocarbon vaporization and can be improved by reducing oil consumption. Carbon deposits from oil degradation originating from reactive hydrocarbons is also related to hydrocarbon vaporization.

1.2. Overall Phenomena Relating to Engine Oil Vaporization

Oil consumption, oil degradation, and carbon deposit buildup on the piston are major concerns for engine power cylinder system development. The vaporization process is closely related to these phenomena acting as both cause and effect. Liquid oil composition determines the vaporization rate and the vaporized oil is a major contributor to oil consumption. When this vaporized oil experiences oxidation/degradation by hot blowby gas, the intensity of deterioration affects the degradation of liquid oil, or further formation of carbon deposits as the oil vapors circulate within the piston ring pack. These results, caused by vaporization process, then in turn change the liquid oil composition and the liquid oil transport behavior. The liquid oil composition changes directly due to the vaporization process, in a quantitative respect, and transforms chemically by oxidation/degradation due to the condensation of deteriorated oil vapor onto the liquid oil film. Solid-state carbon deposit can affect the overall characteristics of liquid oil transport by interrupting the oil flow path, which changes the lubrication condition. Therefore, the mechanical/chemical behavior of vaporized oil transport, including the oil vaporization process, cannot be separated from the mechanical/chemical behavior of liquid oil transport. Several separate studies have been presented about these coupled mechanisms. Lubricant degradation during engine operation was studied in [2] and the relationship between carbon deposit formation and oil consumption was presented in [4]. Several studies about the vaporization process from the cylinder liner in the combustion chamber have also been presented ([5][6][7]).

1.3. Outline of Modeling Work

In the current work, vaporization of the engine oil on the piston, ring and liner surfaces and transport of the oil vapors in the piston ring pack were modeled.

To describe the oil vaporization in the piston ring pack accurately, it needs to couple the vaporization process with the liquid oil transport. However, the liquid oil transport mechanism in the piston ring pack has not been determined. Therefore, complete coupling of oil vaporization and liquid transport is beyond the scope of this work.

The analysis carried out in this work was based on two lubrication conditions. One assumes an infinite oil supply condition within the piston ring pack and the other assumes a finite oil supply condition to a certain region, e.g. the crown land. The term "infinite" oil supply analysis, used in this work, means that there is sufficient oil supply to a certain region such that the composition of the liquid oil in this region remains unchanged. "Finite" oil supply analysis, also used in this work, allows the oil composition and oil amount to change during engine operation.

In what follows, the elements of the model will be described first. Then the model will be applied to a heavy-duty diesel engine with emphasis on the relationship between liquid oil transport and oil vaporization in critical ring pack regions.

The purpose of this modeling work is not prediction of engine oil consumption but the theoretical analysis of effect of engine oil vaporization on the engine oil consumption.

For this work, typical oil consumption data (5g/hr) from the diesel engine experiment was used as a reference data.

2. Model Description

As the first step in modeling the vaporization of engine oil, the engine oil was modeled as being composed of several distinct paraffin hydrocarbons. The vaporization process of each oil component was then modeled as a mass transfer process under the influence of the surrounding gas flow motion. The piston ring pack was divided into nine regions in which this vaporization model would apply. For each oil component, nine equations corresponding to a mass balance in each of the nine regions of the piston ring pack were obtained for the nine unknown oil vapor densities. These equations were then solved numerically.

2.1. Engine Oil Modeling

Engine oil is composed of base stocks and additives. Base stocks are the main constituent of the engine oil and are generally hydrocarbons, which are either paraffinic, naphthenic, or aromatics. Additives may constitute up to 20% of engine oil, as in the case of the premium crankcase oil, and usually contain hydrocarbons and metallic components [1]. The chemical structures of additive components are different according to their roles as an additive. Some structures of base stocks and additives are shown in **Appendix A**.

In this modeling work, both base stocks and additives in the engine oil were modeled as paraffin hydrocarbons. More specifically, the engine oil was modeled as a compound of several different paraffin hydrocarbon components with different liquid-phase mass fractions and boiling points. Properties such as molecular weight, vapor pressure, and gas-phase mass fraction of each oil component were then obtained in order to calculate the vaporization rate of each oil component from the liquid oil film.

2.1.1. Liquid-Phase Mass Fraction and Boiling Point

In order to determine the liquid-phase mass fraction and boiling point of each of the oil components, the distillation curve of a particular engine oil was obtained first. Then

discretization was made to model the engine oil as a compound of a number of paraffin hydrocarbons, as done in [7]. Twenty-one paraffin hydrocarbon components were used to span the whole spectrum of the oils with finer divisions for the light oil components since they are more volatile. **Figure 2-1** shows the discretization for the two oils used in this study.

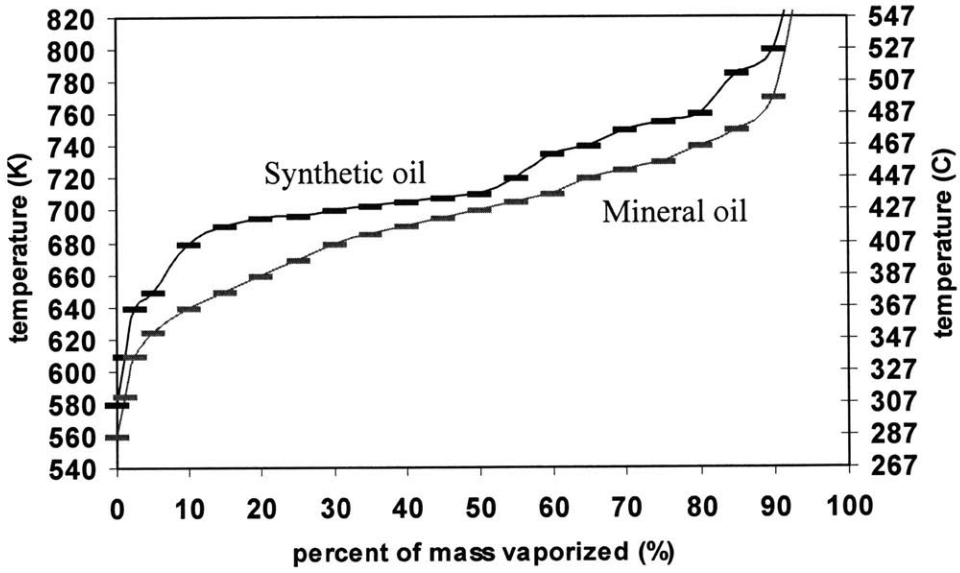

Figure 2-1. Atmospheric boiling point distillation curves of mineral and synthetic oils

For a given percentage of mass vaporized (%), the boiling point of the mineral oil is lower than that of the synthetic oil, and therefore, the mineral oil is composed of lighter oil components. (**Figure 2-1** and **Table 2-1**)

Furthermore, in some cases consecutive points on the flat part of a distillation curve are really the same component, meaning that it is in the middle of distillation. These points are represented by bold fonts and shaded backgrounds in **Table 2-1.** For example, the oil components denoted by 7,8,9,and 10 are all the same oil component with 20% mass fraction and the oil components denoted by 19 and 20 are another oil component with 10% mass fraction in synthetic oil. The oil therefore could be modeled as seventeen oil components instead of twenty-one oil components. Twenty-one oil components were still used, however, with no loss of accuracy.

Synthetic oil (heavy oil)			Mineral oil (light oil)		
Oil component number	Mass fraction (%)	Boiling point (K)	Oil component number	Mass fraction (%)	Boiling point (K)
1	1	580	1	1	560
2	1.5	610	2	1.5	585
3	2.5	640	3	2.5	610
4	5	650	4	5	625
5	5	680	5	5	640
6	5	690	6	5	650
7	**5**	**695**	7	5	660
8	**5**	**697**	8	5	670
9	**5**	**700**	**9**	**5**	**680**
10	**5**	**703**	**10**	**5**	**685**
11	5	706	11	5	690
12	5	708	**12**	**5**	**695**
13	5	710	**13**	**5**	**700**
14	5	720	**14**	**5**	**705**
15	5	735	**15**	**5**	**710**
16	5	740	16	5	720
17	5	750	**17**	**5**	**725**
18	5	755	**18**	**5**	**730**
19	**5**	**760**	19	5	740
20	**5**	**785**	20	5	750
21	10	800	21	5	770

Table 2-1. Mass fractions in the liquid oil and boiling points of synthetic and mineral oil corresponding to the points on the distillation curves in Figure 2-1

2.1.2. Molecular Weights of Oil Components

Once the boiling point of each oil component was found from the distillation curve, the molecular weight of each oil component could be determined using the polynomial relationship between the boiling point and molecular weight of paraffin hydrocarbons [8].

$$M_{oil} = a \cdot BP^4 + b \cdot BP^3 + c \cdot BP^2 + d \cdot BP + e \quad \textbf{(2.1)}$$

where,

M_{oil} (kg/kmol) : The molecular weight of an oil component

$BP(°C)$: The boiling point of an oil component

$a = 6.072 \times 10^{-8}$, $b = -1.01431998 \times 10^{-4}$, $c = 0.691023398$, $d = -19.31502887594$, and $e = 2139.90829605837$

This correlation formula matches well for the paraffin hydrocarbon species: $C_{16}H_{34} \sim C_{100}H_{202}$ (Here, C denotes carbon and H denotes hydrogen atom)

2.1.3. Vapor Pressures of Oil Components on the Liquid Oil Film

Vapor pressure of each oil component could be computed using Antoine Equation [8]. This equation correlates the temperature of a paraffin hydrocarbon oil component and the vapor pressure of that component.

$$\log_{10}[P_{vapor}] = A - \frac{B}{C + T_{oil}} \quad \textbf{(2.2)}$$

where,

$P_{vapor}(mmHg)$: The vapor pressure of an oil component on the oil film

$T_{oil}(°C)$: The oil film temperature

Constants A, B, and C: Antoine constants that are tabulated by the molecular weight of different paraffin hydrocarbons [8].

As shown in **Figure 2-2,** vapor pressure exhibits an exponential increase with temperature for each oil component, and for a given oil film temperature, a light oil component exhibits a high vapor pressure than a heavy oil component.

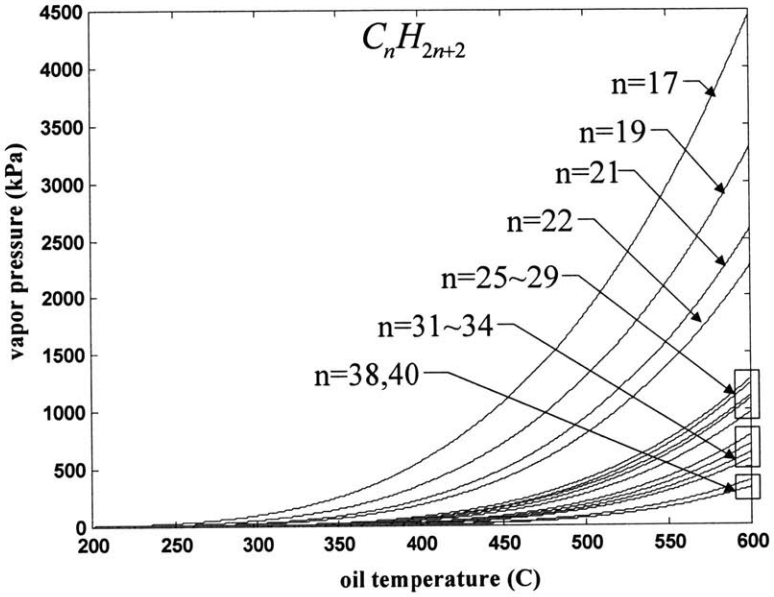

Figure 2-2. Vapor pressures of oil components as a function of oil temperature

2.1.4. Mass Fraction of Oil Components on the Oil Film Surface

Using the relationship between mole fraction and mass fraction and Raoult's law giving relationship between vapor pressure and the surrounding pressure around the oil film surface, the mass fraction of a certain oil component on the oil film surface could be obtained.

2.1.4.1. Relationship between Mole Fraction and Mass Fraction

The mean molecular weight of the mixture or solution is denoted as M and can be expressed as follows:

$$M = \sum x_i M_i = \frac{1}{\sum \frac{mf_i}{M_i}} \tag{2.3}$$

where,

x_i : Mole fraction of species i

mf_i : Mass fraction of species i

M_i : Molecular weight of species i

M : Average molecular weight of mixture or solution

The following relationships govern these quantaties.

$$\sum mf_i = 1 \tag{2.4}$$

$$\sum x_i = 1 \tag{2.5}$$

$$mf_i = \frac{x_i M_i}{\sum x_j M_j} = \frac{x_i M_i}{M} \tag{2.6}$$

$$x_i = \frac{mf_i / M_i}{\sum (mf_j / M_j)} = \frac{mf_i M}{M_i} \tag{2.7}$$

2.1.4.2. Mass Fraction of Oil Vapor on the Oil Film Surface – Raoult's Law

The mass fraction of a certain oil component on the oil film surface could be determined by assuming thermodynamic equilibrium between the liquid and vapor phases. In other words, using equations **(2.3)~(2.7)** and Raoult's law, following relationships could be obtained.

In the liquid oil,

$$x_{i,liquid} = mf_{i,liquid} \frac{M_{liquid}}{M_i} \tag{2.8}$$

$$M_{liquid} = \frac{1}{\sum \frac{mf_{i,liquid}}{M_i}} \tag{2.9}$$

In the gas side,

$$x_{i,gas} = mf_{i,gas} \frac{M_{gas}}{M_i} \tag{2.10}$$

Using the assumption that $mf_{air} >> mf_{i,gas}$ and $mf_{air} \approx 1$

$$M_{gas} = \frac{1}{\sum \frac{mf_{i,gas}}{M_i}} = \frac{1}{\frac{mf_{air}}{M_{air}} + \sum \left(\frac{mf_{i,gas}}{M_i} \right)_{oil}} \approx \frac{1}{\frac{mf_{air}}{M_{air}}} \approx \frac{1}{\frac{1}{M_{air}}} = M_{air} \tag{2.11}$$

where,

$x_{i,liquid}$: Mole fraction of oil component i in the liquid oil

$x_{i,gas}$: Mole fraction of oil component i in the gas-side

$mf_{i,liquid}$: Mass fraction of oil component i in the liquid oil

$mf_{i,gas}$: Mass fraction of oil component i in the gas-side

mf_{air} : Mass fraction of air in the gas-side

M_{liquid} : Average molecular weight of liquid oil

M_{gas} : Average molecular weight of gas (Air-oil vapor mixture)

M_{air} : Molecular weight of air in the gas-side

From **Raoult's law**,

$$P_{i,vapor} \cdot x_{i,liquid} = P_{air} \cdot x_{i,surface} \quad \textbf{(2.12)}$$

where,

$P_{i,vapor}$: Vapor pressure of oil component i just under the oil film surface

P_{air} : Air pressure surrounding the oil film surface

$x_{i,liquid}$: Mole fraction of oil component i in the liquid oil

$x_{i,surface}$: Mole fraction of oil component i just on the oil film surface in the gas-side

Finally, using equations **(2.8)~(2.11),** equation **(2.12)** becomes

$$P_{i,vapor} \cdot mf_{i,liquid} \cdot \frac{M_{liquid}}{M_i} = P_{air} \cdot mf_{i,surface} \cdot \frac{M_{gas}}{M_i} \text{ or}$$

$$mf_{i,surface} = \frac{P_{i,vapor}}{P_{air}} \cdot \frac{M_{liquid}}{M_{gas}} \cdot mf_{i,liquid} \approx \frac{P_{i,vapor}}{P_{air}} \cdot \frac{M_{liquid}}{M_{air}} \cdot mf_{i,liquid} \quad \textbf{(2.13)}$$

It can be clearly seen from equation **(2.2)** and equation **(2.13)** that increasing oil temperature and decreasing surrounding gas pressure both result in higher oil vapor mass fraction at the oil/gas interface and thus higher vaporization rate.

2.2. Vaporization Process Modeling

The oil vaporization process was treated as a mass transfer phenomenon caused by the mass fraction difference between the oil film surface and the gas within the piston ring pack, with the assumption of low mass transfer theory-applicable laminar flow ([9][10]), i.e., the oil vapor mass flux can be represented as following form.

$$m_i'' = g_m (mf_{i,surface} - mf_{i,gas}) \quad \textbf{(2.14)}$$

where,

$m_i''(kg/m^2 \cdot s)$: The oil vaporization rate per unit area or oil vapor mass flux

$mf_{i,surface}$: The mass fraction of oil component i at the oil/gas interface determined in equation **(2.13)**

$mf_{i,gas}$: The mass fraction of the oil component i in the gas stream

$g_m(kg/m^2 \cdot s)$: The mass transfer coefficient determined by resolving the gas flows

First, the applicability of the equation **(2.14)** or the low mass transfer assumption will be validated in section **2.2.1**. In section **2.2.2**, the concept of equivalent diffusion length will be introduced to calculate g_m in equation **(2.14)**. Finally, in sections **2.2.3** and **2.2.4**, the assumptions for the calculation of $mf_{i,surface}$ in equation **(2.14)** will be surveyed and under these assumptions, $mf_{i,surface}$ will be calculated using equation **(2.13)**.

2.2.1. Low Mass Transfer Assumption

2.2.1.1. Molecular Flux and Convective Flux

The total flux of any quantity is composed of two. One is the molecular flux and the other is the convective flux. Molecular flux is arising from potential gradients or driving forces and expressed in the form of constitutive or phenomenological equation for momentum, energy, and mass transport. Momentum, energy, and mass can also be transported by bulk fluid motion or bulk flow and the resulting flux is convective flux.

Momentum and Heat Transfer

When considering momentum and heat transfer from one phase to another across the phase interface as shown in **Figure 2-3(a)**,

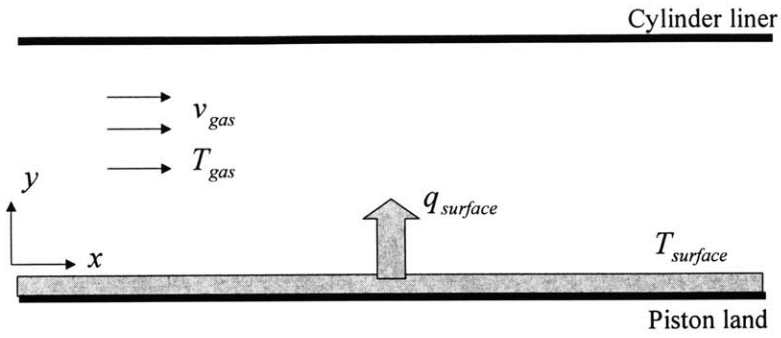

(a) Schematic diagram for momentum and heat transfer

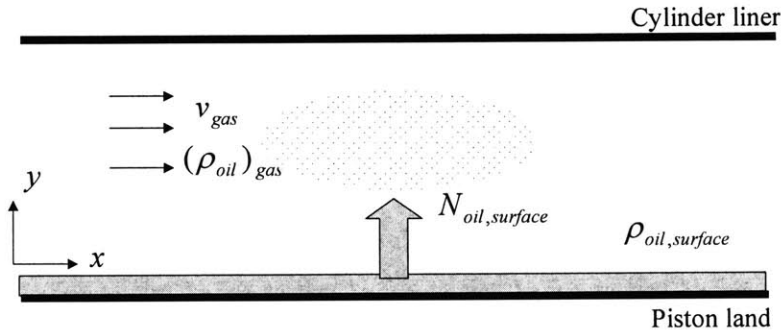

(b) Schematic diagram for mass transfer

Figure 2-3. Air-oil vapor mixture flow over a piston land/piston groove/cylinder liner

The total momentum flux at the wall, $\pi_{yx}\big|_{y=0}$ is

$$\pi_{yx}\big|_{y=0} = \tau_{yx}\big|_{y=0} + (\rho_{gas} v_x v_y)\big|_{y=0} \qquad \textbf{(2.15)}$$

Where,

$\tau_{yx}\big|_{y=0}$: Shear stress at the wall

v_x, v_y : Velocity component of gas in the x direction and y direction in **Figure 2-3(a)** respectively

The terms $\pi_{yx}\big|_{y=0}$ and $\tau_{yx}\big|_{y=0}$ have two subscripts, x that represents the direction of force, and y that represents the direction normal to the surface on which the force is acting.

The total energy flux at the wall, $e_y\big|_{y=0}$ is

$$e_y\big|_{y=0} = q_y\big|_{y=0} + (\rho_{gas}\hat{C}_p T v_y)\big|_{y=0} \tag{2.16}$$

Where,

$q_y\big|_{y=0}$: The molecular or conductive energy flux at the wall

Since the plate (y=0) is stationary, the gas which is contact with the plate is also stagnant and v_x and v_y, therefore, are zeros. As a result, the second terms in equations **(2.15)** and **(2.16)** disappear, i.e.,

$$\pi_{yx}\big|_{y=0} = \tau_{yx}\big|_{y=0} = -\mu\frac{dv_x}{dy}\bigg|_{y=0} = f\cdot\frac{\rho_{gas}v_{gas}^2}{2} \tag{2.17}$$

$$e_y\big|_{y=0} = q_y\big|_{y=0} = -k\frac{dT}{dy}\bigg|_{y=0} = h\cdot(T_{surface} - T_{gas}) \tag{2.18}$$

where,

f : Friction factor

μ : Viscosity of the gas ($kg/m\cdot s$)

k : Thermal conductivity of the gas ($W/m\cdot K$)

h : Convection heat transfer coefficient ($W/m^2\cdot K$)

Mass Transfer

The momentum transfer and the heat transfer have only molecular flux term at the interface as shown in equations **(2.17)** and **(2.18)**. However, mass transfer is composed of molecular mass transfer and self-induced convective mass transfer.

In **Figure 2-3(b)**, a flat plate that represents piston land/groove/cylinder liner with surrounding stream of air-oil vapor mixture having a velocity v_{gas} and an oil component's density $\rho_{oil,gas}$ is shown.

The total mass flux of the oil component $N_{oil,y}\big|_{y=0}$ is composed of the molecular mass flux of the oil component at the oil film surface $J_{oil,y}\big|_{y=0}$ and self-induced convective mass flux $\rho_{oil} v_{mixture,y}\big|_{y=0}$, i.e.,

$$
\begin{aligned}
N_{oil,y}\big|_{y=0} &= J_{oil,y}\big|_{y=0} + \rho_{oil} v_{mixture,y}\big|_{y=0} \\
&= J_{oil,y}\big|_{y=0} + \rho_{oil} \left. \frac{\rho_{oil} v_{oil,y} + \rho_{air} v_{air,y}}{\rho_{mixture}} \right|_{y=0} \\
&= J_{oil,y}\big|_{y=0} + \rho_{oil} \left. \frac{\rho_{oil} v_{oil,y}}{\rho_{mixture}} \right|_{y=0} \\
&\approx J_{oil,y}\big|_{y=0} + \rho_{oil,surface} \frac{\rho_{oil,surface}}{\rho_{air}} \cdot v_{oil,y}\big|_{y=0}
\end{aligned}
\qquad \textbf{(2.19)}
$$

Where,

ρ_{oil}, $\rho_{mixture}$, and ρ_{air} : Densities of oil vapor, air-oil vapor mixture and air, respectively

$\rho_{oil,surface}$: Density of oil vapor on the oil film surface (y=0)

$v_{oil,y}$, $v_{mixture,y}$, and $v_{air,y}$: Velocities of oil, air-oil vapor mixture and air in the y-direction, repsectively

2.2.1.2. Low Mass Transfer

In equation **(2.19)**, the no slip condition at the oil film surface, or $v_{air,y}\big|_{y=0} = 0$, and air dominant air-oil vapor mixture assumption, or $\rho_{mixture} \approx \rho_{air}$, were used. The second term (convective mass flux term induced by particle motion so called Stefan flow) is therefore non-zero compared to momentum flux and heat flux. However, in the vaporization process within the piston ring pack during engine operation, the mass fraction of an oil component on the oil film surface is expected to be negligible compared to unity, and therefore

$$mf_{oil,surface} = \frac{\rho_{oil,surface}}{\rho_{mixture}} \approx \frac{\rho_{oil,surface}}{\rho_{air}} << 1 \qquad \textbf{(2.20)}$$

and the second term in equation **(2.19)** can be neglected. In other words, the low mass transfer theory could be applied instead of high mass transfer theory that considers the second term or convective term induced by moving oil particle itself.

During boiling, the mass fraction of oil vapor on the oil film surface is close to the unity, in which case, high mass transfer theory should be used. A suitable criterion for the application of low mass transfer theory about the mass fraction difference $\Delta mf = mf_{oil,surface} - mf_{oil,gas}$ is that Δmf <0.1 or 0.2 and the error in using that theory is approximately (1/2) Δmf [9].

For the engine studied in this modeling work, the mass fraction of the lightest oil vapor on the oil film surface and the mass fraction of that oil vapor in the air-oil vapor mixture stream are both less than 10%. Therefore, the low mass transfer theory is applicable without a significant loss in accuracy.

2.2.2. Equivalent Diffusion Length with the Assumption of Overall Laminar Flow within the Piston Ring Pack

For the calculation of the vaporization rate of an oil component, the vaporization rate per unit area can be expressed as follows:

$$N_{oil,surface} = J_{oil,surface} = g_m (mf_{oil,surface} - mf_{oil,gas}) = -D_{12} \left. \frac{\partial \rho_{oil}}{\partial y} \right|_{y=0} \quad \textbf{(2.21)}$$

where,

g_m = Convective mass transfer coefficient ($kg / m^2 \cdot s$)

D_{12} = Diffusion coefficient of oil vapor in the gas stream (m^2 / s)

Equation **(2.21)** states that the total convective mass transfer between the oil vapor on the oil film surface and the oil vapor in the gas stream can be calculated by assuming that diffusion mass transfer occurs at the oil/gas interface.

2.2.2.1. Film Model for Mass Transfer

In **Figure 2-4,** the film model for mass transfer is shown.

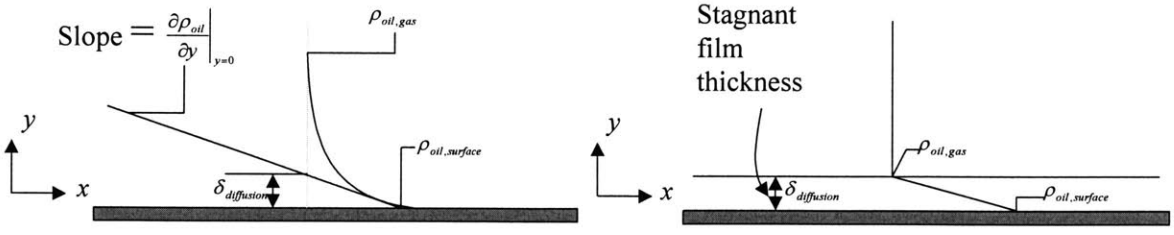

a) Actual case b) Idealized case

Figure 2-4. Film model for mass transfer

The entire resistance to mass transfer is assumed to be due to a stagnant film in the air-oil vapor mixture next to the piston land/groove/cylinder liner. The thickness $\delta_{diffusion}(x)$ is such that it provides the same resistance to mass transfer as the resistance that exists for the actual convection process at a point x.

$$\left.\frac{\partial \rho_{oil}(x,y)}{\partial y}\right|_{y=0} = \frac{\rho_{oil,gas}(x) - \rho_{oil,surface}}{\delta_{diffusion}(x)} = \frac{\rho_m(x) - \rho_{oil,surface}}{\delta_{diffusion}(x)} \tag{2.22}$$

In equation **(2.22)**, the thickness $\delta_{diffusion}(x)$ will be varying along x direction indicated in **Figure 2-4** and $\rho_{oil,gas}(x) = \rho_m(x)$ means the bulk oil-vapor density which will be calculated as follows.

$$\rho_m(x) = \frac{1}{u_{avg} a}\int_0^a \rho(x,y)\cdot u(y)\cdot dy \tag{2.23}$$

However, to make the situation in **Figure 5** be applicable for the whole x direction equally, i.e., to get the constant equivalent diffusion along the x direction, the averaged thickness $\delta_{diffusion}$ can be introduced as follows.

$$\int_0^{\frac{\pi B}{2}} -\left.\frac{\partial \rho}{\partial y}\right|_{y=0} dx = \frac{\pi B}{2}\cdot\frac{\rho_s - \overline{\rho}_m}{\delta_{diffusion}} \tag{2.24}$$

where, B is the cylinder bore or diameter, and

$$\overline{\rho}_m = \frac{2}{\pi B}\int_0^{\frac{\pi B}{2}} \rho_m(x)dx \tag{2.25}$$

Calculations of equations **(2.22)~(2.25)** require the determination of oil vapor density distribution $\rho(x,y)$ and in turn, to determine $\rho(x,y)$, the velocity distribution in the considered region should be known beforehand. In the next section **2.2.2.2**, the flow pattern in the piston ring pack was assumed to determine fully developed velocity distribution.

2.2.2.2. Assumed Flow Pattern within the Piston Ring Pack

Gas flows across the piston lands and along the clearance between rings and their grooves (**Figure 2-5**) significantly influence the oil vaporization process. These flows are expected to be laminar because of their low Reynolds numbers ranging from 1000 to 3000 ([11][12]).

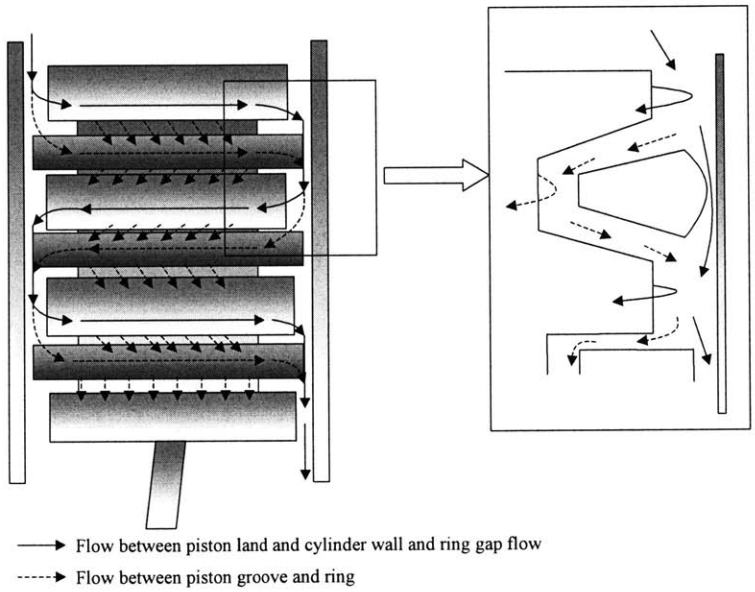

Figure 2-5. Assumed flow pattern within the piston ring pack

As was the case in [11] and [12], these two gas flows were assumed to be pressure-driven fully developed Poiseuille flow, as shown in **Figure 2-6.** The velocity profile is therefore given by:

$$u(y) = 6u_{avg}\frac{y}{a}\left(1-\frac{y}{a}\right) \tag{2.26}$$

where, a is the clearance between the piston land and cylinder liner or, between the groove and the piston ring. Since a is much smaller than the other dimensions of the piston ring pack, the infinite flat plate assumption, and neglect of the curvature, is justified.

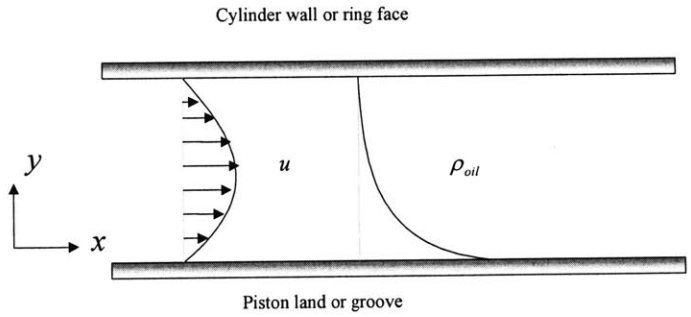

Figure 2-6. Fully developed velocity and density profile within the ring pack

The entrance effect is usually insignificant, and was neglected in this work. The vaporization rate was therefore underestimated.

Using this fully developed velocity distribution, the fully developed oil vapor density profile will be obtained with assumed boundary conditions and in turn the averaged equivalent diffusion length will be decided in the next section **2.2.2.3**.

2.2.2.3. Mass Transfer Equation and Related Boundary Conditions

Away from the piston wall which represents land or groove or cylinder liner, total mass flux is the sum of the molecular flux and the convective flux due to gas flow. Mass transfer Peclet number Pe=ReSc represents the ratio of convective mass flux to molecular mass flux. The flow characteristic is generally laminar (Re~1000-3000) in the piston ring pack and the Schmidt number (Sc) is on the order of unity. Therefore, the Peclet number

(Pe) is much larger than unity and convective mass transfer represents the dominant mass transfer mechanism in the x direction indicated in **Figure 2-6**.

Given that the x direction or air-oil vapor mixture flow direction mass transfer is mainly determined by convective mass transfer, and with the assumption of fully developed Poiseuille flow, the mass transfer equation of oil vapor within the piston ring pack system could be derived in the following manner:

$$u\frac{\partial \rho}{\partial x} = D_{12}\frac{\partial^2 \rho}{\partial y^2} \tag{2.27}$$

With boundary conditions shown in **Figure 2-7**:

$\rho(x, y = 0) = \rho_s$ = Constant = oil vapor density on the oil film surface **(2.28)**

This condition comes from the assumption that temperatures on the piston lands or grooves are uniform in the specified region e.g., crown land.

$$\frac{\partial \rho}{\partial y} = 0 \text{ at y = a = clearance} \tag{2.29}$$

This condition was derived from the fact that oil component cannot permeate into the cylinder liner/ring surface.

$\rho(x = 0, y = a) = \rho_0$ = Oil vapor density on the cylinder liner/ring surface where the air-oil vapor stream starts e.g., liner side where ring gap is positioned. **(2.30)**

This condition comes from the assumption that circumferential air-oil vapor mixture stream starts below the ring gap, or the stream should have a starting point somewhere in the circumferential direction.

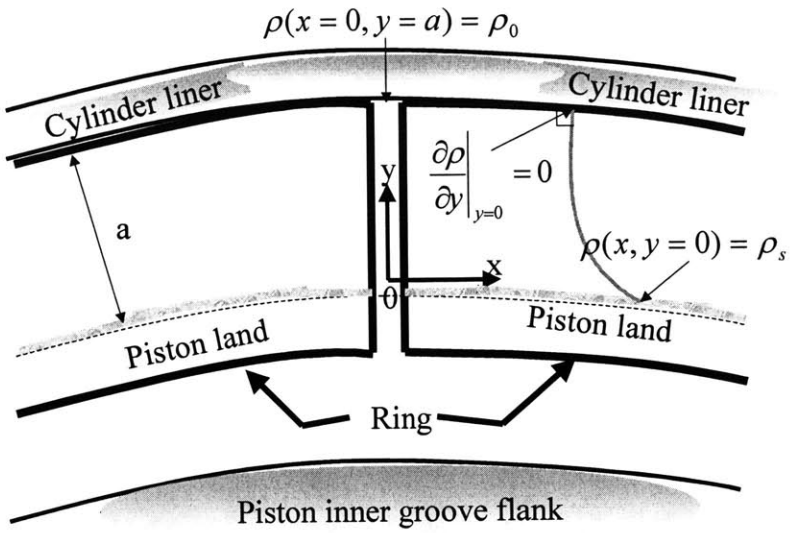

(a) Boundary conditions for the case of mass transfer between piston land and the liner

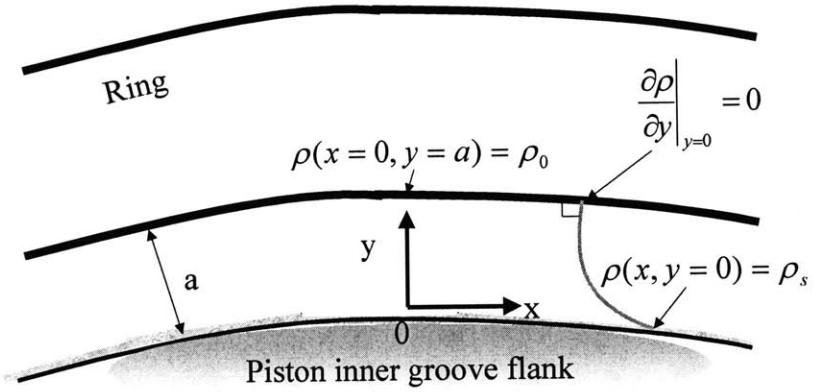

(a) Boundary conditions for the case of mass transfer between inner side of the groove of a piston ring and the inner side of the piston ring

Figure 2-7. Boundary conditions for mass transfer in the piston ring pack

The approximate series solution of equation **(2.27)** with boundary conditions **(2.28)~(2.30)** is

$$\rho(x,y) = \rho_s + \frac{5}{3a}(\rho_0 - \rho_s)\left(y - \frac{y^4}{a^3} + \frac{5}{3}\frac{y^5}{a^4} \right) \cdot e^{-\frac{4}{\mathrm{Re}\,Sc}\left(\frac{x}{a}\right)} \tag{2.31}$$

Here, $\mathrm{Re} = \dfrac{u_{avg}(2a)}{\nu_{air}}$ and ν_{air} is the kinematic viscosity of air.

The bulk oil-vapor density in the air-oil vapor mixture stream is therefore

$$\rho_m(x) = \frac{1}{u_{avg}\,a}\int_0^a \rho(x,y)\cdot u(y)\cdot dy = \rho_s + (\rho_0 - \rho_s)\left(\frac{59}{84}\right)\cdot e^{-\frac{4}{\mathrm{Re}\,Sc}\left(\frac{x}{a}\right)} \tag{2.32}$$

To obtain the average equivalent stagnant film thickness $\delta_{diffusion}$ along the half circumference along the surface in a specified piston ring pack region,

$$\int_0^{\frac{\pi B}{2}} -\left.\frac{\partial \rho}{\partial y}\right|_{y=0} dx = \frac{\pi B}{2}\cdot\frac{\rho_s - \bar{\rho}_m}{\delta_{diffusion}} \tag{2.33}$$

where,

B : Engine cylinder diameter or cylinder bore.

Calculation of equation **(2.33)** using equations **(2.31)** and **(2.32)** gives

$$\delta_{diffusion} = 0.42 \times a \tag{2.34}$$

This result corresponds to

$$Sh = \frac{D_h}{\delta_{diffusion}} = \frac{2a}{0.42a} \approx 4.77 \tag{2.35}$$

Where,

Sh : Mass transfer Sherwood number corresponding to the heat transfer Nusselt number Nu

D_h : Hydraulic diameter of a duct representing the gas-stream flow path in the piston ring pack.

From section **2.2.1**, low mass transfer theory is applicable in this study. Therefore, the Sherwood number Sh can be used as Nusselt number Nu. The value of 4.77 in equation **(2.35)** is the typical Nusselt number in the rectangular duct flow with a specified temperature and heat flux condition.

All the calculation results in this section are for the calculation of equivalent diffusion thickness in equation **(2.34)**. In other words, the oil vapor density distribution in equation **(2.31)** was derived for the purpose of calculation of equivalent diffusion thickness in equation **(2.34)** with condition that there exists oil only one side in a considered region.

The calculation of oil vapor density distribution in the piston ring pack will be done using the equivalent diffusion thickness in equation **(2.34)** with consideration of overall mass conservation including the inflow and outflow of oil vapors and the vaporized oils from all the piston, ring, and liner sides in the piston ring pack and will be treated in section **2.3**.

The detailed derivations of **(2.31)** and **(2.34)** are presented in **Appendix B** and **Appendix C** respectively. In addition, the exact solution of partial differential equation **(2.27)** with boundary conditions **(2.28)~(2.30)** are shown in **Appendix D**.

2.2.2.4. Entrance Length for Mass Transfer

The results derived in section **2.2.2.3** are based on the assumption of steady-state, fully developed flow conditions. In order for these results to be accurate, the entrance length

where unsteady effects are dominant should be small enough to be neglected. The entrance length for the mass transfer along the piston circumference direction is

$$x_{m,e} = \left(\frac{11}{960}\mathrm{Re}\,Sc\right) \times a \qquad \textbf{(2.36)}$$

where,

$x_{m,e}$: Mass transfer entrance length

a : Clearance of a specified region in the piston ring pack.

The derivation of equation **(2.36)** is included in **Appendix E.**

The hydrodynamic entrance length $x_{h,e}$ and thermal entrance length $x_{t,e}$ also should be small enough to allow use the results in section **2.2.2.3**. These lengths were found to be small and are shown with an example for the 2nd land region in **Appendix F**.

2.2.2.5. Uniform Temperatures in the Oil Film

In order to check whether the temperature of the oil layer is uniform or not, the heat transfer Biot number was introduced. The heat transfer Biot number is the ratio of the internal heat transfer resistance to the external heat transfer resistance. For the case of the oil film in the piston ring pack,

$$Bi_T = \frac{h_{air}\delta_{oil}}{k_{oil}} = \frac{Nu \cdot k_{air}}{D_h} \cdot \frac{\delta_{oil}}{k_{oil}} = Nu \cdot \left(\frac{\delta_{oil}}{D_h}\right) \cdot \left(\frac{k_{air}}{k_{oil}}\right) \sim (1)\left(\frac{10^{-5}}{10^{-4}}\right)\left(\frac{10^{-2}}{10^{-1}}\right) << 1 \qquad \textbf{(2.37)}$$

where,

Bi_T : Heat transfer Biot number

h_{air} : Convective heat transfer coefficient $(W/m^2 \cdot K)$ in the oil-air vapor mixture gas.

Nu : Heat transfer Nusselt number

δ_{oil} : Oil film thickness in the piston ring pack

D_h : Hydraulic diameter

k_{air} : Thermal conductivity of air

k_{oil} : Thermal conductivity of oil.

The heat transfer resistance in the oil film is therefore negligible compared to that of air-oil vapor mixture gas, and the temperature of the oil film in the piston ring pack can be assumed to be uniform. In addition, physics requires that the temperature distribution is continuous at the interface of the oil film and the air-oil vapor mixture gas. Therefore, the temperature distribution is determined as shown in **Figure 2-8**.

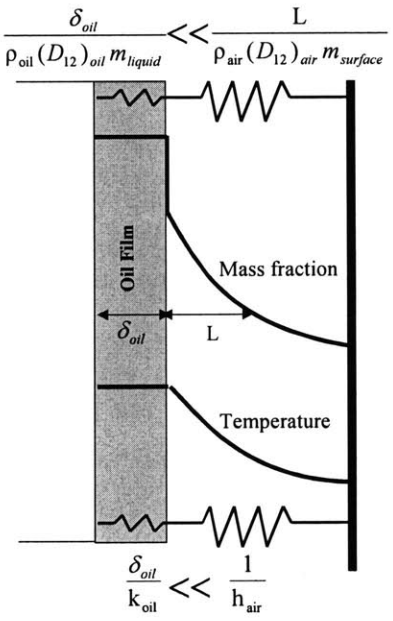

Figure 2-8. Heat transfer resistance and mass transfer resistance

2.2.2.6. Uniform Mass Fractiosn of Oil Components in the Oil Film

The mass transfer Biot number was calculated in a similar way to the heat transfer Biot number in order to check the homogeneity of the mass fraction distribution of an oil component in the oil film in the piston ring pack.

$$R_{diffusion} \sim \frac{\delta_{oil}}{\rho_{oil}(D_{12})_{oil} mf_{oil,liquid}} \tag{2.38}$$

$$R_{convection} = R_{equivalent\_diffusion} \sim \frac{a}{\rho_{air}(D_{12})_{air} mf_{oil,surface}} \tag{2.39}$$

where,

$R_{diffusion}$: Diffusive mass transfer resistance in the oil film

$R_{convection}$: Convective mass transfer resistance in the gas side where air-oil vapor mixture gas flows

$R_{equivalent\_diffusion}$: Diffusive mass transfer resistance that is equivalent to the convective mass transfer resistance $R_{convection}$

$(D_{12})_{air}$ and $(D_{12})_{oil}$: Diffusion coefficient (m^2/s) in the liquid oil and in the air-oil vapor mixture gas, respectively

The mass transfer Biot number Bi_m can be expressed in the following manner:

$$Bi_m = \frac{R_{diffusion}}{R_{convection}} = \frac{R_{diffusion}}{R_{equivalent\_diffusion}} = \frac{\delta_{oil}}{a}\frac{(D_{12})_{air}}{(D_{12})_{oil}}\frac{\rho_{air}}{\rho_{oil}}\frac{mf_{oil,surface}}{mf_{oil,liquid}} \tag{2.40}$$

Using equation **(2.13):**

$$Bi_m = \frac{\delta_{oil}}{a}\frac{(D_{12})_{air}}{(D_{12})_{oil}}\frac{\rho_{air}}{\rho_{oil}}\frac{P_{vapor}}{P_{air}}\frac{M_{oil}}{M_{air}} \sim \frac{10^{-5}}{10^{-4}}\frac{10^{-6}}{10^{-9}}\frac{\rho_{air}}{10^{3}}\frac{P_{vapor}}{P_{air}}\frac{100}{10}$$

$$= \frac{\rho_{air}}{P_{air}} P_{vapor} = \frac{1}{RT_{air}} P_{vapor} \sim \frac{1}{10^4 10^2} P_{vapr} < 10^{-6} \cdot 10^5 << 1 \qquad \textbf{(2.41)}$$

Therefore, the mass fraction of an oil component in the liquid oil film can be assumed to be homogeneous. In contrast to the temperature distribution, the mass fraction at the interface of the oil film and air-oil vapor gas is discontinuous as governed by equation **(2.13)**. Therefore, the mass fraction distribution is determined as shown in **Figure 2-8.**

2.2.2.7. Calculation of diffusion coefficient

The calculation of vaporization rate using equivalent diffusion length requires the value of the diffusion coefficient in the air-oil vapor mixture. The effective binary diffusion approach was used in calculation of multi-component diffusion coefficient. If species 1 is in small concentration, an effective binary diffusion coefficient for species 1 diffusing through the mixture $D_{1,mixture}$ can be defined from the simple kinetic theory in the following way [9].

$$D_{1,mixture} \approx \frac{1 - x_1}{\sum (x_i / D_{1,i})} \text{ and } x_1 << 1 \qquad \textbf{(2.42)}$$

Where,

x_i : Mole fraction of an oil component i in the mixture

$D_{1,i}$: Binary diffusion coefficient between oil component 1 and oil component i

For example, in this study, the oil was modeled as the mixture of twenty-one different paraffin hydrocarbon components. For an oil component 1,

$$D_{1,mixture} = \frac{1 - x_1}{\sum_{i=2}^{n} (x_i / D_{1,i})} = \frac{1 - x_1}{\frac{x_2}{D_{1,2}} + \frac{x_3}{D_{1,3}} + \cdots \frac{x_{21}}{D_{1,21}} + \frac{x_{air}}{D_{1,air}}} \qquad \textbf{(2.43)}$$

Since, $x_i << x_{air} \approx 1$

$$D_{1,mixture} \approx \frac{1}{\frac{x_{air}}{D_{1,air}}} = D_{1,air} \tag{2.44}$$

For other oil components in the air-oil vapor mixture:

$$D_{2,mixture} = D_{2,air}, D_{3,mixture} = D_{3,air}, \ldots, D_{21,mixture} = D_{21,air} \tag{2.45}$$

The values of these effective binary diffusion coefficients were calculated using equation [13]:

$$D_{i,air}(cm^2/\sec) = \left(0.00217 - 0.0005\sqrt{\frac{M_i + M_{air}}{M_i M_{air}}}\right)\frac{T\sqrt{T}}{P}\frac{\sqrt{\frac{M_i + M_{air}}{M_i M_{air}}}}{\sigma_{i,air}^2 \Omega_D} \tag{2.46}$$

where,

M_i (kg/kmol) : Molecular weight of a paraffin hydrocarbon oil component i

$T(K)$: Temperature in the air-oil vapor mixture

$P(atm)$: Pressure in the air-oil vapor mixture

$\sigma_{i,air}(\mathring{A})$: The characteristic Lennard-Jones length or the collision diameter

Ω_D: The diffusion collision integral

$\sigma_{i,air}(\mathring{A})$ and Ω_D are calculated based on the Lennard-Jones 6-12 model in **Appendix G.**

In equation **(2.46)**, pressure is the only variable for a particular oil component. Therefore, diffusion of an oil component is expected to be suppressed by the large combustion chamber pressure around combustion TDC (Top Dead Center).

2.2.2.8. Vaporization Rate of an Oil Component

In summary, the vaporization rate of an oil component could be calculated using the concept of equivalent diffusion length as follows.

$$\dot{m}_{oil}(kg/s) = \frac{(D_{12})_{gas} \cdot A_{vaporization}}{\delta_{diffusion}} (\rho_{oil,surface} - \rho_{oil,gas}) \quad \textbf{(2.47)}$$

where,

$(D_{12})_{gas}$: Diffusive mass transfer coefficient of an oil component in the air-oil vapor gas mixture and can be calculated using equation **(2.46)**

$\delta_{diffusion}$: Equivalent diffusion length and can be calculated using equation **(2.34)**.

$A_{vaporization}$: Vaporization area where the oil components exist and will be determined depending on the lubrication conditions

$\rho_{oil,surface}$: Density of an oil component on the oil film surface and can be calculated using equation **(2.20)** or $\rho_{oil,surface} = \rho_{air} \cdot mf_{oil,surface}$

$\rho_{oil,gas}$: Density of an oil component vapor in the air-oil vapor mixture, which is to be solved.

2.3. Governing Equations

2.3.1. Nine Regions in the Piston Ring Pack System

The piston ring pack system was divided into nine regions as shown in **Figure 2-9**.

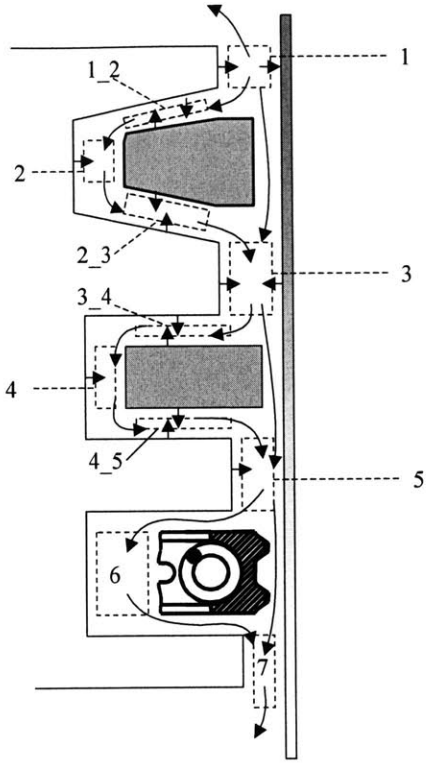

Figure 2-9. Nine regions to be modeled in the piston ring pack

- Region 1: Region between the crown land and the cylinder liner
- Region 1_2: Region between the upper side of the 1st groove and the upper side of the top ring
- Region 2: Region between the inner side of the 1st groove and the inner side of the top ring
- Region 2_3: Region between the lower side of the 1st groove and the lower side of the top ring
- Region 3: Region between the 2nd land and the cylinder liner
- Region 3_4: Region between the upper side of the 2nd groove and the upper side of the 2nd ring
- Region 4: Region between the inner side of the 2nd groove and the inner side of the 2nd ring

- Region 4_5: Region between the lower side of the 2nd groove and the lower side of the 2nd ring
- Region 5: Region between the 3rd land and the cylinder liner

For region 6 and region 7 in **Figure 2-9**, oil vapors in the gas were assumed to be saturated due to the oil sump in the crankcase. This assumption can be relaxed depending on the specific conditions in the oil sump. However, there is no reverse gas flow from regions 6 or 7 to region 5 in the engine studied in this work, and therefore, the validity of this assumption does not influence the results presented here. The mass fraction of the oil vapor in the combustion chamber (region 0) was assumed to be zero due to large amount of cylinder gas relative to the expected small amount of oil vapor.

2.3.2.Conservation of Mass of Oil Vapor

For each region of the piston ring pack, there is a mass balance of oil components originating from vaporization and of oil inflow/outflow due to the gas flow from pressure difference/pumping due to ring dynamics.

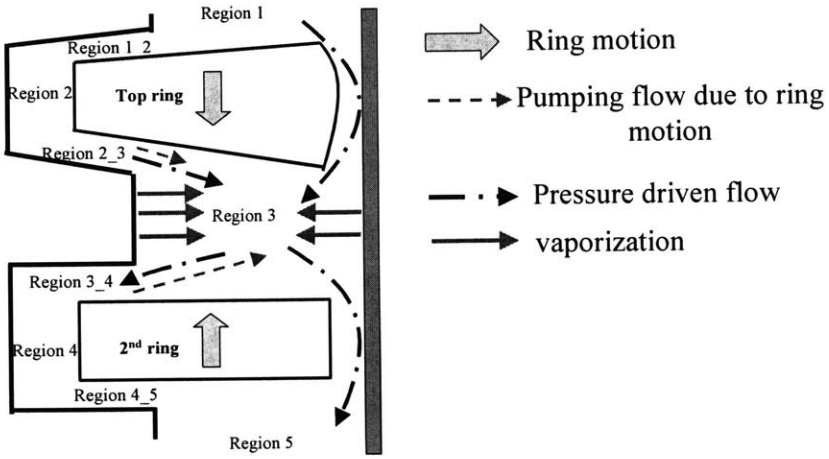

Vaporized oil + oil vapor inflow – oil vapor outflow

= net generation of oil vapor

Figure 2-10. Balance of oil vapor mass in the 2nd land region (region 3)

For example, in the 2nd land region (region 3) in **Figure 2-10**,

$$
\begin{aligned}
&m''_{3,land} A_{3,land} + m''_{3,liner} A_{3,liner} + \begin{Bmatrix} \rho_1 \cdot \dot{V}_{1\to3}(\dot{V}_{1\to3} \geq 0) \\ \rho_3 \cdot \dot{V}_{1\to3}(\dot{V}_{1\to3} \leq 0) \end{Bmatrix} + \begin{Bmatrix} \rho_{2\_3} \cdot \dot{V}_{2\_3\to3}(\dot{V}_{2\_3\to3} \geq 0) \\ \rho_3 \cdot \dot{V}_{2\_3\to3}(\dot{V}_{2\_3\to3} \leq 0) \end{Bmatrix} \\
&- \begin{Bmatrix} \rho_3 \cdot \dot{V}_{3\to3\_4}(\dot{V}_{3\to3\_4} \geq 0) \\ \rho_{3\_4} \cdot \dot{V}_{3\to3\_4}(\dot{V}_{3\to3\_4} \leq 0) \end{Bmatrix} - \begin{Bmatrix} \rho_3 \cdot \dot{V}_{3\to5}(\dot{V}_{3\to5} \geq 0) \\ \rho_5 \cdot \dot{V}_{3\to5}(\dot{V}_{3\to5} \leq 0) \end{Bmatrix} \\
&- \begin{Bmatrix} \rho_3 \cdot \dot{V}_{3\to2\_3,pump}(\dot{V}_{3\to2\_3,pump} \geq 0) \\ \rho_{2\_3} \cdot \dot{V}_{3\to2\_3,pump}(\dot{V}_{3\to2\_3,pump} \leq 0) \end{Bmatrix} - \begin{Bmatrix} \rho_3 \cdot \dot{V}_{3\to3\_4,pump}(\dot{V}_{3\to3\_4,pump} \geq 0) \\ \rho_5 \cdot \dot{V}_{3\to3\_4,pump}(\dot{V}_{3\to3\_4,pump} \leq 0) \end{Bmatrix} \\
&= \dot{m}_3 = \rho_3 \dot{V}_3 + \dot{\rho}_3 V_3
\end{aligned}
\tag{2.48}
$$

where,

$m''_{3,land}$: Vaporized oil mass flux from the 2nd land

$m''_{3,liner}$: Vaporized oil mass flux from the liner in the 2nd land region

$A_{3,land}$: Vaporization area on the 2nd land

$A_{3,liner}$: Vaporization area on the liner in the 2nd land region

$\dot{V}_{i\to j}$: Pressure-driven volume flow rate of air-oil vapor mixture from region i to j

$\dot{V}_{i\to j,pump}$: Volume flow rate of air-oil vapor mixture from region i to j due to pumping

V_3: Volume of region 3

$\dot{V}_3$: Rate of change of volume in region 3

ρ_i: Density of oil vapor in region i

$\dot{\rho}_i$: Rate of change of density of oil vapor in region i

Combining equations **(2.13)** and **(2.47)**,

$$
\begin{aligned}
&m''_{3,land}(kg/m^2 \cdot s) = \frac{(D_{oil,air})_3}{L_{3,land}} (mf_{3,land\_surface} \rho_{3,air} - \rho_3) \\
&= \frac{(D_{oil,air})_3}{L_{3,land}} \cdot (mf_{3,land\_liquid} \frac{P_{vap}(T_{3,land\_surface})}{P_3} \frac{M_{liquid\_oil}}{M_{air}} \rho_{3,air} - \rho_3)
\end{aligned}
\tag{2.49}
$$

$$m''_{3,liner}(kg/m^2 \cdot s) = \frac{(D_{oil,air})_3}{L_{3,liner}}(mf_{3,liner\_surface}\rho_{3,air} - \rho_3)$$
$$= \frac{(D_{oil,air})_3}{L_{3,liner}}(mf_{3,liner\_liquid}\frac{P_{vap}(T_{3,liner\_surface})}{P_3}\frac{M_{liquid\_oil}}{M_{air}}\rho_{3,air} - \rho_3) \quad \textbf{(2.50)}$$

where,

$(D_{oil,air})_3$: Diffusion coefficient of the air-oil vapor mixture in region 3

$mf_{3,land\_surface}$: Mass fractions of a gas-phase oil component on the oil film surface on the 2nd land

$mf_{3,liner\_surface}$: Mass fractions of a gas-phase oil component on the oil film surface on the liner in the 2nd land region

$mf_{3,land\_liquid}$: Mass fractions of a liquid-phase oil component in the oil film on the 2nd land

$mf_{3,land\_liquid}$: Mass fractions of a liquid-phase oil component in the oil film on the liner in the 2nd land region

$T_{3,land\_surface}$: Temperature of oil film on the 2nd land

$T_{3,liner\_surface}$: Temperatures of oil film on the liner in the 2nd land region

$L_{3,land}$: Equivalent diffusion lengths for the oil component on the 2nd land

$L_{3,liner}$: Equivalent diffusion lengths for the oil component on the liner in the 2nd land region

P_3 : Pressure in region 3

$\rho_{3,air}$: Air density in region 3

P_3 and $\rho_{3,air}$ are related to each other by the ideal gas law, which is $P_3 = \rho_{3,air}\widetilde{R}T_{3,air}$. Here, $\widetilde{R}$ is the universal gas constant ($\approx 8314(J/kg \cdot K)$) and $T_{3,air}$ is assumed to be the average of the 2nd land temperature and the liner temperature in the 2nd land region, i.e.

$$T_{3,air} = \frac{T_{3,land\_surface} + T_{3,liner\_surface}}{2}.$$

The other regions are dealt with in a similar manner and are summarized in the next section.

2.3.3. Basic Equations

Nine governing equations are derived for the nine regions in the piston ring pack system (**Figure 2-9**) using the mass conservation law as described in section **2.3.2**. The nine unknowns to be solved in these equations are oil vapor densities in each region $\rho_1, \rho_{1\_2}, \rho_2, \rho_{2\_3}, \rho_3, \rho_{3\_4}, \rho_4, \rho_{4\_5}, \rho_5$.

2.3.3.1. Calculation of Quantities Related to Thermodynamic Properties

Before deriving governing equations, the boundary conditions created by oil vapor densities in region 0 (combustion chamber), region 6 (oil control ring groove region), and region 7 (crankcase) and the air densities in the whole piston ring pack should be decided.

For the oil vapor densities,

$$\rho_0 \approx 0,\ \rho_6 = \frac{P_{vap}(T_6) \cdot M_{oil\_compo}}{\widetilde{R} \cdot T_6}, \text{ and } \rho_7 = \frac{P_{vap}(T_7) \cdot M_{oil\_compo}}{\widetilde{R} \cdot T_7} \quad \textbf{(2.51)}$$

where,

T_6 : Gas temperature in region 6

T_7 : Gas temperature in region 7

$P_{vap}(T_6)$: Vapor pressure of an oil component in region 6

$P_{vap}(T_7)$: Vapor pressure of an oil component in region 7

M_{oil_compo} : Molecular weight of the oil component

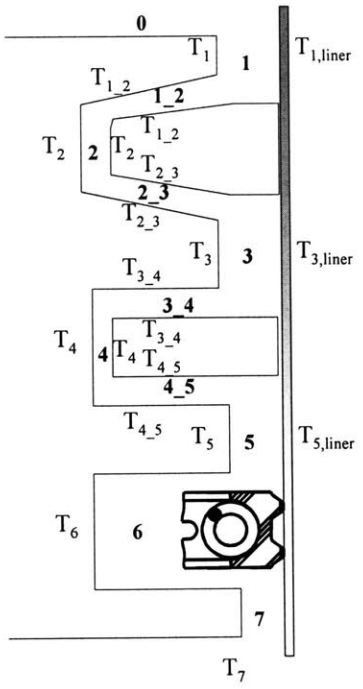

Groove temperature

$$T_{1\_2} = \frac{T_1 + T_2}{2} \qquad T_{2\_3} = \frac{T_2 + T_3}{2}$$

$$T_{3\_4} = \frac{T_3 + T_4}{2} \qquad T_{4\_5} = \frac{T_4 + T_5}{2}$$

Air temperature

$$T_{air,1} = \frac{T_1 + T_{1,liner}}{2} \qquad T_{air,1\_2} = T_{1\_2}$$

$$T_{air,2} = T_2 \qquad T_{air,2\_3} = T_{2\_3}$$

$$T_{air,3} = \frac{T_3 + T_{3,liner}}{2} \qquad T_{air,3\_4} = T_{3\_4}$$

$$T_{air,4} = T_4 \qquad T_{air,4\_5} = T_{4\_5}$$

$$T_{air,5} = \frac{T_5 + T_{5,liner}}{2}$$

Figure 2-11. Temperature distribution in the piston ring pack

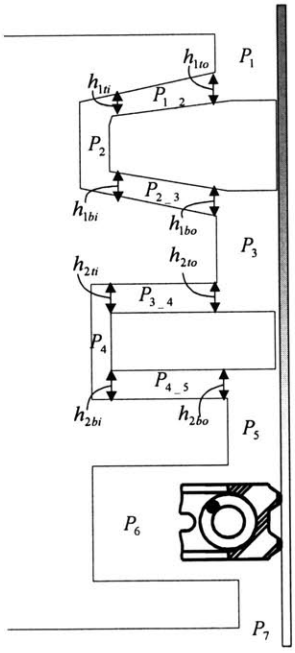

Pressures in groove regions

$$P_{1\_2} = \frac{P_1 \cdot h_{1to} + P_2 \cdot h_{1ti}}{h_{1to} + h_{1ti}}$$

$$P_{2\_3} = \frac{P_2 \cdot h_{1bi} + P_3 \cdot h_{1bo}}{h_{1bi} + h_{1bo}}$$

$$P_{3\_4} = \frac{P_3 \cdot h_{2to} + P_4 \cdot h_{2ti}}{h_{2to} + h_{2ti}}$$

$$P_{4\_5} = \frac{P_4 \cdot h_{2bi} + P_5 \cdot h_{2bo}}{h_{2bi} + h_{2bo}}$$

Figure 2-12. Pressure distribution in the piston ring pack

It is assumed that the piston ring pack temperatures in these regions are the same as the gas temperatures in these regions as shown in **Figure 2-11**.

Using the ideal gas law, and temperature & pressure relationship shown in **Figure 2-12**,

$$\rho_{air,i} = \frac{P_i \cdot M_{air}}{\tilde{R} \cdot T_{air,i}} \quad \text{for} \quad i=1,1\_2,2,2\_3,3,3\_4,4,4\_5,5 \tag{2.52}$$

The pressure and density of a groove region can be zero when the ring in that groove has complete contact with the groove side. In that case, the pressure-driven flow is also zero but the pumping flow is not zero. (**Figure 2-13**)

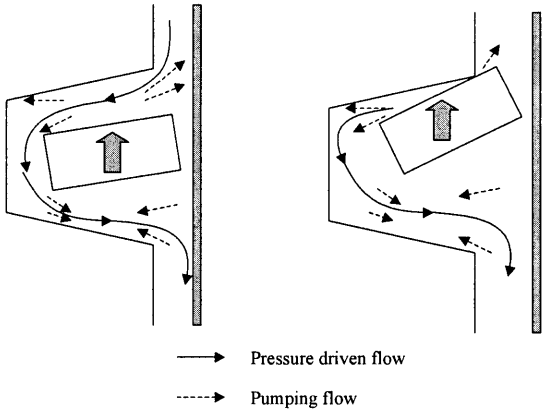

Figure 2-13. Pumping flow in the piston ring pack

The diffusion coefficient is a function of temperature and pressure. Therefore, the diffusion coefficient of an oil component in the region k is given by:

$$(D_{oil,air})_k = \left(0.00217 - 0.0005\sqrt{\frac{M_{oil}+M_{air}}{M_{oil}M_{air}}}\right)\frac{T_{air,k}\sqrt{T_{air,k}}}{P_k}\frac{\sqrt{\frac{M_{oil}+M_{air}}{M_{oil}M_{air}}}}{\sigma^2_{oil,air}\Omega_D(T_{air,k})}\times 10^{-6}(m^2/s) \tag{2.53}$$

where,

$M_{oil}(kg/kmol)$: The molecular weight of an oil component considered.

2.3.3.2. Vaporization Equations in the Piston Ring Pack

Nine vaporization equations were derived using the information in section **2.3.3.1,** for the piston ring pack.

Parameters $v_{1,land}$, $v_{1,liner}$, v_{1_2} , v_2 , v_{2_3} , $v_{3,land}$, $v_{3,liner}$, v_{3_4} , v_4 , v_{4_5} , $v_{5,land}$, $v_{5,liner}$ are introduced to represent the proportion of oil vapor, on the oil film surface, that has the potential to vaporize. If this parameter is equal to unity, all of the oil present is able to vaporize. If this parameter is equal to zero, only condensation can occur.

Parameters $l_{1,land}$, $l_{1,liner}$, l_{1_2} , l_2 , l_{2_3} , $l_{3,land}$, $l_{3,liner}$, l_{3_4} , l_4 , l_{4_5} , $l_{5,land}$, $l_{5,liner}$ are introduced to represent the lubrication condition. If this parameter is equal to unity, that means fully-flooded lubrication condition. If this parameter is equal to zero, that means dry lubrication condition. For the parameter having values between 0 and 1, partial lubrication condition can be represented.

For the region 1,

$$m''_{1,land}A_{1,land} + m''_{1,liner}A_{1,liner} + \begin{Bmatrix} \rho_0 \cdot \dot{V}_{0\to1}(\dot{V}_{0\to1} \geq 0) \\ \rho_1 \cdot \dot{V}_{0\to1}(\dot{V}_{0\to1} \leq 0) \end{Bmatrix} - \begin{Bmatrix} \rho_1 \cdot \dot{V}_{1\to2}(\dot{V}_{1\to2} \geq 0) \\ \rho_{1\_2} \cdot \dot{V}_{1\to2}(\dot{V}_{1\to2} \leq 0) \end{Bmatrix}$$
$$- \begin{Bmatrix} \rho_1 \cdot \dot{V}_{1\to3}(\dot{V}_{1\to3} \geq 0) \\ \rho_3 \cdot \dot{V}_{1\to3}(\dot{V}_{1\to3} \leq 0) \end{Bmatrix} - \begin{Bmatrix} \rho_1 \cdot \dot{V}_{1\to1\_2,pump}(\dot{V}_{1\to1\_2,pump} \geq 0) \\ \rho_{1\_2} \cdot \dot{V}_{1\to1\_2,pump}(\dot{V}_{1\to1\_2,pump} \leq 0) \end{Bmatrix} = \dot{m}_1 = \rho_1\dot{V}_1 + \dot{\rho}_1 V_1 \quad \textbf{(2.54)}$$

$$m''_{1,land}(kg/m^2 \cdot s) = \frac{(D_{oil,air})_1}{L_{1,land}}(mf_{1,land\_surface}\rho_{air,1} \cdot v_{1,land} - \rho_1) \cdot l_{1,land}$$
$$= \frac{(D_{oil,air})_1}{L_{1,land}}(mf_{1,land\_liquid}\frac{P_{vap}(T_{1,land\_surface})}{P_1}\frac{M_{liquid\_oil}}{M_{air}}\rho_{air,1} \cdot v_{1,land} - \rho_1) \cdot l_{1,land} \quad \textbf{(2.55)}$$

$$m''_{1,liner}(kg/m^2\cdot s)=\frac{(D_{oil,air})_1}{L_{1,liner}}(mf_{1,liner\_surface}\rho_{air,1}\cdot v_{1,liner}-\rho_1)\cdot l_{1,liner}$$
$$=\frac{(D_{oil,air})_1}{L_{1,liner}}(mf_{1,liner\_liquid}\frac{P_{vap}(T_{1,liner\_surface})}{P_1}\frac{M_{liquid\_oil}}{M_{air}}\rho_{air,1}\cdot v_{1,liner}-\rho_1)\cdot l_{1,liner} \quad \textbf{(2.56)}$$

For the region 1_2,

$$m''_{1\_2,groove}A_{1\_2,groove}+m''_{1\_2,ring}A_{1\_2,ring}+\begin{Bmatrix}\rho_1\cdot\dot{V}_{1\to2}(\dot{V}_{1\to2}\geq 0)\\ \rho_{1\_2}\cdot\dot{V}_{1\to2}(\dot{V}_{1\to2}\leq 0)\end{Bmatrix}-\begin{Bmatrix}\rho_{1\_2}\cdot\dot{V}_{1\to2}(\dot{V}_{1\to2}\geq 0)\\ \rho_2\cdot\dot{V}_{1\to2}(\dot{V}_{1\to2}\leq 0)\end{Bmatrix}$$
$$+\begin{Bmatrix}\rho_1\cdot\dot{V}_{1\to1\_2,pump}(\dot{V}_{1\to1\_2,pump}\geq 0)\\ \rho_{1\_2}\cdot\dot{V}_{1\to1\_2,pump}(\dot{V}_{1\to1\_2,pump}\leq 0)\end{Bmatrix}+\begin{Bmatrix}\rho_2\cdot\dot{V}_{2\to1\_2,pump}(\dot{V}_{2\to1\_2,pump}\geq 0)\\ \rho_{1\_2}\cdot\dot{V}_{2\to1\_2,pump}(\dot{V}_{2\to1\_2,pump}\leq 0)\end{Bmatrix}$$
$$=\dot{m}_{1\_2}=\rho_{1\_2}\dot{V}_{1\_2}+\dot{\rho}_{1\_2}V_{1\_2} \quad \textbf{(2.57)}$$

$$m''_{1\_2,groove}(kg/m^2\cdot s)=\frac{(D_{oil,air})_{1\_2}}{L_{1\_2,groove}}(mf_{1\_2,groove\_surface}\rho_{air,1\_2}\cdot v_{1\_2}-\rho_{1\_2})\cdot l_{1\_2}$$
$$=\frac{(D_{oil,air})_{1\_2}}{L_{1\_2,groove}}(mf_{1\_2,groove\_liquid}\frac{P_{vap}(T_{1\_2,groove\_surface})}{P_{1\_2}}\frac{M_{liquid\_oil}}{M_{air}}\rho_{air,1\_2}\cdot v_{1\_2}-\rho_{1\_2})\cdot l_{1\_2} \quad \textbf{(2.58)}$$

$$m''_{1\_2,groove}A_{1\_2,groove}=m''_{1\_2,ring}A_{1\_2,ring} \quad \textbf{(2.59)}$$

For the region 2,

$$m''_{2,groove}A_{2,groove}+\begin{Bmatrix}\rho_{1\_2}\cdot\dot{V}_{1\to2}(\dot{V}_{1\to2}\geq 0)\\ \rho_2\cdot\dot{V}_{1\to2}(\dot{V}_{1\to2}\leq 0)\end{Bmatrix}-\begin{Bmatrix}\rho_2\cdot\dot{V}_{2\to3}(\dot{V}_{2\to3}\geq 0)\\ \rho_{2\_3}\cdot\dot{V}_{2\to3}(\dot{V}_{2\to3}\leq 0)\end{Bmatrix}$$
$$-\begin{Bmatrix}\rho_2\cdot\dot{V}_{2\to1\_2,pump}(\dot{V}_{2\to1\_2,pump}\geq 0)\\ \rho_{1\_2}\cdot\dot{V}_{2\to1\_2,pump}(\dot{V}_{2\to1\_2,pump}\leq 0)\end{Bmatrix}-\begin{Bmatrix}\rho_2\cdot\dot{V}_{2\to2\_3,pump}(\dot{V}_{2\to2\_3,pump}\geq 0)\\ \rho_{2\_3}\cdot\dot{V}_{2\to2\_3,pump}(\dot{V}_{2\to2\_3,pump}\leq 0)\end{Bmatrix} \quad \textbf{(2.60)}$$
$$=\dot{m}_2=\rho_2\dot{V}_2+\dot{\rho}_2V_2$$

$$m''_{2,groove}(kg/m^2\cdot s)=\frac{(D_{oil,air})_2}{L_{2,groove}}(mf_{2,groove\_surface}\rho_{air,2}\cdot v_2-\rho_2)\cdot l_2$$
$$=\frac{(D_{oil,air})_2}{L_{2,groove}}(mf_{2,groove\_liquid}\frac{P_{vap}(T_{2,groove\_surface})}{P_2}\frac{M_{liquid\_oil}}{M_{air}}\rho_{air,2}\cdot v_2-\rho_2)\cdot l_2 \quad \textbf{(2.61)}$$

For the region 2_3,

$$m''_{2\_3,groove}A_{2\_3,groove}+m''_{2\_3,ring}A_{2\_3,ring}+\begin{Bmatrix}\rho_2\cdot\dot{V}_{2\to3}(\dot{V}_{2\to3}\geq0)\\ \rho_{2\_3}\cdot\dot{V}_{2\to3}(\dot{V}_{2\to3}\leq0)\end{Bmatrix}-\begin{Bmatrix}\rho_{2\_3}\cdot\dot{V}_{2\to3}(\dot{V}_{2\to3}\geq0)\\ \rho_3\cdot\dot{V}_{2\to3}(\dot{V}_{2\to3}\leq0)\end{Bmatrix}$$
$$+\begin{Bmatrix}\rho_2\cdot\dot{V}_{2\to2\_3,pump}(\dot{V}_{2\to2\_3,pump}\geq0)\\ \rho_{2\_3}\cdot\dot{V}_{2\to2\_3,pump}(\dot{V}_{2\to2\_3,pump}\leq0)\end{Bmatrix}+\begin{Bmatrix}\rho_3\cdot\dot{V}_{3\to2\_3,pump}(\dot{V}_{3\to2\_3,pump}\geq0)\\ \rho_{2\_3}\cdot\dot{V}_{3\to2\_3,pump}(\dot{V}_{3\to2\_3,pump}\leq0)\end{Bmatrix}$$
$$=\dot{m}_{2\_3}=\rho_{2\_3}\dot{V}_{2\_3}+\dot{\rho}_{2\_3}V_{2\_3} \quad \textbf{(2.62)}$$

$$m''_{2\_3,groove}(kg/m^2\cdot s)=\frac{(D_{oil,air})_{2\_3}}{L_{2\_3,groove}}(mf_{2\_3,groove\_surface}\rho_{air,2\_3}\cdot v_{2\_3}-\rho_{2\_3})\cdot l_{2\_3}$$
$$=\frac{(D_{oil,air})_{2\_3}}{L_{2\_3,groove}}(mf_{2\_3,groove\_liquid}\frac{P_{vap}(T_{2\_3,groove\_surface})}{P_{2\_3}}\frac{M_{liquid\_oil}}{M_{air}}\rho_{air,2\_3}\cdot v_{2\_3}-\rho_{2\_3})\cdot l_{2\_3} \quad \textbf{(2.63)}$$

$$m''_{2\_3,groove}A_{2\_3,groove}=m''_{2\_3,ring}A_{2\_3,ring} \quad \textbf{(2.64)}$$

For the region 3,

$$m''_{3,land}A_{3,land}+m''_{3,liner}A_{3,liner}+\begin{Bmatrix}\rho_1\cdot\dot{V}_{1\to3}(\dot{V}_{1\to3}\geq0)\\ \rho_3\cdot\dot{V}_{1\to3}(\dot{V}_{1\to3}\leq0)\end{Bmatrix}+\begin{Bmatrix}\rho_{2\_3}\cdot\dot{V}_{2\_3\to3}(\dot{V}_{2\_3\to3}\geq0)\\ \rho_3\cdot\dot{V}_{2\_3\to3}(\dot{V}_{2\_3\to3}\leq0)\end{Bmatrix}$$
$$-\begin{Bmatrix}\rho_3\cdot\dot{V}_{3\to3\_4}(\dot{V}_{3\to3\_4}\geq0)\\ \rho_{3\_4}\cdot\dot{V}_{3\to3\_4}(\dot{V}_{3\to3\_4}\leq0)\end{Bmatrix}-\begin{Bmatrix}\rho_3\cdot\dot{V}_{3\to5}(\dot{V}_{3\to5}\geq0)\\ \rho_5\cdot\dot{V}_{3\to5}(\dot{V}_{3\to5}\leq0)\end{Bmatrix} \quad \textbf{(2.65)}$$
$$-\begin{Bmatrix}\rho_3\cdot\dot{V}_{3\to2\_3,pump}(\dot{V}_{3\to2\_3,pump}\geq0)\\ \rho_{2\_3}\cdot\dot{V}_{3\to2\_3,pump}(\dot{V}_{3\to2\_3,pump}\leq0)\end{Bmatrix}-\begin{Bmatrix}\rho_3\cdot\dot{V}_{3\to3\_4,pump}(\dot{V}_{3\to3\_4,pump}\geq0)\\ \rho_{3\_4}\cdot\dot{V}_{3\to3\_4,pump}(\dot{V}_{3\to3\_4,pump}\leq0)\end{Bmatrix}$$
$$=\dot{m}_3=\rho_3\dot{V}_3+\dot{\rho}_3V_3$$

$$m''_{3,land}(kg/m^2\cdot s)=\frac{(D_{oil,air})_3}{L_{3,land}}(mf_{3,land\_surface}\rho_{air,3}\cdot v_{3,land}-\rho_3)\cdot l_{3,land}$$
$$=\frac{(D_{oil,air})_3}{L_{3,land}}(mf_{3,land\_liquid}\frac{P_{vap}(T_{3,land\_surface})}{P_3}\frac{M_{liquid\_oil}}{M_{air}}\rho_{air,3}\cdot v_{3,land}-\rho_3)\cdot l_{3,land} \quad \textbf{(2.66)}$$

$$m''_{3,liner}(kg/m^2\cdot s)=\frac{(D_{oil,air})_3}{L_{3,liner}}(mf_{3,liner\_surface}\rho_{air,3}\cdot v_{3,liner}-\rho_3)\cdot l_{3,liner}$$
$$=\frac{(D_{oil,air})_3}{L_{3,liner}}(mf_{3,liner\_liquid}\frac{P_{vap}(T_{3,liner\_surface})}{P_3}\frac{M_{liquid\_oil}}{M_{air}}\rho_{air,3}\cdot v_{3,liner}-\rho_3)\cdot l_{3,liner} \quad \textbf{(2.67)}$$

For the region 3_4,

$$m''_{3\_4,groove}A_{3\_4,groove}+m''_{3\_4,ring}A_{3\_4,ring}+\begin{Bmatrix}\rho_3\cdot\dot{V}_{3\to4}(\dot{V}_{3\to4}\ge0)\\ \rho_{3\_4}\cdot\dot{V}_{3\to4}(\dot{V}_{3\to4}\le0)\end{Bmatrix}-\begin{Bmatrix}\rho_{3\_4}\cdot\dot{V}_{3\to4}(\dot{V}_{3\to4}\ge0)\\ \rho_4\cdot\dot{V}_{3\to4}(\dot{V}_{3\to4}\le0)\end{Bmatrix}$$
$$+\begin{Bmatrix}\rho_3\cdot\dot{V}_{3\to3\_4,pump}(\dot{V}_{3\to3\_4,pump}\ge0)\\ \rho_{3\_4}\cdot\dot{V}_{3\to3\_4,pump}(\dot{V}_{3\to3\_4,pump}\le0)\end{Bmatrix}+\begin{Bmatrix}\rho_4\cdot\dot{V}_{4\to3\_4,pump}(\dot{V}_{4\to3\_4,pump}\ge0)\\ \rho_{3\_4}\cdot\dot{V}_{4\to3\_4,pump}(\dot{V}_{4\to3\_4,pump}\le0)\end{Bmatrix}$$
$$=\dot{m}_{3\_4}=\rho_{3\_4}\dot{V}_{3\_4}+\dot{\rho}_{3\_4}V_{3\_4} \quad \textbf{(2.68)}$$

$$m''_{3\_4,groove}(kg/m^2\cdot s)=\frac{(D_{oil,air})_{3\_4}}{L_{3\_4,groove}}(mf_{3\_4,groove\_surface}\rho_{air,3\_4}\cdot v_{3\_4}-\rho_{3\_4})\cdot l_{3\_4}$$
$$=\frac{(D_{oil,air})_{3\_4}}{L_{3\_4,groove}}(mf_{3\_4,groove\_liquid}\frac{P_{vap}(T_{3\_4,groove\_surface})}{P_{3\_4}}\frac{M_{liquid\_oil}}{M_{air}}\rho_{air,3\_4}\cdot v_{3\_4}-\rho_{3\_4})\cdot l_{3\_4} \quad \textbf{(2.69)}$$

$$m''_{3\_4,groove}A_{3\_4,groove}=m''_{3\_4,ring}A_{3\_4,ring} \quad \textbf{(2.70)}$$

For the region 4,

$$m''_{4,groove}A_{4,groove} + \begin{Bmatrix} \rho_{3\_4}\cdot\dot{V}_{3\to4}(\dot{V}_{3\to4}\geq 0) \\ \rho_4\cdot\dot{V}_{3\to4}(\dot{V}_{3\to4}\leq 0) \end{Bmatrix} - \begin{Bmatrix} \rho_4\cdot\dot{V}_{4\to5}(\dot{V}_{4\to5}\geq 0) \\ \rho_{4\_5}\cdot\dot{V}_{4\to5}(\dot{V}_{4\to5}\leq 0) \end{Bmatrix}$$
$$- \begin{Bmatrix} \rho_4\cdot\dot{V}_{4\to3\_4,pump}(\dot{V}_{4\to3\_4,pump}\geq 0) \\ \rho_{3\_4}\cdot\dot{V}_{4\to3\_4,pump}(\dot{V}_{4\to3\_4,pump}\leq 0) \end{Bmatrix} - \begin{Bmatrix} \rho_4\cdot\dot{V}_{4\to4\_5,pump}(\dot{V}_{4\to4\_5,pump}\geq 0) \\ \rho_{4\_5}\cdot\dot{V}_{4\to4\_5,pump}(\dot{V}_{4\to4\_5,pump}\leq 0) \end{Bmatrix} \quad \textbf{(2.71)}$$
$$= \dot{m}_4 = \rho_4\dot{V}_4 + \dot{\rho}_4 V_4$$

$$m''_{4,groove}(kg/m^2\cdot s) = \frac{(D_{oil,air})_4}{L_{4,groove}}(mf_{4,groove\_surface}\rho_{air,4}\cdot v_4 - \rho_4)\cdot l_4$$
$$= \frac{(D_{oil,air})_4}{L_{4,groove}}(mf_{4,groove\_liquid}\frac{P_{vap}(T_{4,groove\_surface})}{P_4}\frac{M_{liquid\_oil}}{M_{air}}\rho_{air,4}\cdot v_4 - \rho_4)\cdot l_4 \quad \textbf{(2.72)}$$

For the region 4_5,

$$m''_{4\_5,groove}A_{4\_5,groove} + m''_{4\_5,ring}A_{4\_5,ring} + \begin{Bmatrix} \rho_4\cdot\dot{V}_{4\to5}(\dot{V}_{4\to5}\geq 0) \\ \rho_{4\_5}\cdot\dot{V}_{4\to5}(\dot{V}_{4\to5}\leq 0) \end{Bmatrix} - \begin{Bmatrix} \rho_{4\_5}\cdot\dot{V}_{4\to5}(\dot{V}_{4\to5}\geq 0) \\ \rho_5\cdot\dot{V}_{4\to5}(\dot{V}_{4\to5}\leq 0) \end{Bmatrix}$$
$$+ \begin{Bmatrix} \rho_4\cdot\dot{V}_{4\to4\_5,pump}(\dot{V}_{4\to4\_5,pump}\geq 0) \\ \rho_{4\_5}\cdot\dot{V}_{4\to4\_5,pump}(\dot{V}_{4\to4\_5,pump}\leq 0) \end{Bmatrix} + \begin{Bmatrix} \rho_5\cdot\dot{V}_{5\to4\_5,pump}(\dot{V}_{5\to4\_5,pump}\geq 0) \\ \rho_{4\_5}\cdot\dot{V}_{5\to4\_5,pump}(\dot{V}_{5\to4\_5,pump}\leq 0) \end{Bmatrix}$$
$$= \dot{m}_{4\_5} = \rho_{4\_5}\dot{V}_{4\_5} + \dot{\rho}_{4\_5}V_{4\_5} \quad \textbf{(2.73)}$$

$$m''_{4\_5,groove}(kg/m^2\cdot s) = \frac{(D_{oil,air})_{4\_5}}{L_{4\_5,groove}}(mf_{4\_5,groove\_surface}\rho_{air,4\_5}\cdot v_{4\_5} - \rho_{4\_5})\cdot l_{4\_5}$$
$$= \frac{(D_{oil,air})_{4\_5}}{L_{4\_5,groove}}(mf_{4\_5,groove\_liquid}\frac{P_{vap}(T_{4\_5,groove\_surface})}{P_{4\_5}}\frac{M_{liquid\_oil}}{M_{air}}\rho_{air,4\_5}\cdot v_{4\_5} - \rho_{4\_5})\cdot l_{4\_5} \quad \textbf{(2.74)}$$

$$m''_{4\_5,groove}A_{4\_5,groove} = m''_{4\_5,ring}A_{4\_5,ring} \quad \textbf{(2.75)}$$

For the region 5,

$$m''_{5,land}A_{5,land} + m''_{5,liner}A_{5,liner} + \begin{Bmatrix} \rho_3 \cdot \dot{V}_{3\to5}(\dot{V}_{3\to5} \geq 0) \\ \rho_5 \cdot \dot{V}_{3\to5}(\dot{V}_{3\to5} \leq 0) \end{Bmatrix} + \begin{Bmatrix} \rho_{4\_5} \cdot \dot{V}_{4\to5}(\dot{V}_{4\to5} \geq 0) \\ \rho_5 \cdot \dot{V}_{4\to5}(\dot{V}_{4\to5} \leq 0) \end{Bmatrix}$$
$$- \begin{Bmatrix} \rho_5 \cdot \dot{V}_{5\to6}(\dot{V}_{5\to6} \geq 0) \\ \rho_6 \cdot \dot{V}_{5\to6}(\dot{V}_{5\to6} \leq 0) \end{Bmatrix} - \begin{Bmatrix} \rho_5 \cdot \dot{V}_{5\to7}(\dot{V}_{5\to7} \geq 0) \\ \rho_7 \cdot \dot{V}_{5\to7}(\dot{V}_{5\to7} \leq 0) \end{Bmatrix} - \begin{Bmatrix} \rho_5 \cdot \dot{V}_{5\to4\_5,pump}(\dot{V}_{5\to4\_5,pump} \geq 0) \\ \rho_{4\_5} \cdot \dot{V}_{5\to4\_5,pump}(\dot{V}_{5\to4\_5,pump} \leq 0) \end{Bmatrix}$$
$$= \dot{m}_5 = \rho_5 \dot{V}_5 + \dot{\rho}_5 V_5 \qquad \textbf{(2.76)}$$

$$m''_{5,land}(kg/m^2 \cdot s) = \frac{(D_{oil,air})_5}{L_{5,land}}(mf_{5,land\_surface}\rho_{air,5} \cdot v_{5,land} - \rho_5) \cdot l_{5,land}$$
$$= \frac{(D_{oil,air})_5}{L_{5,land}}(mf_{5,land\_liquid}\frac{P_{vap}(T_{5,land\_surface})}{P_5}\frac{M_{liquid\_oil}}{M_{air}}\rho_{air,5} \cdot v_{5,land} - \rho_5) \cdot l_{5,land} \qquad \textbf{(2.77)}$$

$$m''_{5,liner}(kg/m^2 \cdot s) = \frac{(D_{oil,air})_5}{L_{5,liner}}(mf_{5,liner\_surface}\rho_{air,5} \cdot v_{5,liner} - \rho_5) \cdot l_{5,liner}$$
$$= \frac{(D_{oil,air})_5}{L_{5,liner}}(mf_{5,liner\_liquid}\frac{P_{vap}(T_{5,liner\_surface})}{P_5}\frac{M_{liquid\_oil}}{M_{air}}\rho_{air,5} \cdot v_{5,liner} - \rho_5) \cdot l_{5,liner} \qquad \textbf{(2.78)}$$

In equations **(2.59), (2.64), (2.70),** and **(2.75),** the lubrication conditions of the upper ring side and lower ring side were assumed to be the same as the lubrication conditions of the corresponding upper groove and lower groove respectively. This assumption comes from the fact that the ring moves up and down due to inertia during engine operation, and this motion makes it possible for the ring to come into contact with the groove flanks in case of non-dry lubrication condition. In addition, the temperature of the side of a ring was assumed to be the same as the temperature of the groove side it faces. Therefore, following notations will replace the old ones in equations **(2.57), (2.62), (2.68),** and **(2.73).**

$$m''_{1\_2}A_{1\_2} = 2 \times m''_{1\_2,groove}A_{1\_2,groove} = 2 \times m''_{1\_2,ring}A_{1\_2,ring} \qquad \textbf{(2.79)}$$

$$m''_{2\_3} A_{2\_3} = 2 \times m''_{2\_3,groove} A_{2\_3,groove} = 2 \times m''_{2\_3,ring} A_{2\_3,ring} \quad \textbf{(2.80)}$$

$$m''_{3\_4} A_{3\_4} = 2 \times m''_{3\_4,groove} A_{3\_4,groove} = 2 \times m''_{3\_4,ring} A_{3\_4,ring} \quad \textbf{(2.81)}$$

$$m''_{4\_5} A_{4\_5} = 2 \times m''_{4\_5,groove} A_{4\_5,groove} = 2 \times m''_{4\_5,ring} A_{4\_5,ring} \quad \textbf{(2.82)}$$

2.3.4. Normalized Equations

In order to solve the nine equations shown in section **2.3.3**, we must first normalize them to be of order one. For the oil density in a region, the normalization factors are mass fraction of an oil component on the oil film surface, and the air density in the region. For the time derivative or crank angle variation during the engine cycle, engine speed (Rev/sec) was used as a normalization factor.

$$\rho_1 = \hat{\rho}_1 \cdot mf_{1,land\_surface} \cdot \rho_{air,1} \quad \textbf{(2.83)}$$

$$\rho_{1\_2} = \hat{\rho}_{1\_2} \cdot mf_{1\_2,groove\_surface} \cdot \rho_{air,1\_2} \quad \textbf{(2.84)}$$

$$\rho_2 = \hat{\rho}_2 \cdot mf_{2,groove\_surface} \cdot \rho_{air,2} \quad \textbf{(2.85)}$$

$$\rho_{2\_3} = \hat{\rho}_{2\_3} \cdot mf_{2\_3,groove\_surface} \cdot \rho_{air,2\_3} \quad \textbf{(2.86)}$$

$$\rho_3 = \hat{\rho}_3 \cdot mf_{3,land\_surface} \cdot \rho_{air,3} \quad \textbf{(2.87)}$$

$$\rho_{3\_4} = \hat{\rho}_{3\_4} \cdot mf_{3\_4,groove\_surface} \cdot \rho_{air,3\_4} \quad \textbf{(2.88)}$$

$$\rho_4 = \hat{\rho}_4 \cdot mf_{4,groove\_surface} \cdot \rho_{air,4} \quad \textbf{(2.89)}$$

$$\rho_{4\_5} = \hat{\rho}_{4\_5} \cdot mf_{4\_5,groove\_surface} \cdot \rho_{air,4\_5} \quad \textbf{(2.90)}$$

$$\rho_5 = \hat{\rho}_5 \cdot mf_{5,land\_surface} \cdot \rho_{air,5} \quad \textbf{(2.91)}$$

$$t = \frac{\hat{t}}{N(rps)} \quad \textbf{(2.92)}$$

Here, $\hat{\rho}_1, \hat{\rho}_{1\_2}, \hat{\rho}_2, \hat{\rho}_{2\_3}, \hat{\rho}_3, \hat{\rho}_{3\_4}, \hat{\rho}_4, \hat{\rho}_{4\_5}, \hat{\rho}_5$ are normalized oil vapor densities and $\hat{t}$ is the normalized time. For example,

$$mf_{1,land\_surface} \cdot \rho_{air,1} = \left(mf_{1,land\_liquid} \cdot \frac{P_{vap}(T_{1,land\_surface})}{P_1} \cdot \frac{M_{liquid\_oil}}{M_{air}} \right) \cdot \left(\frac{P_1}{\widetilde{R} T_{air,1}} \right)$$
$$= mf_{1,land\_liquid} \cdot \frac{P_{vap}(T_{1,land\_surface})}{\widetilde{R} T_{air,1}} \cdot \frac{M_{liquid\_oil}}{M_{air}} \quad \textbf{(2.93)}$$

Since, pressure is the only variable with respect to the crank angle or time in equation **(2.93)**, $mf_{1,land\_surface} \cdot \rho_{air,1}$ in equation **(2.93)** is an invariant. Therefore,

$$\frac{d\rho_1}{dt} = \frac{d(\hat{\rho}_1 \cdot mf_{1,land\_surface} \cdot \rho_{air,1})}{d(\hat{t} / N)} = (mf_{1,land\_surface} \cdot \rho_{air,1}) \cdot N \cdot \frac{d\hat{\rho}_1}{d\hat{t}} \quad \textbf{(2.94)}$$

As an another example,

Volume flow rate $\dot{V}_{0\to1} = \frac{dV_{0\to1}}{dt} = N \frac{dV_{0\to1}}{d\hat{t}}$ **(2.95)**

Rate of change of volume $\dot{V}_1 = \frac{dV_1}{dt} = N \frac{dV_1}{d\hat{t}}$ **(2.96)**

The following equations are normalized equations using normalizing factors **(2.83)~(2.92)** and with consideration of equations **(2.94)~(2.96).**

For the region 1,

$$\frac{d\hat{\rho}_1}{d\hat{t}} + \frac{\hat{\rho}_1}{V_1}\frac{dV_1}{d\hat{t}} - \frac{(D_{oil,air})_1 A_{1,land}}{NL_{1,land}V_1}(v_{1,land} - \hat{\rho}_1)l_{1,land}$$

$$- \frac{(D_{oil,air})_1 A_{1,liner}}{NL_{1,liner}V_1}\left(\frac{mf_{1,liner\_surface}}{mf_{1,land\_surface}}v_{1,liner} - \hat{\rho}_1\right)l_{1,liner} - \left\{\begin{array}{l} 0(\dot{V}_{0\to1} \geq 0) \\ \frac{\hat{\rho}_1}{V_1}\frac{dV_{0\to1}}{d\hat{t}}(\dot{V}_{0\to1} \leq 0) \end{array}\right\}$$

$$+ \left\{\begin{array}{l} \frac{\hat{\rho}_1}{V_1}\frac{dV_{1\to2}}{d\hat{t}}(\dot{V}_{1\to2} \geq 0) \\ \frac{mf_{1\_2,groove\_surface}}{mf_{1,land\_surface}}\frac{\rho_{air,1\_2}}{\rho_{air,1}}\frac{\hat{\rho}_{1\_2}}{V_1}\frac{dV_{1\to2}}{d\hat{t}}(\dot{V}_{1\to2} \leq 0) \end{array}\right\}$$

$$+ \left\{\begin{array}{l} \frac{\hat{\rho}_1}{V_1}\frac{dV_{1\to3}}{d\hat{t}}(\dot{V}_{1\to3} \geq 0) \\ \frac{mf_{3,land\_surface}}{mf_{1,land\_surface}}\frac{\rho_{air,3}}{\rho_{air,1}}\frac{\hat{\rho}_3}{V_1}\frac{dV_{1\to3}}{d\hat{t}}(\dot{V}_{1\to3} \leq 0) \end{array}\right\}$$

$$+ \left\{\begin{array}{l} \frac{\hat{\rho}_1}{V_1}\frac{dV_{1\to1\_2,pump}}{d\hat{t}}(\dot{V}_{1\to1\_2,pump} \geq 0) \\ \frac{mf_{1\_2,groove\_surface}}{mf_{1,land\_surface}}\frac{\rho_{air,1\_2}}{\rho_{air,1}}\frac{\hat{\rho}_{1\_2}}{V_1}\frac{dV_{1\to1\_2,pump}}{d\hat{t}}(\dot{V}_{1\to1\_2,pump} \leq 0) \end{array}\right\} = 0 \qquad \textbf{(2.97)}$$

For the region 1_2,

$$\frac{d\hat{\rho}_{1\_2}}{d\hat{t}}+\frac{\hat{\rho}_{1\_2}}{V_{1\_2}}\frac{dV_{1\_2}}{d\hat{t}}-\frac{(D_{oil,air})_{1\_2}A_{1\_2}}{NL_{1\_2,groove}V_{1\_2}}(v_{1\_2}-\hat{\rho}_{1\_2})l_{1\_2}$$
$$-\left\{\begin{array}{l}\dfrac{mf_{1,land\_surface}}{mf_{1\_2,groove\_surface}}\dfrac{\rho_{air,1}}{\rho_{air,1\_2}}\dfrac{\hat{\rho}_1}{V_{1\_2}}\dfrac{dV_{1\to2}}{d\hat{t}}(\dot{V}_{1\to2}\geq 0)\\ \dfrac{\hat{\rho}_{1\_2}}{V_{1\_2}}\dfrac{dV_{1\to2}}{d\hat{t}}(\dot{V}_{1\to2}\leq 0)\end{array}\right\}$$
$$+\left\{\begin{array}{l}\dfrac{\hat{\rho}_{1\_2}}{V_{1\_2}}\dfrac{dV_{1\to2}}{d\hat{t}}(\dot{V}_{1\to2}\geq 0)\\ \dfrac{mf_{2,groove\_surface}}{mf_{1\_2,groove\_surface}}\dfrac{\rho_{air,2}}{\rho_{air,1\_2}}\dfrac{\hat{\rho}_2}{V_{1\_2}}\dfrac{dV_{1\to2}}{d\hat{t}}(\dot{V}_{1\to2}\leq 0)\end{array}\right\}$$
$$-\left\{\begin{array}{l}\dfrac{mf_{1,land\_surface}}{mf_{1\_2,groove\_surface}}\dfrac{\rho_{air,1}}{\rho_{air,1\_2}}\dfrac{\hat{\rho}_1}{V_{1\_2}}\dfrac{dV_{1\to1\_2,pump}}{d\hat{t}}(\dot{V}_{1\to1\_2,pump}\geq 0)\\ \dfrac{\hat{\rho}_{1\_2}}{V_{1\_2}}\dfrac{dV_{1\to1\_2,pump}}{d\hat{t}}(\dot{V}_{1\to1\_2,pump}\leq 0)\end{array}\right\}$$
$$-\left\{\begin{array}{l}\dfrac{mf_{2,groove\_surface}}{mf_{1\_2,groove\_surface}}\dfrac{\rho_{air,2}}{\rho_{air,1\_2}}\dfrac{\hat{\rho}_2}{V_{1\_2}}\dfrac{dV_{2\to1\_2,pump}}{d\hat{t}}(\dot{V}_{2\to1\_2,pump}\geq 0)\\ \dfrac{\hat{\rho}_{1\_2}}{V_{1\_2}}\dfrac{dV_{2\to1\_2,pump}}{d\hat{t}}(\dot{V}_{2\to1\_2,pump}\leq 0)\end{array}\right\}=0 \qquad \textbf{(2.98)}$$

For the region 2,

$$\frac{d\hat{\rho}_2}{d\hat{t}} + \frac{\hat{\rho}_2}{V_2}\frac{dV_2}{d\hat{t}} - \frac{(D_{oil,air})_2 A_{2,groove}}{NL_{2,groove}V_2}(v_2 - \hat{\rho}_2)l_2$$

$$- \begin{Bmatrix} \frac{mf_{1\_2,groove\_surface}}{mf_{2,groove\_surface}}\frac{\rho_{air,1\_2}}{\rho_{air,2}}\frac{\hat{\rho}_{1\_2}}{V_2}\frac{dV_{1\to 2}}{d\hat{t}}(\dot{V}_{1\to 2} \geq 0) \\ \frac{\hat{\rho}_2}{V_2}\frac{dV_{1\to 2}}{d\hat{t}}(\dot{V}_{1\to 2} \leq 0) \end{Bmatrix}$$

$$+ \begin{Bmatrix} \frac{\hat{\rho}_2}{V_2}\frac{dV_{2\to 3}}{d\hat{t}}(\dot{V}_{2\to 3} \geq 0) \\ \frac{mf_{2\_3,groove\_surface}}{mf_{2,groove\_surface}}\frac{\rho_{air,2\_3}}{\rho_{air,2}}\frac{\hat{\rho}_{2\_3}}{V_2}\frac{dV_{2\to 3}}{d\hat{t}}(\dot{V}_{2\to 3} \leq 0) \end{Bmatrix}$$

$$+ \begin{Bmatrix} \frac{\hat{\rho}_2}{V_2}\frac{dV_{2\to 1\_2,pump}}{d\hat{t}}(\dot{V}_{2\to 1\_2,pump} \geq 0) \\ \frac{mf_{1\_2,groove\_surface}}{mf_{2,groove\_surface}}\frac{\rho_{air,1\_2}}{\rho_{air,2}}\frac{\hat{\rho}_{1\_2}}{V_2}\frac{dV_{2\to 1\_2,pump}}{d\hat{t}}(\dot{V}_{2\to 1\_2,pump} \leq 0) \end{Bmatrix}$$

$$+ \begin{Bmatrix} \frac{\hat{\rho}_2}{V_2}\frac{dV_{2\to 2\_3,pump}}{d\hat{t}}(\dot{V}_{2\to 2\_3,pump} \geq 0) \\ \frac{mf_{2\_3,groove\_surface}}{mf_{2,groove\_surface}}\frac{\rho_{air,2\_3}}{\rho_{air,2}}\frac{\hat{\rho}_{2\_3}}{V_2}\frac{dV_{2\to 2\_3,pump}}{d\hat{t}}(\dot{V}_{2\to 2\_3,pump} \leq 0) \end{Bmatrix} = 0 \quad \textbf{(2.99)}$$

For the region 2_3,

$$\frac{d\hat{\rho}_{2\_3}}{d\hat{t}}+\frac{\hat{\rho}_{2\_3}}{V_{2\_3}}\frac{dV_{2\_3}}{d\hat{t}}-\frac{(D_{oil,air})_{2\_3}A_{2\_3}}{NL_{2\_3,groove}V_{2\_3}}(v_{2\_3}-\hat{\rho}_{2\_3})l_{2\_3}$$
$$-\left\{\begin{array}{l}\dfrac{mf_{2,groove\_surface}}{mf_{2\_3,groove\_surface}}\dfrac{\rho_{air,2}}{\rho_{air,2\_3}}\dfrac{\hat{\rho}_2}{V_{2\_3}}\dfrac{dV_{2\to3}}{d\hat{t}}(\dot{V}_{2\to3}\geq 0)\\ \dfrac{\hat{\rho}_{2\_3}}{V_{2\_3}}\dfrac{dV_{2\to3}}{d\hat{t}}(\dot{V}_{2\to3}\leq 0)\end{array}\right\}$$
$$+\left\{\begin{array}{l}\dfrac{\hat{\rho}_{2\_3}}{V_{2\_3}}\dfrac{dV_{2\to3}}{d\hat{t}}(\dot{V}_{2\to3}\geq 0)\\ \dfrac{mf_{3,land\_surface}}{mf_{2\_3,groove\_surface}}\dfrac{\rho_{air,3}}{\rho_{air,2\_3}}\dfrac{\hat{\rho}_3}{V_{2\_3}}\dfrac{dV_{2\to3}}{d\hat{t}}(\dot{V}_{2\to3}\leq 0)\end{array}\right\}$$
$$-\left\{\begin{array}{l}\dfrac{mf_{2,groove\_surface}}{mf_{2\_3,groove\_surface}}\dfrac{\rho_{air,2}}{\rho_{air,2\_3}}\dfrac{\hat{\rho}_2}{V_{2\_3}}\dfrac{dV_{2\to2\_3,pump}}{d\hat{t}}(\dot{V}_{2\to2\_3,pump}\geq 0)\\ \dfrac{\hat{\rho}_{2\_3}}{V_{2\_3}}\dfrac{dV_{2\to2\_3,pump}}{d\hat{t}}(\dot{V}_{2\to2\_3,pump}\leq 0)\end{array}\right\}$$
$$-\left\{\begin{array}{l}\dfrac{mf_{3,groove\_surface}}{mf_{2\_3,groove\_surface}}\dfrac{\rho_{air,3}}{\rho_{air,2\_3}}\dfrac{\hat{\rho}_3}{V_{2\_3}}\dfrac{dV_{3\to2\_3,pump}}{d\hat{t}}(\dot{V}_{3\to2\_3,pump}\geq 0)\\ \dfrac{\hat{\rho}_{2\_3}}{V_{2\_3}}\dfrac{dV_{3\to2\_3,pump}}{d\hat{t}}(\dot{V}_{3\to2\_3,pump}\leq 0)\end{array}\right\}=0 \qquad \textbf{(2.100)}$$

For the region 3,

$$\frac{d\hat{\rho}_3}{d\hat{t}} + \frac{\hat{\rho}_3}{V_3}\frac{dV_3}{d\hat{t}} - \frac{(D_{oil,air})_3 A_{13land}}{NL_{3,land}V_3}(v_{3,land} - \hat{\rho}_3)l_{3,land}$$

$$- \frac{(D_{oil,air})_3 A_{3,liner}}{NL_{3,liner}V_3}\left(\frac{mf_{3,liner\_surface}}{mf_{3,land\_surface}}v_{3,liner} - \hat{\rho}_3\right)l_{3,liner}$$

$$- \left\{\begin{array}{l} \dfrac{mf_{1,land\_surface}}{mf_{3,land\_surface}}\dfrac{\rho_{air,1}}{\rho_{air,3}}\dfrac{\hat{\rho}_1}{V_3}\dfrac{dV_{1\to3}}{d\hat{t}}(\dot{V}_{1\to3} \geq 0) \\ \dfrac{\hat{\rho}_3}{V_3}\dfrac{dV_{1\to3}}{d\hat{t}}(\dot{V}_{1\to3} \leq 0) \end{array}\right\}$$

$$- \left\{\begin{array}{l} \dfrac{mf_{2\_3,groove\_surface}}{mf_{3,land\_surface}}\dfrac{\rho_{air,2\_3}}{\rho_{air,3}}\dfrac{\hat{\rho}_{2\_3}}{V_3}\dfrac{dV_{2\to3}}{d\hat{t}}(\dot{V}_{2\to3} \geq 0) \\ \dfrac{\hat{\rho}_3}{V_3}\dfrac{dV_{2\to3}}{d\hat{t}}(\dot{V}_{2\to3} \leq 0) \end{array}\right\}$$

$$+ \left\{\begin{array}{l} \dfrac{\hat{\rho}_3}{V_3}\dfrac{dV_{3\to4}}{d\hat{t}}(\dot{V}_{3\to4} \geq 0) \\ \dfrac{mf_{3\_4,groove\_surface}}{mf_{3,land\_surface}}\dfrac{\rho_{air,3\_4}}{\rho_{air,3}}\dfrac{\hat{\rho}_{3\_4}}{V_3}\dfrac{dV_{3\to4}}{d\hat{t}}(\dot{V}_{3\to4} \leq 0) \end{array}\right\}$$

$$+ \left\{\begin{array}{l} \dfrac{\hat{\rho}_3}{V_3}\dfrac{dV_{3\to5}}{d\hat{t}}(\dot{V}_{3\to5} \geq 0) \\ \dfrac{mf_{5,land\_surface}}{mf_{3,land\_surface}}\dfrac{\rho_{air,5}}{\rho_{air,3}}\dfrac{\hat{\rho}_5}{V_3}\dfrac{dV_{3\to5}}{d\hat{t}}(\dot{V}_{3\to5} \leq 0) \end{array}\right\}$$

$$+ \left\{\begin{array}{l} \dfrac{\hat{\rho}_3}{V_3}\dfrac{dV_{3\to2\_3,pump}}{d\hat{t}}(\dot{V}_{3\to2\_3,pump} \geq 0) \\ \dfrac{mf_{2\_3,groove\_surface}}{mf_{3,land\_surface}}\dfrac{\rho_{air,2\_3}}{\rho_{air,3}}\dfrac{\hat{\rho}_{2\_3}}{V_3}\dfrac{dV_{3\to2\_3,pump}}{d\hat{t}}(\dot{V}_{3\to2\_3,pump} \leq 0) \end{array}\right\}$$

$$+ \left\{\begin{array}{l} \dfrac{\hat{\rho}_3}{V_3}\dfrac{dV_{3\to3\_4,pump}}{d\hat{t}}(\dot{V}_{3\to3\_4,pump} \geq 0) \\ \dfrac{mf_{3\_4,groove\_surface}}{mf_{3,land\_surface}}\dfrac{\rho_{air,3\_4}}{\rho_{air,3}}\dfrac{\hat{\rho}_{3\_4}}{V_3}\dfrac{dV_{3\to3\_4,pump}}{d\hat{t}}(\dot{V}_{3\to3\_4,pump} \leq 0) \end{array}\right\} = 0 \qquad \textbf{(2.101)}$$

For the region 3_4,

$$\frac{d\hat{\rho}_{3\_4}}{d\hat{t}}+\frac{\hat{\rho}_{3\_4}}{V_{3\_4}}\frac{dV_{3\_4}}{d\hat{t}}-\frac{(D_{oil,air})_{3\_4}A_{3\_4}}{NL_{3\_4,groove}V_{3\_4}}(v_{3\_4}-\hat{\rho}_{3\_4})l_{3\_4}$$
$$-\left\{\begin{array}{l}\dfrac{mf_{3,land\_surface}}{mf_{3\_4,groove\_surface}}\dfrac{\rho_{air,3}}{\rho_{air,3\_4}}\dfrac{\hat{\rho}_3}{V_{3\_4}}\dfrac{dV_{3\to4}}{d\hat{t}}(\dot{V}_{3\to4}\geq 0)\\ \dfrac{\hat{\rho}_{3\_4}}{V_{3\_4}}\dfrac{dV_{3\to4}}{d\hat{t}}(\dot{V}_{3\to4}\leq 0)\end{array}\right\}$$
$$+\left\{\begin{array}{l}\dfrac{\hat{\rho}_{3\_4}}{V_{3\_4}}\dfrac{dV_{3\to4}}{d\hat{t}}(\dot{V}_{3\to4}\geq 0)\\ \dfrac{mf_{4,groove\_surface}}{mf_{3\_4,groove\_surface}}\dfrac{\rho_{air,4}}{\rho_{air,3\_4}}\dfrac{\hat{\rho}_4}{V_{3\_4}}\dfrac{dV_{3\to4}}{d\hat{t}}(\dot{V}_{3\to4}\leq 0)\end{array}\right\}$$
$$-\left\{\begin{array}{l}\dfrac{mf_{3,land\_surface}}{mf_{3\_4,groove\_surface}}\dfrac{\rho_{air,3}}{\rho_{air,3\_4}}\dfrac{\hat{\rho}_3}{V_{3\_4}}\dfrac{dV_{3\to3\_4,pump}}{d\hat{t}}(\dot{V}_{3\to3\_4,pump}\geq 0)\\ \dfrac{\hat{\rho}_{3\_4}}{V_{3\_4}}\dfrac{dV_{3\to3\_4,pump}}{d\hat{t}}(\dot{V}_{3\to3\_4,pump}\leq 0)\end{array}\right\}$$
$$-\left\{\begin{array}{l}\dfrac{mf_{4,groove\_surface}}{mf_{3\_4,groove\_surface}}\dfrac{\rho_{air,4}}{\rho_{air,3\_4}}\dfrac{\hat{\rho}_4}{V_{3\_4}}\dfrac{dV_{4\to3\_4,pump}}{d\hat{t}}(\dot{V}_{4\to3\_4,pump}\geq 0)\\ \dfrac{\hat{\rho}_{3\_4}}{V_{3\_4}}\dfrac{dV_{4\to3\_4,pump}}{d\hat{t}}(\dot{V}_{4\to3\_4,pump}\leq 0)\end{array}\right\}=0 \qquad \textbf{(2.102)}$$

For the region 4,

$$\frac{d\hat{\rho}_4}{d\hat{t}} + \frac{\hat{\rho}_4}{V_4}\frac{dV_4}{d\hat{t}} - \frac{(D_{oil,air})_4 A_{4,groove}}{NL_{4,groove}V_4}(v_{4,groove} - \hat{\rho}_4)l_{4,groove}$$

$$- \begin{Bmatrix} \frac{mf_{3\_4,groove\_surface}}{mf_{4,groove\_surface}}\frac{\rho_{air,3\_4}}{\rho_{air,4}}\frac{\hat{\rho}_{3\_4}}{V_4}\frac{dV_{3\to4}}{d\hat{t}}(\dot{V}_{3\to4} \geq 0) \\ \frac{\hat{\rho}_4}{V_4}\frac{dV_{3\to4}}{d\hat{t}}(\dot{V}_{3\to4} \leq 0) \end{Bmatrix}$$

$$+ \begin{Bmatrix} \frac{\hat{\rho}_4}{V_4}\frac{dV_{4\to5}}{d\hat{t}}(\dot{V}_{4\to5} \geq 0) \\ \frac{mf_{4\_5,groove\_surface}}{mf_{4,groove\_surface}}\frac{\rho_{air,4\_5}}{\rho_{air,4}}\frac{\hat{\rho}_{4\_5}}{V_4}\frac{dV_{4\to5}}{d\hat{t}}(\dot{V}_{4\to5} \leq 0) \end{Bmatrix}$$

$$+ \begin{Bmatrix} \frac{\hat{\rho}_4}{V_4}\frac{dV_{4\to3\_4,pump}}{d\hat{t}}(\dot{V}_{4\to3\_4,pump} \geq 0) \\ \frac{mf_{3\_4,groove\_surface}}{mf_{4,groove\_surface}}\frac{\rho_{air,3\_4}}{\rho_{air,4}}\frac{\hat{\rho}_{3\_4}}{V_4}\frac{dV_{4\to3\_4,pump}}{d\hat{t}}(\dot{V}_{4\to3\_4,pump} \leq 0) \end{Bmatrix}$$

$$+ \begin{Bmatrix} \frac{\hat{\rho}_4}{V_4}\frac{dV_{4\to4\_5,pump}}{d\hat{t}}(\dot{V}_{4\to4\_5,pump} \geq 0) \\ \frac{mf_{4\_5,groove\_surface}}{mf_{4,groove\_surface}}\frac{\rho_{air,4\_5}}{\rho_{air,4}}\frac{\hat{\rho}_{4\_5}}{V_4}\frac{dV_{4\to4\_5,pump}}{d\hat{t}}(\dot{V}_{4\to4\_5,pump} \leq 0) \end{Bmatrix} = 0 \qquad \textbf{(2.103)}$$

For the region 4_5,

$$\frac{d\hat{\rho}_{4\_5}}{d\hat{t}}+\frac{\hat{\rho}_{4\_5}}{V_{4\_5}}\frac{dV_{4\_5}}{d\hat{t}}-\frac{(D_{oil,air})_{4\_5}A_{4\_5}}{NL_{4\_5,groove}V_{4\_5}}(v_{4\_5}-\hat{\rho}_{4\_5})l_{4\_5}$$
$$-\left\{\begin{array}{l}\dfrac{mf_{4,groove\_surface}}{mf_{4\_5,groove\_surface}}\dfrac{\rho_{air,4}}{\rho_{air,4\_5}}\dfrac{\hat{\rho}_4}{V_{4\_5}}\dfrac{dV_{4\to5}}{d\hat{t}}(\dot{V}_{4\to5}\geq 0)\\ \dfrac{\hat{\rho}_{4\_5}}{V_{4\_5}}\dfrac{dV_{4\to5}}{d\hat{t}}(\dot{V}_{4\to5}\leq 0)\end{array}\right\}$$
$$+\left\{\begin{array}{l}\dfrac{\hat{\rho}_{4\_5}}{V_{4\_5}}\dfrac{dV_{4\to5}}{d\hat{t}}(\dot{V}_{4\to5}\geq 0)\\ \dfrac{mf_{5,land\_surface}}{mf_{4\_5,groove\_surface}}\dfrac{\rho_{air,5}}{\rho_{air,4\_5}}\dfrac{\hat{\rho}_5}{V_{4\_5}}\dfrac{dV_{4\to5}}{d\hat{t}}(\dot{V}_{4\to5}\leq 0)\end{array}\right\}$$
$$-\left\{\begin{array}{l}\dfrac{mf_{4,groove\_surface}}{mf_{4\_5,groove\_surface}}\dfrac{\rho_{air,4}}{\rho_{air,4\_5}}\dfrac{\hat{\rho}_4}{V_{4\_5}}\dfrac{dV_{4\to4\_5,pump}}{d\hat{t}}(\dot{V}_{4\to4\_5,pump}\geq 0)\\ \dfrac{\hat{\rho}_{4\_5}}{V_{4\_5}}\dfrac{dV_{4\to4\_5,pump}}{d\hat{t}}(\dot{V}_{4\to4\_5,pump}\leq 0)\end{array}\right\}$$
$$-\left\{\begin{array}{l}\dfrac{mf_{5,land\_surface}}{mf_{4\_5,groove\_surface}}\dfrac{\rho_{air,5}}{\rho_{air,4\_5}}\dfrac{\hat{\rho}_5}{V_{4\_5}}\dfrac{dV_{5\to4\_5,pump}}{d\hat{t}}(\dot{V}_{5\to4\_5,pump}\geq 0)\\ \dfrac{\hat{\rho}_{4\_5}}{V_{4\_5}}\dfrac{dV_{5\to4\_5,pump}}{d\hat{t}}(\dot{V}_{5\to4\_5,pump}\leq 0)\end{array}\right\}=0 \qquad \textbf{(2.104)}$$

For the region 5,

$$\frac{d\hat{\rho}_5}{d\hat{t}} + \frac{\hat{\rho}_5}{V_5}\frac{dV_5}{d\hat{t}} - \frac{(D_{oil,air})_5 A_{5,land}}{NL_{5,land}V_5}(v_{5,land} - \hat{\rho}_5)l_{5,land}$$

$$- \frac{(D_{oil,air})_5 A_{5,liner}}{NL_{5,liner}V_5}\left(\frac{mf_{5,liner\_surface}}{mf_{5,land\_surface}}v_{1,liner} - \hat{\rho}_5\right)l_{5,liner}$$

$$- \left\{\begin{array}{l} \dfrac{mf_{3,land\_surface}}{mf_{5,land\_surface}}\dfrac{\rho_{air,3}}{\rho_{air,5}}\dfrac{\hat{\rho}_3}{V_5}\dfrac{dV_{3\to5}}{d\hat{t}}(\dot{V}_{3\to5} \geq 0) \\ \dfrac{\hat{\rho}_5}{V_5}\dfrac{dV_{3\to5}}{d\hat{t}}(\dot{V}_{3\to5} \leq 0) \end{array}\right\}$$

$$- \left\{\begin{array}{l} \dfrac{mf_{4\_5,groove\_surface}}{mf_{5,land\_surface}}\dfrac{\rho_{air,4\_5}}{\rho_{air,5}}\dfrac{\hat{\rho}_{4\_5}}{V_5}\dfrac{dV_{4\to5}}{d\hat{t}}(\dot{V}_{4\to5} \geq 0) \\ \dfrac{\hat{\rho}_5}{V_5}\dfrac{dV_{4\to5}}{d\hat{t}}(\dot{V}_{4\to5} \leq 0) \end{array}\right\}$$

$$+ \left\{\begin{array}{l} \dfrac{\hat{\rho}_5}{V_5}\dfrac{dV_{5\to6}}{d\hat{t}}(\dot{V}_{5\to6} \geq 0) \\ \dfrac{\hat{\rho}_6}{mf_{5,land\_surface}\rho_{air,5}V_5}\dfrac{dV_{5\to6}}{d\hat{t}}(\dot{V}_{5\to6} \leq 0) \end{array}\right\}$$

$$+ \left\{\begin{array}{l} \dfrac{\hat{\rho}_5}{V_5}\dfrac{dV_{5\to7}}{d\hat{t}}(\dot{V}_{5\to7} \geq 0) \\ \dfrac{\hat{\rho}_7}{mf_{5,land\_surface}\rho_{air,5}V_5}\dfrac{dV_{5\to7}}{d\hat{t}}(\dot{V}_{5\to7} \leq 0) \end{array}\right\}$$

$$+ \left\{\begin{array}{l} \dfrac{\hat{\rho}_5}{V_5}\dfrac{dV_{5\to4\_5,pump}}{d\hat{t}}(\dot{V}_{5\to4\_5,pump} \geq 0) \\ \dfrac{mf_{4\_5,groove\_surface}}{mf_{5,land\_surface}}\dfrac{\rho_{air,4\_5}}{\rho_{air,5}}\dfrac{\hat{\rho}_{4\_5}}{V_{15}}\dfrac{dV_{5\to4\_5,pump}}{d\hat{t}}(\dot{V}_{5\to4\_5,pump} \leq 0) \end{array}\right\} = 0 \qquad \textbf{(2.105)}$$

2.3.5. Discretized Equations

The normalized equations in section 2.3.4 were then discretized. The disretized equations are based on the time step $\Delta\hat{t} = \frac{1}{360}$. An implicit method was used in order to achieve numerical stability.

For example, for the rate of change of oil vapor density in the region 1,

$$\frac{d\hat{\rho}_1}{d\hat{t}} \approx \frac{\hat{\rho}_1(\hat{t}) - \hat{\rho}_1(\hat{t} - \Delta\hat{t})}{\Delta\hat{t}} \tag{2.106}$$

and, for the rate of change of volume in the region 1,

$$\frac{dV_1}{d\hat{t}} \approx \frac{V_1(\hat{t}) - V_1(\hat{t} - \Delta\hat{t})}{\Delta\hat{t}} \tag{2.107}$$

Other time-dependent quantities such as the pressure-driven volume flow rate $\dot{V}_{0\to1}$, and the pumping flow rate $\dot{V}_{1\to1\_2,pump}$ at a certain time or a crank angle during the engine operation, were calculated by the existing ring dynamics model.

The following discretized equations were used for the numerical calculation.

For the region 1,

$$(1 + A_{11}^{(1)} + A_{11,pump} + A_{11}^{(2)} + A_{11}^{(3)} + A_{11}^{(4)}) \cdot \hat{\rho}_1(\hat{t}) + (A_{12}^{(1)} + A_{12,pump}) \cdot \hat{\rho}_{1\_2}(\hat{t}) + A_{15} \cdot \hat{\rho}_3(\hat{t}) = B_1 \tag{2.108}$$

$$A_{11}^{(1)} = \frac{1}{V_1}\frac{dV_1}{d\hat{t}}\Delta\hat{t} + \frac{(D_{oil,air})_1 \cdot A_{1,land}}{NL_{1,land}V_1}\Delta\hat{t} \cdot l_{1,land} + \frac{(D_{oil,air})_1 \cdot A_{1,liner}}{NL_{1,liner}V_1}\Delta\hat{t} \cdot l_{1,liner} \tag{2.109}$$

$$A_{11}^{(2)} = \begin{Bmatrix} 0(\dot{V}_{0\to 1} \geq 0) \\ -\frac{1}{V_1}\frac{dV_{0\to 1}}{d\hat{t}}\Delta\hat{t}(\dot{V}_{0\to 1} \leq 0) \end{Bmatrix} \quad \textbf{(2.110)}$$

$$A_{11}^{(3)} = \begin{Bmatrix} \frac{1}{V_1}\frac{dV_{1\to 2}}{d\hat{t}}\Delta\hat{t}(\dot{V}_{1\to 2} \geq 0) \\ 0(\dot{V}_{1\to 2} \leq 0) \end{Bmatrix} \quad \textbf{(2.111)}$$

$$A_{11,pump} = \begin{Bmatrix} \frac{1}{V_1}\frac{dV_{1\to 1\_2,pump}}{d\hat{t}}\Delta\hat{t}(\dot{V}_{1\to 1\_2,pump} \geq 0) \\ 0(\dot{V}_{1\to 1\_2,pump} \leq 0) \end{Bmatrix} \quad \textbf{(2.112)}$$

$$A_{11}^{(4)} = \begin{Bmatrix} \frac{1}{V_1}\frac{dV_{1\to 3}}{d\hat{t}}\Delta\hat{t}(\dot{V}_{1\to 3} \geq 0) \\ 0(\dot{V}_{1\to 3} \leq 0) \end{Bmatrix} \quad \textbf{(2.113)}$$

$$A_{12}^{(1)} = \begin{Bmatrix} 0(\dot{V}_{1\to 2} \geq 0) \\ \frac{mf_{1\_2,groove\_surface}}{mf_{1,land\_surface}}\frac{\rho_{air,1\_2}}{\rho_{air,1}}\frac{1}{V_1}\frac{dV_{1\to 2}}{d\hat{t}}\Delta\hat{t}(\dot{V}_{1\to 2} \leq 0) \end{Bmatrix} \quad \textbf{(2.114)}$$

$$A_{12,pump} = \begin{Bmatrix} 0(\dot{V}_{1\to 1\_2,pump} \geq 0) \\ \frac{mf_{1\_2,groove\_surface}}{mf_{1,land\_surface}}\frac{\rho_{air,1\_2}}{\rho_{air,1}}\frac{1}{V_1}\frac{dV_{1\to 1\_2,pump}}{d\hat{t}}\Delta\hat{t}(\dot{V}_{1\to 1\_2,pump} \leq 0) \end{Bmatrix} \quad \textbf{(2.115)}$$

$$A_{15} = \begin{Bmatrix} 0(\dot{V}_{1\to 3} \geq 0) \\ \frac{mf_{3,land\_surface}}{mf_{1,land\_surface}}\frac{\rho_{air,3}}{\rho_{air,1}}\frac{1}{V_1}\frac{dV_{1\to 3}}{d\hat{t}}\Delta\hat{t}(\dot{V}_{1\to 3} \leq 0) \end{Bmatrix} \quad \textbf{(2.116)}$$

$$B_1 = \hat{\rho}_1(\hat{t} - \Delta\hat{t}) + \frac{(D_{oil,air})_1 A_{1,land} \cdot v_{1,land} \cdot l_{1,land}}{NL_{1,land} V_1} \Delta\hat{t} + \frac{mf_{1,liner\_surface}}{mf_{1,land\_surface}} \frac{(D_{oil,air})_1 A_{1,liner} \cdot v_{1,liner} \cdot l_{1,liner}}{NL_{1,liner} V_1} \Delta\hat{t} \tag{2.117}$$

For the region 1_2,

$$\begin{aligned}&(A_{21}^{(1)} + A_{21,pump}) \cdot \hat{\rho}_1(\hat{t}) + (1 + A_{22}^{(1)} + A_{22}^{(2)} + A_{22,pump1} + A_{22,pump2}) \cdot \hat{\rho}_{1\_2}(\hat{t}) \\ &+ (A_{23}^{(1)} + A_{23,pump}) \cdot \hat{\rho}_2(\hat{t}) = B_2\end{aligned} \tag{2.118}$$

$$A_{21}^{(1)} = \left\{ \begin{array}{l} -\frac{mf_{1,land\_surface}}{mf_{1\_2,groove\_suface}} \frac{\rho_{air,1}}{\rho_{air,1\_2}} \frac{1}{V_{1\_2}} \frac{dV_{1\to 2}}{d\hat{t}} \Delta\hat{t} (\dot{V}_{1\to 2} \geq 0) \\ 0 (\dot{V}_{1\to 2} \leq 0) \end{array} \right\} \tag{2.119}$$

$$A_{21,pump} = \left\{ \begin{array}{l} -\frac{mf_{1,land\_surface}}{mf_{1\_2,groove\_suface}} \frac{\rho_{air,1}}{\rho_{air,1\_2}} \frac{1}{V_{1\_2}} \frac{dV_{1\to 1\_2,pump}}{d\hat{t}} \Delta\hat{t} (\dot{V}_{1\to 1\_2,pump} \geq 0) \\ 0 (\dot{V}_{1\to 1\_2,pump} \leq 0) \end{array} \right\} \tag{2.120}$$

$$A_{22}^{(1)} = \frac{1}{V_{1\_2}} \frac{dV_{1\_2}}{d\hat{t}} \Delta\hat{t} + \frac{(D_{oil,air})_{1\_2} A_{1\_2} \cdot l_{1\_2}}{NL_{1\_2} V_{1\_2}} \Delta\hat{t} \tag{2.121}$$

$$A_{22}^{(2)} = \left\{ \begin{array}{l} \frac{1}{V_{1\_2}} \frac{dV_{1\to 2}}{d\hat{t}} \Delta\hat{t} (\dot{V}_{1\to 2} \geq 0) \\ -\frac{1}{V_{1\_2}} \frac{dV_{1\to 2}}{d\hat{t}} \Delta\hat{t} (\dot{V}_{1\to 2} \leq 0) \end{array} \right\} \tag{2.122}$$

$$A_{22,pump1} = \left\{ \begin{array}{l} 0 (\dot{V}_{1\to 1\_2,pump} \geq 0) \\ -\frac{1}{V_{1\_2}} \frac{dV_{1\to 1\_2,pump}}{d\hat{t}} \Delta\hat{t} (\dot{V}_{1\to 1\_2,pump} \leq 0) \end{array} \right\} \tag{2.123}$$

$$A_{22,pump2} = \begin{Bmatrix} 0(\dot{V}_{2\to 1\_2,pump} \geq 0) \\ -\frac{1}{V_{1\_2}} \frac{dV_{2\to 1\_2,pump}}{d\hat{t}} \Delta\hat{t}(\dot{V}_{2\to 1\_2,pump} \leq 0) \end{Bmatrix} \quad \textbf{(2.124)}$$

$$A_{23}^{(1)} = \begin{Bmatrix} 0(\dot{V}_{1\to 2} \geq 0) \\ \frac{mf_{2,groove\_surface}}{mf_{1\_2,groove\_surface}} \frac{\rho_{air,2}}{\rho_{air,1\_2}} \frac{1}{V_{1\_2}} \frac{dV_{1\to 2}}{d\hat{t}} \Delta\hat{t}(\dot{V}_{1\to 2} \leq 0) \end{Bmatrix} \quad \textbf{(2.125)}$$

$$A_{23,pump} = \begin{Bmatrix} -\frac{mf_{2,groove\_surface}}{mf_{1\_2,groove\_surface}} \frac{\rho_{air,2}}{\rho_{air,1\_2}} \frac{1}{V_{1\_2}} \frac{dV_{2\to 1\_2,pump}}{d\hat{t}} \Delta\hat{t}(\dot{V}_{2\to 1\_2,pump} \geq 0) \\ 0(\dot{V}_{2\to 1\_2,pump} \leq 0) \end{Bmatrix} \quad \textbf{(2.126)}$$

$$B_2 = \hat{\rho}_{1\_2}(\hat{t} - \Delta\hat{t}) + \frac{(D_{oil,air})_{1\_2} A_{1\_2} \cdot v_{1\_2} \cdot l_{1\_2}}{NL_{1\_2} V_{1\_2}} \Delta\hat{t} \quad \textbf{(2.127)}$$

For the region 2,

$$\begin{aligned} &(A_{32}^{(1)} + A_{32,pump}) \cdot \hat{\rho}_{1\_2}(\hat{t}) + (1 + A_{33}^{(1)} + A_{33}^{(2)} + A_{33}^{(3)} + A_{33,pump1} + A_{33,pump2}) \cdot \hat{\rho}_2(\hat{t}) \\ &+ (A_{34}^{(1)} + A_{34,pump}) \cdot \hat{\rho}_{2\_3}(\hat{t}) = B_3 \end{aligned} \quad \textbf{(2.128)}$$

$$A_{32}^{(1)} = \begin{Bmatrix} -\frac{mf_{1\_2,groove\_surface}}{mf_{2,groove\_suface}} \frac{\rho_{air,1\_2}}{\rho_{air,2}} \frac{1}{V_2} \frac{dV_{1\to 2}}{d\hat{t}} \Delta\hat{t}(\dot{V}_{1\to 2} \geq 0) \\ 0(\dot{V}_{1\to 2} \leq 0) \end{Bmatrix} \quad \textbf{(2.129)}$$

$$A_{32,pump} = \begin{Bmatrix} 0(\dot{V}_{2\to 1\_2,pump} \geq 0) \\ \frac{mf_{1\_2,groove\_surface}}{mf_{2,groove\_suface}} \frac{\rho_{air,1\_2}}{\rho_{air,2}} \frac{1}{V_2} \frac{dV_{2\to 1\_2,pump}}{d\hat{t}} \Delta\hat{t}(\dot{V}_{2\to 1\_2,pump} \leq 0) \end{Bmatrix} \quad \textbf{(2.130)}$$

$$A_{33}^{(1)} = \frac{1}{V_2}\frac{dV_2}{d\hat{t}}\Delta\hat{t} + \frac{(D_{oil,air})_2 A_{2,groove}\cdot l_2}{NL_{2,groove}V_2}\Delta\hat{t} \tag{2.131}$$

$$A_{33}^{(2)} = \begin{Bmatrix} 0(\dot{V}_{1\to 2} \geq 0) \\ -\frac{1}{V_2}\frac{dV_{1\to 2}}{d\hat{t}}\Delta\hat{t}(\dot{V}_{1\to 2} \leq 0) \end{Bmatrix} \tag{2.132}$$

$$A_{33}^{(3)} = \begin{Bmatrix} \frac{1}{V_2}\frac{dV_{2\to 3}}{d\hat{t}}\Delta\hat{t}(\dot{V}_{2\to 3} \geq 0) \\ 0(\dot{V}_{2\to 3} \leq 0) \end{Bmatrix} \tag{2.133}$$

$$A_{33,pump1} = \begin{Bmatrix} \frac{1}{V_2}\frac{dV_{2\to 1\_2,pump}}{d\hat{t}}\Delta\hat{t}(\dot{V}_{2\to 1\_2,pump} \geq 0) \\ 0(\dot{V}_{2\to 1\_2,pump} \leq 0) \end{Bmatrix} \tag{2.134}$$

$$A_{33,pump2} = \begin{Bmatrix} \frac{1}{V_2}\frac{dV_{2\to 2\_3,pump}}{d\hat{t}}\Delta\hat{t}(\dot{V}_{2\to 2\_3,pump} \geq 0) \\ 0(\dot{V}_{2\to 2\_3,pump} \leq 0) \end{Bmatrix} \tag{2.135}$$

$$A_{34}^{(1)} = \begin{Bmatrix} 0(\dot{V}_{2\to 3} \geq 0) \\ \frac{mf_{2\_3,groove\_surface}}{mf_{2,groove\_surface}}\frac{\rho_{air,2\_3}}{\rho_{air,2}}\frac{1}{V_2}\frac{dV_{2\to 3}}{d\hat{t}}\Delta\hat{t}(\dot{V}_{2\to 3} \leq 0) \end{Bmatrix} \tag{2.136}$$

$$A_{34,pump} = \begin{Bmatrix} 0(\dot{V}_{2\to 2\_3,pump} \geq 0) \\ \frac{mf_{2\_3,groove\_surface}}{mf_{2,groove\_surface}}\frac{\rho_{air,2\_3}}{\rho_{air,2}}\frac{1}{V_2}\frac{dV_{2\to 2\_3,pump}}{d\hat{t}}\Delta\hat{t}(\dot{V}_{2\to 2\_3,pump} \leq 0) \end{Bmatrix} \tag{2.137}$$

$$B_3 = \hat{\rho}_2(\hat{t} - \Delta\hat{t}) + \frac{(D_{oil,air})_2 A_{2,groove}\cdot v_2 \cdot l_2}{NL_{2,groove}V_2}\Delta\hat{t} \tag{2.138}$$

For the region 2_3,

$$(A_{43}^{(1)} + A_{43,pump})\hat{\rho}_2(\hat{t}) + (1 + A_{44}^{(1)} + A_{44}^{(2)} + A_{44,pump1} + A_{44,pump2})\hat{\rho}_{2\_3}(\hat{t}) + (A_{45}^{(1)} + A_{45,pump})\hat{\rho}_3(\hat{t}) = B_4 \tag{2.139}$$

$$A_{43}^{(1)} = \begin{Bmatrix} -\dfrac{mf_{2,groove\_surface}}{mf_{2\_3,groove\_suface}} \dfrac{\rho_{air,2}}{\rho_{air,2\_3}} \dfrac{1}{V_{2\_3}} \dfrac{dV_{2\to3}}{d\hat{t}} \Delta\hat{t}(\dot{V}_{2\to3} \geq 0) \\ 0(\dot{V}_{2\to3} \leq 0) \end{Bmatrix} \tag{2.140}$$

$$A_{43,pump} = \begin{Bmatrix} -\dfrac{mf_{2,groove\_surface}}{mf_{2\_3,groove\_suface}} \dfrac{\rho_{air,2}}{\rho_{air,2\_3}} \dfrac{1}{V_{2\_3}} \dfrac{dV_{2\to2\_3,pump}}{d\hat{t}} \Delta\hat{t}(\dot{V}_{2\to2\_3,pump} \geq 0) \\ 0(\dot{V}_{2\to2\_3,pump} \leq 0) \end{Bmatrix} \tag{2.141}$$

$$A_{44}^{(1)} = \frac{1}{V_{2\_3}} \frac{dV_{2\_3}}{d\hat{t}} \Delta\hat{t} + \frac{(D_{oil,air})_{2\_3} A_{2\_3} \cdot l_{2\_3}}{NL_{2\_3} V_{2\_3}} \Delta\hat{t} \tag{2.142}$$

$$A_{44}^{(2)} = \begin{Bmatrix} \dfrac{1}{V_{2\_3}} \dfrac{dV_{2\to3}}{d\hat{t}} \Delta\hat{t}(\dot{V}_{2\to3} \geq 0) \\ -\dfrac{1}{V_{2\_3}} \dfrac{dV_{2\to3}}{d\hat{t}} \Delta\hat{t}(\dot{V}_{2\to3} \leq 0) \end{Bmatrix} \tag{2.143}$$

$$A_{44,pump1} = \begin{Bmatrix} 0(\dot{V}_{2\to2\_3,pump} \geq 0) \\ -\dfrac{1}{V_{2\_3}} \dfrac{dV_{2\to2\_3,pump}}{d\hat{t}} \Delta\hat{t}(\dot{V}_{2\to2\_3,pump} \leq 0) \end{Bmatrix} \tag{2.144}$$

$$A_{44,pump2} = \begin{Bmatrix} 0(\dot{V}_{3\to2\_3,pump} \geq 0) \\ -\dfrac{1}{V_{2\_3}} \dfrac{dV_{3\to2\_3,pump}}{d\hat{t}} \Delta\hat{t}(\dot{V}_{3\to2\_3,pump} \leq 0) \end{Bmatrix} \tag{2.145}$$

$$A_{45}^{(1)} = \begin{Bmatrix} 0(\dot{V}_{2\to3} \geq 0) \\ \dfrac{mf_{3,land\_surface}}{mf_{2\_3,groove\_surface}} \dfrac{\rho_{air,3}}{\rho_{air,2\_3}} \dfrac{1}{V_{2\_3}} \dfrac{dV_{2\to3}}{d\hat{t}} \Delta\hat{t}(\dot{V}_{2\to3} \leq 0) \end{Bmatrix} \quad \textbf{(2.146)}$$

$$A_{45,pump} = \begin{Bmatrix} -\dfrac{mf_{3,land\_surface}}{mf_{2\_3,groove\_surface}} \dfrac{\rho_{air,3}}{\rho_{air,2\_3}} \dfrac{1}{V_{2\_3}} \dfrac{dV_{3\to2\_3,pump}}{d\hat{t}} \Delta\hat{t}(\dot{V}_{3\to2\_3,pump} \geq 0) \\ 0(\dot{V}_{3\to2\_3,pump} \leq 0) \end{Bmatrix} \quad \textbf{(2.147)}$$

$$B_4 = \hat{\rho}_{2\_3}(\hat{t} - \Delta\hat{t}) + \frac{(D_{oil,air})_{2\_3} A_{2\_3} \cdot v_{2\_3} \cdot l_{2\_3}}{NL_{2\_3} V_{2\_3}} \Delta\hat{t} \quad \textbf{(2.148)}$$

For the region 3,

$$A_{51}\hat{\rho}_1(\hat{t}) + (A_{54}^{(1)} + A_{54,pump})\hat{\rho}_{2\_3}(\hat{t}) + (1 + A_{55}^{(1)} + A_{55}^{(2)} + A_{55}^{(3)} + A_{55}^{(4)} + A_{55}^{(5)} + A_{55,pump1} + A_{55,pump2})\hat{\rho}_3(\hat{t}) + (A_{56}^{(1)} + A_{56,pump})\hat{\rho}_{3\_4}(\hat{t}) + A_{59}\hat{\rho}_5(\hat{t}) = 0 \quad \textbf{(2.149)}$$

$$A_{51} = \begin{Bmatrix} -\dfrac{mf_{1,land\_surface}}{mf_{3,land\_surface}} \dfrac{\rho_{air,1}}{\rho_{air,3}} \dfrac{1}{V_3} \dfrac{dV_{1\to3}}{d\hat{t}} \Delta\hat{t}(\dot{V}_{1\to3} \geq 0) \\ 0(\dot{V}_{1\to3} \leq 0) \end{Bmatrix} \quad \textbf{(2.150)}$$

$$A_{54}^{(1)} = \begin{Bmatrix} -\dfrac{mf_{2\_3,groove\_surface}}{mf_{3,land\_surface}} \dfrac{\rho_{air,2\_3}}{\rho_{air,3}} \dfrac{1}{V_3} \dfrac{dV_{2\to3}}{d\hat{t}} \Delta\hat{t}(\dot{V}_{2\to3} \geq 0) \\ 0(\dot{V}_{2\to3} \leq 0) \end{Bmatrix} \quad \textbf{(2.151)}$$

$$A_{54,pump} = \begin{Bmatrix} 0(\dot{V}_{3\to2\_3,pump} \geq 0) \\ \dfrac{mf_{2\_3,groove\_surface}}{mf_{3,land\_surface}} \dfrac{\rho_{air,2\_3}}{\rho_{air,3}} \dfrac{1}{V_3} \dfrac{dV_{3\to2\_3,pump}}{d\hat{t}} \Delta\hat{t}(\dot{V}_{3\to2\_3,pump} \leq 0) \end{Bmatrix} \quad \textbf{(2.152)}$$

$$A_{55}^{(1)} = \frac{1}{V_3}\frac{dV_3}{d\hat{t}}\Delta\hat{t} + \frac{(D_{oil,air})_3 \cdot A_{3,land}}{NL_{3,land}V_3}\Delta\hat{t}\cdot l_{3,land} + \frac{(D_{oil,air})_3 \cdot A_{3,liner}}{NL_{3,liner}V_3}\Delta\hat{t}\cdot l_{3,liner} \quad \textbf{(2.153)}$$

$$A_{55}^{(2)} = \begin{Bmatrix} 0(\dot{V}_{1\to3} \geq 0) \\ -\frac{1}{V_3}\frac{dV_{1\to3}}{d\hat{t}}\Delta\hat{t}(\dot{V}_{1\to3} \leq 0) \end{Bmatrix} \quad \textbf{(2.154)}$$

$$A_{55}^{(3)} = \begin{Bmatrix} 0(\dot{V}_{2\to3} \geq 0) \\ -\frac{1}{V_3}\frac{dV_{2\to3}}{d\hat{t}}\Delta\hat{t}(\dot{V}_{2\to3} \leq 0) \end{Bmatrix} \quad \textbf{(2.155)}$$

$$A_{55}^{(4)} = \begin{Bmatrix} \frac{1}{V_3}\frac{dV_{3\to4}}{d\hat{t}}\Delta\hat{t}(\dot{V}_{3\to4} \geq 0) \\ 0(\dot{V}_{3\to4} \leq 0) \end{Bmatrix} \quad \textbf{(2.156)}$$

$$A_{55}^{(5)} = \begin{Bmatrix} \frac{1}{V_3}\frac{dV_{3\to5}}{d\hat{t}}\Delta\hat{t}(\dot{V}_{3\to5} \geq 0) \\ 0(\dot{V}_{3\to5} \leq 0) \end{Bmatrix} \quad \textbf{(2.157)}$$

$$A_{55,pump1} = \begin{Bmatrix} \frac{1}{V_3}\frac{dV_{3\to2\_3,pump}}{d\hat{t}}\Delta\hat{t}(\dot{V}_{3\to2\_3,pump} \geq 0) \\ 0(\dot{V}_{3\to2\_3,pump} \leq 0) \end{Bmatrix} \quad \textbf{(2.158)}$$

$$A_{55,pump2} = \begin{Bmatrix} \frac{1}{V_3}\frac{dV_{3\to3\_4,pump}}{d\hat{t}}\Delta\hat{t}(\dot{V}_{3\to3\_4,pump} \geq 0) \\ 0(\dot{V}_{3\to3\_4,pump} \leq 0) \end{Bmatrix} \quad \textbf{(2.159)}$$

$$A_{56}^{(1)} = \begin{Bmatrix} 0(\dot{V}_{3\to4} \geq 0) \\ \frac{mf_{3\_4,groove\_surface}}{mf_{3,land\_surface}}\frac{\rho_{air,3\_4}}{\rho_{air,3}}\frac{1}{V_3}\frac{dV_{3\to4}}{d\hat{t}}\Delta\hat{t}(\dot{V}_{3\to4} \leq 0) \end{Bmatrix} \quad \textbf{(2.160)}$$

$$A_{56,pump} = \begin{Bmatrix} 0(\dot{V}_{3\to 3\_4,pump} \geq 0) \\ \frac{mf_{3\_4,groove\_surface}}{mf_{3,land\_surface}} \frac{\rho_{air,3\_4}}{\rho_{air,3}} \frac{1}{V_3} \frac{dV_{3\to 3\_4,pump}}{d\hat{t}} \Delta\hat{t}(\dot{V}_{3\to 3\_4,pump} \leq 0) \end{Bmatrix} \quad \textbf{(2.161)}$$

$$A_{59} = \begin{Bmatrix} 0(\dot{V}_{3\to 5} \geq 0) \\ \frac{mf_{5,land\_surface}}{mf_{3,land\_surface}} \frac{\rho_{air,5}}{\rho_{air,3}} \frac{1}{V_3} \frac{dV_{3\to 5}}{d\hat{t}} \Delta\hat{t}(\dot{V}_{3\to 5} \leq 0) \end{Bmatrix} \quad \textbf{(2.162)}$$

$$B_5 = \hat{\rho}_3(\hat{t} - \Delta\hat{t}) + \frac{(D_{oil,air})_3 A_{3,land} \cdot v_{3,land} \cdot l_{3,land}}{NL_{3,land} V_3} \Delta\hat{t} + \frac{mf_{3,liner\_surface}}{mf_{3,land\_surface}} \frac{(D_{oil,air})_3 A_{3,liner} \cdot v_{3,liner} \cdot l_{3,liner}}{NL_{3,liner} V_3} \Delta\hat{t}$$

$$\textbf{(2.163)}$$

For the region 3_4,

$$\begin{aligned} &(A_{65}^{(1)} + A_{65,pump}) \cdot \hat{\rho}_3(\hat{t}) + (1 + A_{66}^{(1)} + A_{66}^{(2)} + A_{66,pump1} + A_{66,pump2}) \cdot \hat{\rho}_{3\_4}(\hat{t}) \\ &+ (A_{67}^{(1)} + A_{67,pump}) \cdot \hat{\rho}_4(\hat{t}) = B_6 \end{aligned} \quad \textbf{(2.164)}$$

$$A_{65}^{(1)} = \begin{Bmatrix} -\frac{mf_{3,land\_surface}}{mf_{3\_4,groove\_suface}} \frac{\rho_{air,3}}{\rho_{air,3\_4}} \frac{1}{V_{3\_4}} \frac{dV_{3\to 4}}{d\hat{t}} \Delta\hat{t}(\dot{V}_{3\to 4} \geq 0) \\ 0(\dot{V}_{3\to 4} \leq 0) \end{Bmatrix} \quad \textbf{(2.165)}$$

$$A_{65,pump} = \begin{Bmatrix} -\frac{mf_{3,land\_surface}}{mf_{3\_4,groove\_suface}} \frac{\rho_{air,3}}{\rho_{air,3\_4}} \frac{1}{V_{3\_4}} \frac{dV_{3\to 3\_4,pump}}{d\hat{t}} \Delta\hat{t}(\dot{V}_{3\to 3\_4,pump} \geq 0) \\ 0(\dot{V}_{3\to 3\_4,pump} \leq 0) \end{Bmatrix} \quad \textbf{(2.166)}$$

$$A_{66}^{(1)} = \frac{1}{V_{3\_4}} \frac{dV_{3\_4}}{d\hat{t}} \Delta\hat{t} + \frac{(D_{oil,air})_{3\_4} A_{3\_4} \cdot l_{3\_4}}{NL_{3\_4} V_{3\_4}} \Delta\hat{t} \quad \textbf{(2.167)}$$

$$A_{66}^{(2)} = \left\{ \begin{array}{l} \dfrac{1}{V_{3\_4}} \dfrac{dV_{3\to4}}{d\hat{t}} \Delta\hat{t} (\dot{V}_{3\to4} \geq 0) \\ -\dfrac{1}{V_{3\_4}} \dfrac{dV_{3\to4}}{d\hat{t}} \Delta\hat{t} (\dot{V}_{3\to4} \leq 0) \end{array} \right\} \tag{2.168}$$

$$A_{66,pump1} = \left\{ \begin{array}{l} 0 (\dot{V}_{3\to3\_4,pump} \geq 0) \\ -\dfrac{1}{V_{3\_4}} \dfrac{dV_{3\to3\_4,pump}}{d\hat{t}} \Delta\hat{t} (\dot{V}_{3\to3\_4,pump} \leq 0) \end{array} \right\} \tag{2.169}$$

$$A_{66,pump2} = \left\{ \begin{array}{l} 0 (\dot{V}_{4\to3\_4,pump} \geq 0) \\ -\dfrac{1}{V_{3\_4}} \dfrac{dV_{4\to3\_4,pump}}{d\hat{t}} \Delta\hat{t} (\dot{V}_{4\to3\_4,pump} \leq 0) \end{array} \right\} \tag{2.170}$$

$$A_{67}^{(1)} = \left\{ \begin{array}{l} 0 (\dot{V}_{3\to4} \geq 0) \\ \dfrac{mf_{4,groove\_surface}}{mf_{3\_4,groove\_surface}} \dfrac{\rho_{air,4}}{\rho_{air,3\_4}} \dfrac{1}{V_{3\_4}} \dfrac{dV_{3\to4}}{d\hat{t}} \Delta\hat{t} (\dot{V}_{3\to4} \leq 0) \end{array} \right\} \tag{2.171}$$

$$A_{67,pump} = \left\{ \begin{array}{l} -\dfrac{mf_{4,groove\_surface}}{mf_{3\_4,groove\_surface}} \dfrac{\rho_{air,4}}{\rho_{air,3\_4}} \dfrac{1}{V_{3\_4}} \dfrac{dV_{4\to3\_4,pump}}{d\hat{t}} \Delta\hat{t} (\dot{V}_{4\to3\_4,pump} \geq 0) \\ 0 (\dot{V}_{4\to3\_4,pump} \leq 0) \end{array} \right\} \tag{2.172}$$

$$B_6 = \hat{\rho}_{3\_4} (\hat{t} - \Delta\hat{t}) + \frac{(D_{oil,air})_{3\_4} A_{3\_4} \cdot v_{3\_4} \cdot l_{3\_4}}{NL_{3\_4} V_{3\_4}} \Delta\hat{t} \tag{2.173}$$

For the region 4,

$$\begin{aligned} &(A_{76}^{(1)} + A_{76,pump}) \cdot \hat{\rho}_{3\_4} (\hat{t}) + (1 + A_{77}^{(1)} + A_{77}^{(2)} + A_{77}^{(3)} + A_{77,pump1} + A_{77,pump2}) \cdot \hat{\rho}_4 (\hat{t}) \\ &+ (A_{78}^{(1)} + A_{78,pump}) \cdot \hat{\rho}_{4\_5} (\hat{t}) = B_7 \end{aligned} \tag{2.174}$$

$$A_{76}^{(1)} = \left\{ \begin{array}{l} -\dfrac{mf_{3\_4,groove\_surface}}{mf_{4,groove\_suface}} \dfrac{\rho_{air,3\_4}}{\rho_{air,4}} \dfrac{1}{V_4} \dfrac{dV_{3\to4}}{d\hat{t}} \Delta\hat{t} (\dot{V}_{3\to4} \geq 0) \\ 0(\dot{V}_{3\to4} \leq 0) \end{array} \right\} \tag{2.175}$$

$$A_{76,pump} = \left\{ \begin{array}{l} 0(\dot{V}_{4\to3\_4,pump} \geq 0) \\ \dfrac{mf_{3\_4,groove\_surface}}{mf_{4,groove\_suface}} \dfrac{\rho_{air,3\_4}}{\rho_{air,4}} \dfrac{1}{V_4} \dfrac{dV_{4\to3\_4,pump}}{d\hat{t}} \Delta\hat{t} (\dot{V}_{4\to3\_4,pump} \leq 0) \end{array} \right\} \tag{2.176}$$

$$A_{77}^{(1)} = \frac{1}{V_4} \frac{dV_4}{d\hat{t}} \Delta\hat{t} + \frac{(D_{oil,air})_4 A_{4,groove} \cdot l_4}{NL_{4,groove} V_4} \Delta\hat{t} \tag{2.177}$$

$$A_{77}^{(2)} = \left\{ \begin{array}{l} 0(\dot{V}_{3\to4} \geq 0) \\ -\dfrac{1}{V_4} \dfrac{dV_{3\to4}}{d\hat{t}} \Delta\hat{t} (\dot{V}_{3\to4} \leq 0) \end{array} \right\} \tag{2.178}$$

$$A_{77}^{(3)} = \left\{ \begin{array}{l} \dfrac{1}{V_4} \dfrac{dV_{4\to5}}{d\hat{t}} \Delta\hat{t} (\dot{V}_{4\to5} \geq 0) \\ 0(\dot{V}_{4\to5} \leq 0) \end{array} \right\} \tag{2.179}$$

$$A_{77,pump1} = \left\{ \begin{array}{l} \dfrac{1}{V_4} \dfrac{dV_{4\to3\_4,pump}}{d\hat{t}} \Delta\hat{t} (\dot{V}_{4\to3\_4,pump} \geq 0) \\ 0(\dot{V}_{4\to3\_4,pump} \leq 0) \end{array} \right\} \tag{2.180}$$

$$A_{77,pump2} = \left\{ \begin{array}{l} \dfrac{1}{V_4} \dfrac{dV_{4\to4\_5,pump}}{d\hat{t}} \Delta\hat{t} (\dot{V}_{4\to4\_5,pump} \geq 0) \\ 0(\dot{V}_{4\to4\_5,pump} \leq 0) \end{array} \right\} \tag{2.181}$$

$$A_{78}^{(1)} = \left\{ \begin{array}{l} 0(\dot{V}_{4\to5} \geq 0) \\ \dfrac{mf_{4\_5,groove\_surface}}{mf_{4,groove\_surface}} \dfrac{\rho_{air,4\_5}}{\rho_{air,4}} \dfrac{1}{V_4} \dfrac{dV_{4\to5}}{d\hat{t}} \Delta\hat{t} (\dot{V}_{4\to5} \leq 0) \end{array} \right\} \tag{2.182}$$

$$A_{78,pump} = \left\{ \begin{array}{l} 0(\dot{V}_{4\to 4\_5,pump} \geq 0) \\ \dfrac{mf_{4\_5,groove\_surface}}{mf_{4,groove\_surface}} \dfrac{\rho_{air,4\_5}}{\rho_{air,4}} \dfrac{1}{V_4} \dfrac{dV_{4\to 4\_5,pump}}{d\hat{t}} \Delta\hat{t}(\dot{V}_{4\to 4\_5,pump} \leq 0) \end{array} \right\} \quad \textbf{(2.183)}$$

$$B_7 = \hat{\rho}_4(\hat{t} - \Delta\hat{t}) + \frac{(D_{oil,air})_4 A_{4,groove} \cdot v_4 \cdot l_4}{NL_{4,groove} V_4} \Delta\hat{t} \quad \textbf{(2.184)}$$

For the region 4_5,

$$\begin{array}{l} (A_{87}^{(1)} + A_{87,pump}) \cdot \hat{\rho}_4(\hat{t}) + (1 + A_{88}^{(1)} + A_{88}^{(2)} + A_{88,pump1} + A_{88,pump2}) \cdot \hat{\rho}_{4\_5}(\hat{t}) \\ + (A_{89}^{(1)} + A_{89,pump}) \cdot \hat{\rho}_5(\hat{t}) = B_8 \end{array} \quad \textbf{(2.185)}$$

$$A_{87}^{(1)} = \left\{ \begin{array}{l} -\dfrac{mf_{4,groove\_surface}}{mf_{4\_5,groove\_suface}} \dfrac{\rho_{air,4}}{\rho_{air,4\_5}} \dfrac{1}{V_{4\_5}} \dfrac{dV_{4\to 5}}{d\hat{t}} \Delta\hat{t}(\dot{V}_{4\to 5} \geq 0) \\ 0(\dot{V}_{4\to 5} \leq 0) \end{array} \right\} \quad \textbf{(2.186)}$$

$$A_{87,pump} = \left\{ \begin{array}{l} -\dfrac{mf_{4,groove\_surface}}{mf_{4\_5,groove\_suface}} \dfrac{\rho_{air,4}}{\rho_{air,4\_5}} \dfrac{1}{V_{4\_5}} \dfrac{dV_{4\to 4\_5,pump}}{d\hat{t}} \Delta\hat{t}(\dot{V}_{4\to 4\_5,pump} \geq 0) \\ 0(\dot{V}_{4\to 4\_5,pump} \leq 0) \end{array} \right\} \quad \textbf{(2.187)}$$

$$A_{88}^{(1)} = \frac{1}{V_{4\_5}} \frac{dV_{4\_5}}{d\hat{t}} \Delta\hat{t} + \frac{(D_{oil,air})_{4\_5} A_{4\_5} \cdot l_{4\_5}}{NL_{4\_5} V_{4\_5}} \Delta\hat{t} \quad \textbf{(2.188)}$$

$$A_{88}^{(2)} = \left\{ \begin{array}{l} \dfrac{1}{V_{4\_5}} \dfrac{dV_{4\to 5}}{d\hat{t}} \Delta\hat{t}(\dot{V}_{4\to 5} \geq 0) \\ -\dfrac{1}{V_{4\_5}} \dfrac{dV_{4\to 5}}{d\hat{t}} \Delta\hat{t}(\dot{V}_{4\to 5} \leq 0) \end{array} \right\} \quad \textbf{(2.189)}$$

$$A_{88,pump1} = \left\{ \begin{array}{l} 0(\dot{V}_{4\to 4\_5,pump} \geq 0) \\ -\dfrac{1}{V_{4\_5}} \dfrac{dV_{4\to 4\_5,pump}}{d\hat{t}} \Delta\hat{t}(\dot{V}_{4\to 4\_5,pump} \leq 0) \end{array} \right\} \tag{2.190}$$

$$A_{88,pump2} = \left\{ \begin{array}{l} 0(\dot{V}_{5\to 4\_5,pump} \geq 0) \\ -\dfrac{1}{V_{4\_5}} \dfrac{dV_{5\to 4\_5,pump}}{d\hat{t}} \Delta\hat{t}(\dot{V}_{5\to 4\_5,pump} \leq 0) \end{array} \right\} \tag{2.191}$$

$$A_{89}^{(1)} = \left\{ \begin{array}{l} 0(\dot{V}_{4\to 5} \geq 0) \\ \dfrac{mf_{5,land\_surface}}{mf_{4\_5,groove\_surface}} \dfrac{\rho_{air,5}}{\rho_{air,4\_5}} \dfrac{1}{V_{4\_5}} \dfrac{dV_{4\to 5}}{d\hat{t}} \Delta\hat{t}(\dot{V}_{4\to 5} \leq 0) \end{array} \right\} \tag{2.192}$$

$$A_{89,pump} = \left\{ \begin{array}{l} -\dfrac{mf_{5,land\_surface}}{mf_{4\_5,groove\_surface}} \dfrac{\rho_{air,5}}{\rho_{air,4\_5}} \dfrac{1}{V_{4\_5}} \dfrac{dV_{5\to 4\_5,pump}}{d\hat{t}} \Delta\hat{t}(\dot{V}_{5\to 4\_5,pump} \geq 0) \\ 0(\dot{V}_{5\to 4\_5,pump} \leq 0) \end{array} \right\} \tag{2.193}$$

$$B_8 = \hat{\rho}_{4\_5}(\hat{t} - \Delta\hat{t}) + \frac{(D_{oil,air})_{4\_5} A_{4\_5} \cdot v_{4\_5} \cdot l_{4\_5}}{NL_{4\_5} V_{4\_5}} \Delta\hat{t} \tag{2.194}$$

For the region 5,

$$\begin{aligned} &A_{95}\hat{\rho}_3(\hat{t}) + (A_{98}^{(1)} + A_{98,pump})\hat{\rho}_{4\_5}(\hat{t}) + (1 + A_{99}^{(1)} + A_{99}^{(2)} + A_{99}^{(3)} + A_{99}^{(4)} + A_{99}^{(5)} + A_{99,pump})\hat{\rho}_5(\hat{t}) \\ &= B_9^{(1)} + B_9^{(2)} + B_9^{(3)} \end{aligned} \tag{2.195}$$

$$A_{95} = \left\{ \begin{array}{l} -\dfrac{mf_{3,land\_surface}}{mf_{5,land\_suface}} \dfrac{\rho_{air,3}}{\rho_{air,5}} \dfrac{1}{V_5} \dfrac{dV_{3\to 5}}{d\hat{t}} \Delta\hat{t}(\dot{V}_{3\to 5} \geq 0) \\ 0(\dot{V}_{3\to 5} \leq 0) \end{array} \right\} \tag{2.196}$$

$$A_{98}^{(1)} = \left\{ \begin{array}{l} -\dfrac{mf_{4\_5,groove\_surface}}{mf_{5,land\_suface}} \dfrac{\rho_{air,4\_5}}{\rho_{air,5}} \dfrac{1}{V_5} \dfrac{dV_{4\to5}}{d\hat{t}} \Delta\hat{t} (\dot{V}_{4\to5} \geq 0) \\ 0(\dot{V}_{4\to5} \leq 0) \end{array} \right\} \tag{2.197}$$

$$A_{98,pump} = \left\{ \begin{array}{l} 0(\dot{V}_{5\to4\_5,pump} \geq 0) \\ \dfrac{mf_{4\_5,groove\_surface}}{mf_{5,land\_suface}} \dfrac{\rho_{air,4\_5}}{\rho_{air,5}} \dfrac{1}{V_5} \dfrac{dV_{5\to4\_5,pump}}{d\hat{t}} \Delta\hat{t} (\dot{V}_{5\to4\_5,pump} \leq 0) \end{array} \right\} \tag{2.198}$$

$$A_{99}^{(1)} = \frac{1}{V_5} \frac{dV_5}{d\hat{t}} \Delta\hat{t} + \frac{(D_{oil,air})_5 \cdot A_{5,land}}{NL_{5,land} V_5} \Delta\hat{t} \cdot l_{5,land} + \frac{(D_{oil,air})_5 \cdot A_{5,liner}}{NL_{5,liner} V_5} \Delta\hat{t} \cdot l_{5,liner} \tag{2.199}$$

$$A_{99}^{(2)} = \left\{ \begin{array}{l} 0(\dot{V}_{3\to5} \geq 0) \\ -\dfrac{1}{V_5} \dfrac{dV_{3\to5}}{d\hat{t}} \Delta\hat{t} (\dot{V}_{3\to5} \leq 0) \end{array} \right\} \tag{2.200}$$

$$A_{99}^{(3)} = \left\{ \begin{array}{l} 0(\dot{V}_{4\to5} \geq 0) \\ -\dfrac{1}{V_5} \dfrac{dV_{4\to5}}{d\hat{t}} \Delta\hat{t} (\dot{V}_{4\to5} \leq 0) \end{array} \right\} \tag{2.201}$$

$$A_{99}^{(4)} = \left\{ \begin{array}{l} \dfrac{1}{V_5} \dfrac{dV_{5\to6}}{d\hat{t}} \Delta\hat{t} (\dot{V}_{5\to6} \geq 0) \\ 0(\dot{V}_{5\to6} \leq 0) \end{array} \right\} \tag{2.202}$$

$$A_{99}^{(5)} = \left\{ \begin{array}{l} \dfrac{1}{V_5} \dfrac{dV_{5\to7}}{d\hat{t}} \Delta\hat{t} (\dot{V}_{5\to7} \geq 0) \\ 0(\dot{V}_{5\to7} \leq 0) \end{array} \right\} \tag{2.203}$$

$$A_{99,pump} = \left\{ \begin{array}{l} \dfrac{1}{V_5} \dfrac{dV_{5\to4\_5,pump}}{d\hat{t}} \Delta\hat{t} (\dot{V}_{5\to4\_5,pump} \geq 0) \\ 0(\dot{V}_{5\to4\_5,pump} \leq 0) \end{array} \right\} \tag{2.204}$$

$$B_9^{(1)} = \hat{\rho}_5(\hat{t} - \Delta\hat{t}) + \frac{(D_{oil,air})_5 A_{5,land} \cdot v_{5,land} \cdot l_{5,land}}{NL_{5,land} V_5} \Delta\hat{t} + \frac{mf_{5,liner\_surface}}{mf_{5,land\_surface}} \frac{(D_{oil,air})_5 A_{5,liner} \cdot v_{5,liner} \cdot l_{5,liner}}{NL_{5,liner} V_5} \Delta\hat{t}$$

(2.205)

$$B_9^{(2)} = \begin{Bmatrix} 0(\dot{V}_{5\to6} \geq 0) \\ -\frac{1}{mf_{5,land\_surface}} \frac{\rho_6}{\rho_{air,5}} \frac{dV_{5\to6}}{d\hat{t}} \Delta\hat{t}(\dot{V}_{5\to6} \leq 0) \end{Bmatrix} \quad \textbf{(2.206)}$$

$$B_9^{(3)} = \begin{Bmatrix} 0(\dot{V}_{5\to7} \geq 0) \\ -\frac{1}{mf_{5,land\_surface}} \frac{\rho_7}{\rho_{air,5}} \frac{dV_{5\to7}}{d\hat{t}} \Delta\hat{t}(\dot{V}_{5\to7} \leq 0) \end{Bmatrix} \quad \textbf{(2.207)}$$

2.3.6. Matrix Representation of Governing Equations

In order to represent the discretized equations in section **2.3.5** in matrix form, the coefficients in equations **(2.108)~(2.207)** are denoted as follows:

$$A_{11} = 1 + A_{11}^{(1)} + A_{11,pump} + A_{11}^{(2)} + A_{11}^{(3)} + A_{11}^{(4)} \quad \textbf{(2.208)}$$

$$A_{12} = A_{12}^{(1)} + A_{12,pump} \quad \textbf{(2.209)}$$

$$A_{15} = A_{15} \quad \textbf{(2.210)}$$

$$A_{21} = A_{21}^{(1)} + A_{21,pump} \quad \textbf{(2.211)}$$

$$A_{22} = 1 + A_{22}^{(1)} + A_{22}^{(2)} + A_{22,pump1} + A_{22,pump2} \quad \textbf{(2.212)}$$

$$A_{23} = A_{23}^{(1)} + A_{23,pump} \quad \textbf{(2.213)}$$

$$A_{32} = A_{32}^{(1)} + A_{32,pump} \quad \textbf{(2.214)}$$

$$A_{33} = 1 + A_{33}^{(1)} + A_{33}^{(2)} + A_{33}^{(3)} + A_{33,pump1} + A_{33,pump2} \quad \textbf{(2.215)}$$

$$A_{34} = A_{34}^{(1)} + A_{34,pump} \quad \textbf{(2.216)}$$

$$A_{43} = A_{43}^{(1)} + A_{43,pump} \tag{2.217}$$

$$A_{44} = 1 + A_{44}^{(1)} + A_{44}^{(2)} + A_{44}^{(3)} + A_{44,pump1} + A_{44,pump2} \tag{2.218}$$

$$A_{45} = A_{45}^{(1)} + A_{45,pump} \tag{2.219}$$

$$A_{51} = A_{51} \tag{2.220}$$

$$A_{54} = A_{54}^{(1)} + A_{54,pump} \tag{2.221}$$

$$A_{55} = 1 + A_{55}^{(1)} + A_{55}^{(2)} + A_{55}^{(3)} + A_{55}^{(4)} + A_{55}^{(5)} + A_{55,pump1} + A_{55,pump2} \tag{2.222}$$

$$A_{56} = A_{56}^{(1)} + A_{56,pump} \tag{2.223}$$

$$A_{59} = A_{59} \tag{2.224}$$

$$A_{65} = A_{65}^{(1)} + A_{65,pump} \tag{2.225}$$

$$A_{66} = 1 + A_{66}^{(1)} + A_{66}^{(2)} + A_{66,pump1} + A_{66,pump2} \tag{2.226}$$

$$A_{67} = A_{67}^{(1)} + A_{67,pump} \tag{2.227}$$

$$A_{76} = A_{76}^{(1)} + A_{76,pump} \tag{2.228}$$

$$A_{77} = 1 + A_{77}^{(1)} + A_{77}^{(2)} + A_{77}^{(3)} + A_{77,pump1} + A_{77,pump2} \tag{2.229}$$

$$A_{78} = A_{78}^{(1)} + A_{78,pump} \tag{2.230}$$

$$A_{87} = A_{87}^{(1)} + A_{87,pump} \tag{2.231}$$

$$A_{88} = 1 + A_{88}^{(1)} + A_{88}^{(2)} + A_{88,pump1} + A_{88,pump2} \tag{2.232}$$

$$A_{89} = A_{89}^{(1)} + A_{89,pump} \tag{2.233}$$

$$A_{95} = A_{95} \tag{2.234}$$

$$A_{98} = A_{98}^{(1)} + A_{98,pump} \tag{2.235}$$

$$A_{99} = 1 + A_{99}^{(1)} + A_{99}^{(2)} + A_{99}^{(3)} + A_{99}^{(4)} + A_{99}^{(5)} + A_{77,pump} \tag{2.236}$$

$$B_1 = B_1 \tag{2.237}$$

$$B_2 = B_2 \tag{2.238}$$

$$B_3 = B_3 \tag{2.239}$$

$$B_4 = B_4 \tag{2.240}$$

$$B_5 = B_5 \tag{2.241}$$

$$B_6 = B_6 \tag{2.242}$$

$$B_7 = B_7 \tag{2.243}$$

$$B_8 = B_8 \tag{2.244}$$

$$B_9 = B_9^{(1)} + B_9^{(2)} + B_9^{(3)} \tag{2.245}$$

$$\begin{bmatrix} A_{11} & A_{12} & 0 & 0 & A_{15} & 0 & 0 & 0 & 0 \\ A_{21} & A_{22} & A_{23} & 0 & 0 & 0 & 0 & 0 & 0 \\ 0 & A_{32} & A_{33} & A_{34} & 0 & 0 & 0 & 0 & 0 \\ 0 & 0 & A_{43} & A_{44} & A_{45} & 0 & 0 & 0 & 0 \\ A_{51} & 0 & 0 & A_{54} & A_{55} & A_{56} & 0 & 0 & A_{59} \\ 0 & 0 & 0 & 0 & A_{65} & A_{66} & A_{67} & 0 & 0 \\ 0 & 0 & 0 & 0 & 0 & A_{76} & A_{77} & A_{78} & 0 \\ 0 & 0 & 0 & 0 & 0 & 0 & A_{87} & A_{88} & A_{89} \\ 0 & 0 & 0 & 0 & A_{95} & 0 & 0 & A_{98} & A_{99} \end{bmatrix} \begin{bmatrix} \hat{\rho}_1 \\ \hat{\rho}_{1\_2} \\ \hat{\rho}_2 \\ \hat{\rho}_{2\_3} \\ \hat{\rho}_3 \\ \hat{\rho}_{3\_4} \\ \hat{\rho}_4 \\ \hat{\rho}_{4\_5} \\ \hat{\rho}_5 \end{bmatrix} = \begin{bmatrix} B_1 \\ B_2 \\ B_3 \\ B_4 \\ B_5 \\ B_6 \\ B_7 \\ B_8 \\ B_9 \end{bmatrix} \tag{2.246}$$

The characteristics of the coefficient matrix in equation **(2.246)** are:

- The diagonal elements are always positive

$$A_{ii} > 0 (i = 1, \cdots, 9) \tag{2.247}$$

- Off-diagonal elements have properties such that

$$- A_{ij} \le 0 \,(\mathrm{i} \ne \mathrm{j} \text{ and } \mathrm{i}, \mathrm{j} = 1, \cdots, 9) \tag{2.248}$$

- And more specifically,

$$\text{If } A_{ij} = 0, \text{ then } A_{ji} < 0, \text{ and If } A_{ij} < 0, \text{ then } A_{ji} = 0 \tag{2.249}$$

- The elements in the right hand side are always positive

$$B_i > 0 (i = 1, \cdots, 9) \tag{2.250}$$

If the coefficient matrix in **(2.246)** is denoted as A, and the 9×9 identity matrix is denoted as I, then the determinant of A can be calculated as follows.

$$\begin{aligned}&\det|A|\\&=\{A_{11}\cdot A_{22}\cdot A_{33}\cdot A_{44}\cdot A_{55}+A_{12}\cdot A_{23}\cdot A_{34}\cdot A_{45}\cdot A_{51}+A_{21}\cdot A_{32}\cdot A_{43}\cdot A_{54}\cdot A_{51}\}\\&\times(A_{66}\cdot A_{77}\cdot A_{88}\cdot A_{99})\end{aligned} \qquad \textbf{(2.251)}$$

The values of $A_{12}\cdot A_{23}\cdot A_{34}\cdot A_{45}\cdot A_{51}$ and $A_{21}\cdot A_{32}\cdot A_{43}\cdot A_{54}\cdot A_{51}$ are always zero due to the coefficient characteristics of **(2.249)** and these were confirmed heuristically by numerical calculation. Therefore, from **(2.247)** and **(2.251)**,

$$\det|A| = A_{11}\cdot A_{22}\cdot A_{33}\cdot A_{44}\cdot A_{55}\cdot A_{66}\cdot A_{77}\cdot A_{88}\cdot A_{99} > 0 \qquad \textbf{(2.252)}$$

Therefore, the equation **(2.246)** always has a solution set, or oil vapor density, in each region. In addition, if the pumping effects are neglected, the large negative value of volume change due to ring flutter can make a negative oil vapor density in a region. The negative density is meaningless in terms of physics. Therefore, it is necessary to include the pumping effect in nine vaporization equations.[1]

[1] If the regions 1_2, 2_3,3_4, and 4_5 are not considered, the governing equation can be reduced to 5 by 5 matrix equations. In that case, the pumping effect can be neglected and the corresponding oil vapor densities in region 1,2,3,4, and 5 are almost same when using 9 by 9 matrix equations which consider pumping effects.

(This page was intentionally left blank)

3. Application of the Model

3.1. Model Inputs

3.1.1. Engine Specification

The piston ring pack used in this model is shown in **Figure 3-1**. This is the piston arrangement for a heavy-duty diesel engine. The rated power condition (1700 rpm) was studied in this work.

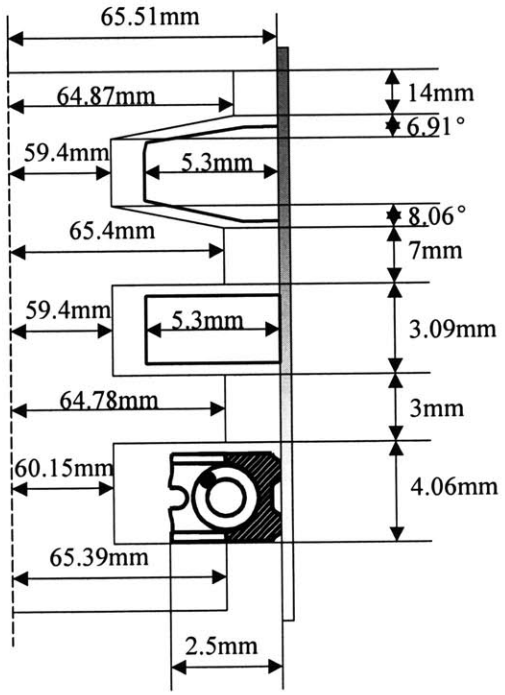

Figure 3-1. Engine specification

This piston, one of many tested in the experiment has a relatively large 3rd land volume resulting in less 3rd land pressure. As a result, oil control ring flutter occurs and large blowby gas flow occurs. This then leads to a drop in 2nd land pressure, and top ring reverse flutter causing a high amount of reverse flow towards the combustion chamber is avoided. **Figure 3-2** shows the land pressure and ring dynamics calculated by the MIT

ring dynamics and gas flow model ([11][14]). The gas flow rates from this model were used as the input for the vaporization model.

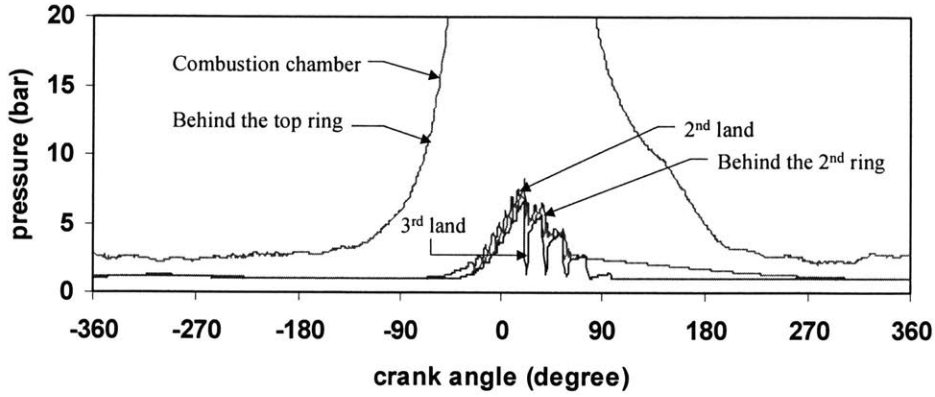

(a) Pressure in the piston ring pack

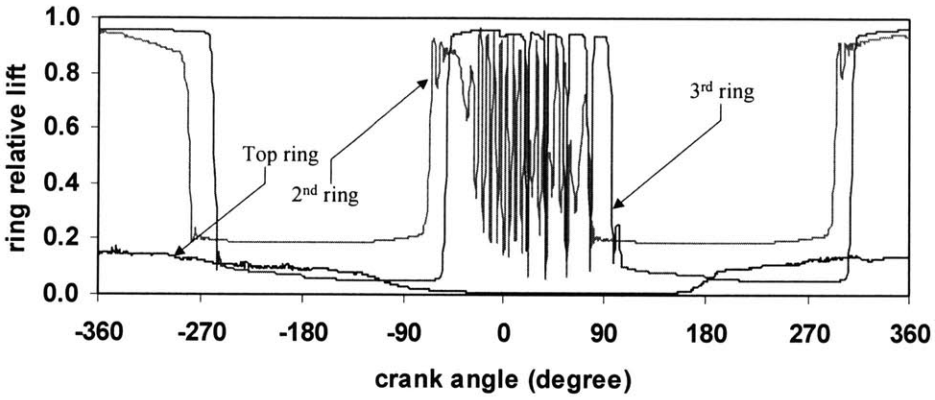

(b) Ring axial lift at the center of gravity normalized by axial clearance between a ring and its groove

Figure 3-2. Pressure and relative ring lift during engine operation

3.1.2. Oil Specification

Oil Specification used in modeling work

Light mineral oil (molecular weight = 374 kg/kmol) and heavy synthetic oil (molecular weight = 412 kg/kmol) were used in this study and modeled from distillation curves in

Figure 2-1. Twenty-one different oil components were modeled by choosing twenty-one different points of each distillation curve. The physical properties, such as volatility and viscosity, of these oils are given in **Table 3-1** [7].

	Mineral	Synthetic
SAE viscosity	10W-30	0W-30
Sulfur (wt.%)	1.51	1.68
Volatility (Noack) (% loss)	16.8	13.5
Viscosity @100 $°C$ (cSt)	10.77	11.22
HTHS viscosity (cP)	3.04	3.04

Where, $1\text{cP} = 1\text{mPa}\cdot\text{s}$; $1\text{cSt} = 1\text{mm}^2/s$

HTHS (High Temperature High Shear): 150$°C$ and $10^6 s^{-1}$

Noack test: wt. % loss at 250$°C$

Table 3-1. Oil specification used in modeling work

Oil Specification used in the Experiment

The engine oil (15W-40) used in the experiment using the heavy-duty diesel engine is more viscous than the oil used in the modeling work. The kinematic viscosity at 100 $°C$ is 15.2 (cSt) and the HTHS viscosity is 3.7 (cP). The sulfur content is about 0.6-0.7 (wt.%) and the volatility (Noack) is about 13 % loss. The distillation curve of the test engine oil is not available at the moment, but, from comparison with those used in [5] and [6], it is expected to be similar to the synthetic oil.

3.1.3.Required Pre-Evaluation

The evaluation of variables such as the volume of each region, volume change of each region, volume flow rate of gas and pressure change due to ring motion during the engine operation was needed to calculate matrix coefficients in equations **(2.208)~(2.245)** and was done using the existing ring dynamics model ([11][14]). The results are shown in **Appendix H**.

Piston and liner temperature data were also needed and were obtained from an FEA (Finite Element Analysis) calculation (**Figure 3-3**). The temperature of an upper groove and a lower groove was evaluated by averaging temperatures of adjacent piston parts. The temperature of air in a specified region was also calculated by averaging temperatures of adjacent parts.

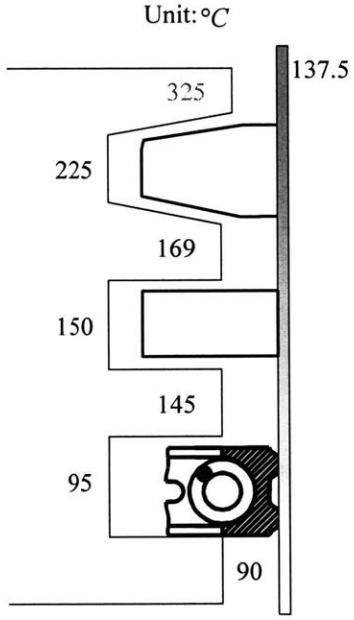

Figure 3-3. Temperature distribution in the piston ring pack of the test engine

The ring face temperature is the same as the temperature of the corresponding piston parts or linter side as shown in **Figure 2-11** in section **2.3.3.1.** This temperature condition for a ring was considered when calculating the vaporization from the upper and the lower grooves and the upper and the lower faces of a ring.

To calculate vaporization rate (Equations **(2.20)** and **(2.47)**), matrix coefficients, i.e., equations **(2.208)~(2.245)**, equivalent diffusion length $L_{diffusion}$, vaporization area $A_{vaporizaton}$, diffusion coefficient $D_{oil,air}$, mass fraction on the oil film surface $mf_{oil,surface}$, and air density ρ_{air} should be evaluated first. All these results are presented in **Appendix I**.

3.2. Infinite Oil Supply Analysis

It is expected that the engine oil may not be able to move into all of the regions in the piston ring pack and even in the wetted region, the oil composition may not be the same as that of the crankcase oil. Accurate description of the oil vaporization in the piston ring pack require coupling the vaporization process with the liquid oil transport and it is beyond the scope of the present work. In this work, the lubrication condition in the piston ring pack was arbitrarily changed to examine its effects on the vaporization. First, the infinite oil supply condition, namely, all the piston ring pack regions have sufficient fresh oil, was examined. This was followed by gradually drying different hot piston regions.

3.2.1. Oil Vapor Density Distribution in the Piston Ring Pack

In **Figure 3-4**, the oil vapor density distribution of the lightest oil component at fully wetted lubrication condition is shown.

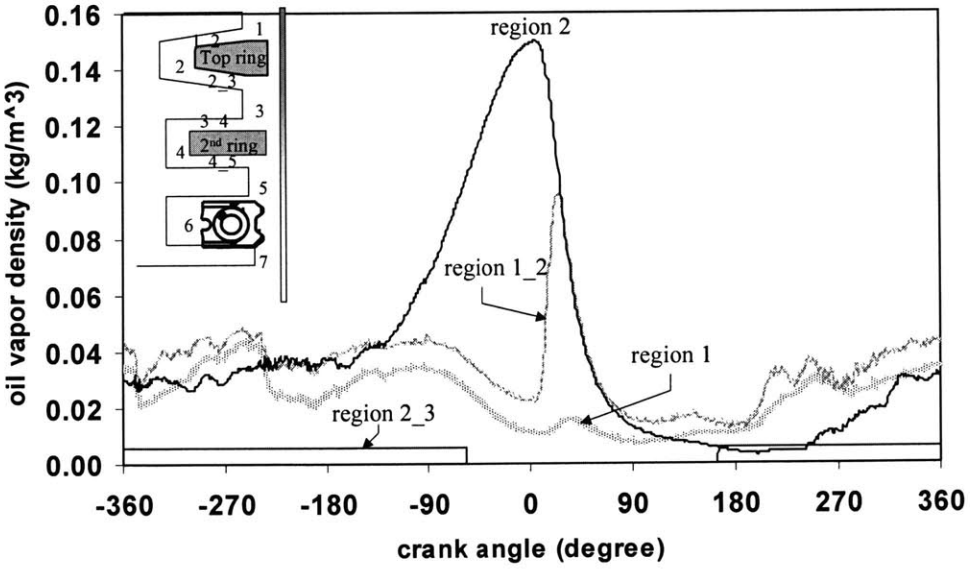

(a) Oil vapor distribution near the top ring region

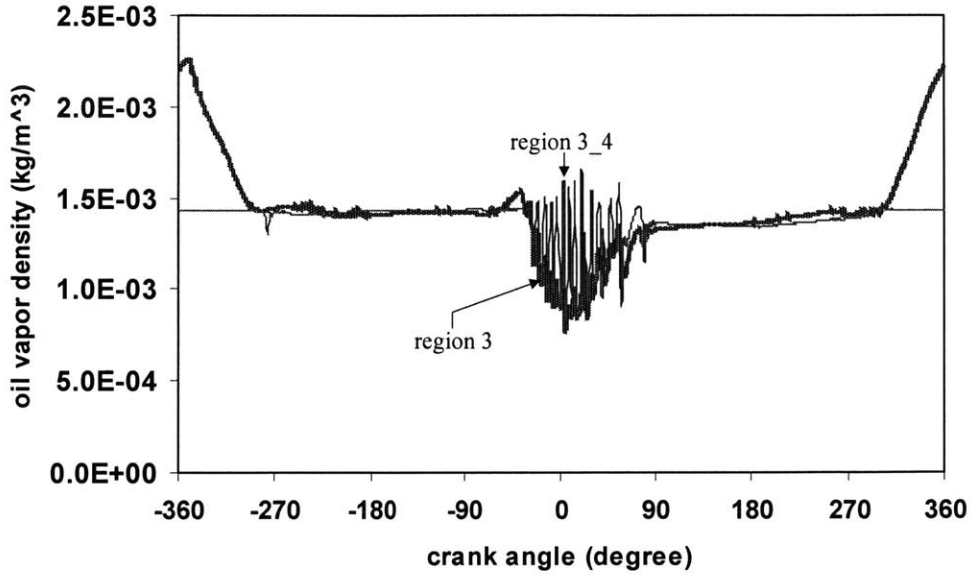

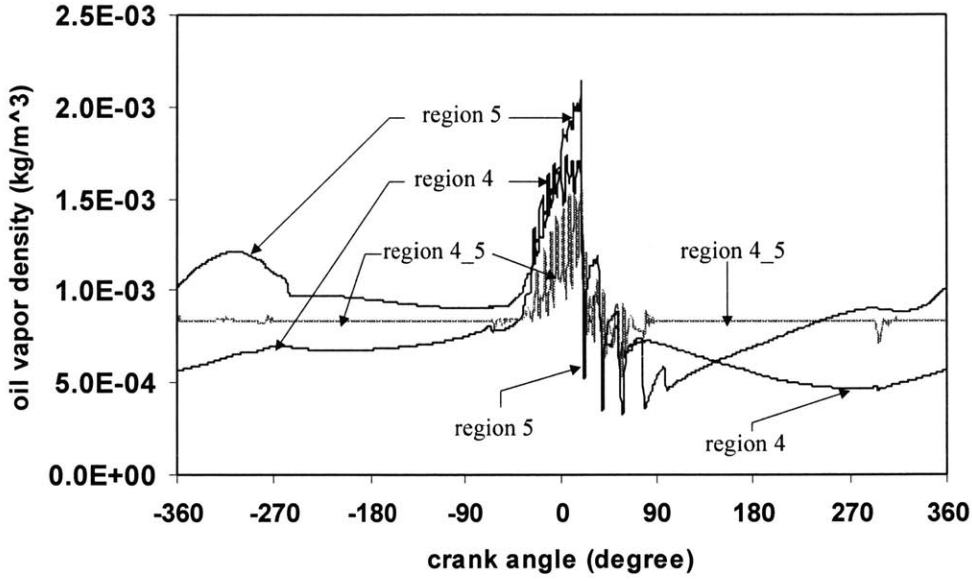

(b) Oil vapor density distribution near 2nd ring and oil control ring region

Figure 3-4. Oil vapor density distribution in the piston ring pack at fully wetted lubrication condition with infinite oil supply (This is the result of the lightest oil component whose boiling point is about 307 $^{\circ}C$ and mass fraction in the liquid oil is about 1%)

The piston tested in this modeling work has zero gas flow through the region 2_3 due to the fact that the top ring is always held on the lower flank of the groove by the high pressure in the combustion chamber (**Figure 3-4(a)**).

During the second half of the compression stroke the oil vapor in region 2 starts to accumulate due to gas flow from region 1 and region 1_2 with the help of the gas-blocking top ring configuration at region 2_3. While the oil vapor is accumulating in region 2, the oil vapors in region 1_2 and in region 1 are decreasing until the cylinder pressure reaches its maximum shortly after TDC. Then, gas starts to flow back from region 2 to region 1. Therefore, the oil vapor stored in region 2 starts to decrease and the oil vapor in region 1_2 increases sharply during this interval largely due to the gas stream from region 2 carrying large amount of oil vapor. At the same time, the oil vapor in region 1 slightly increases as a result of the balance of oil inflow from region 1_2 and oil outflow into the combustion chamber.

During the second half of the expansion stroke, all the amount of oil vapor in region 2, region 1_2, and region 1 decrease because of the shortage of oil vapor source.

There is much less vaporized oil in the lower cold regions in the piston ring pack than in the hot crown land region (**Figure 3-4(b)**). The fluctuating behaviors of oil vapors near combustion TDC is due to 2nd ring and oil control ring flutter (**Figure 3-2(b)** and **Figure 3-4(b)**).

For the other oil components, the overall behaviors are similar but of a different magnitude.

3.2.2. Vaporization Rates of Oil Components in the Piston Ring Pack

Vaporization rate of oil vapor in the piston ring pack is expected to be inversely proportional to the pressure since, among the parameters determining the vaporization rate, the diffusion coefficient dominates and is inversely proportional to the pressure.

In **Figure 3-5**, the vaporization behavior of the lightest oil component at full lubrication condition is shown. A positive rate means vaporization from the oil film surface and a negative rate means condensation onto the oil film surface.

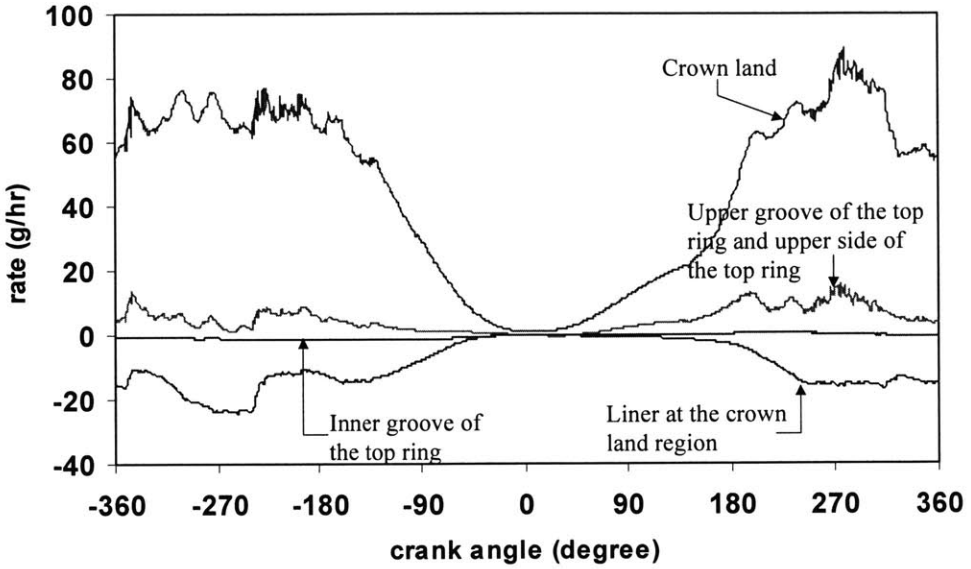

(a) Vaporization rate near crown land

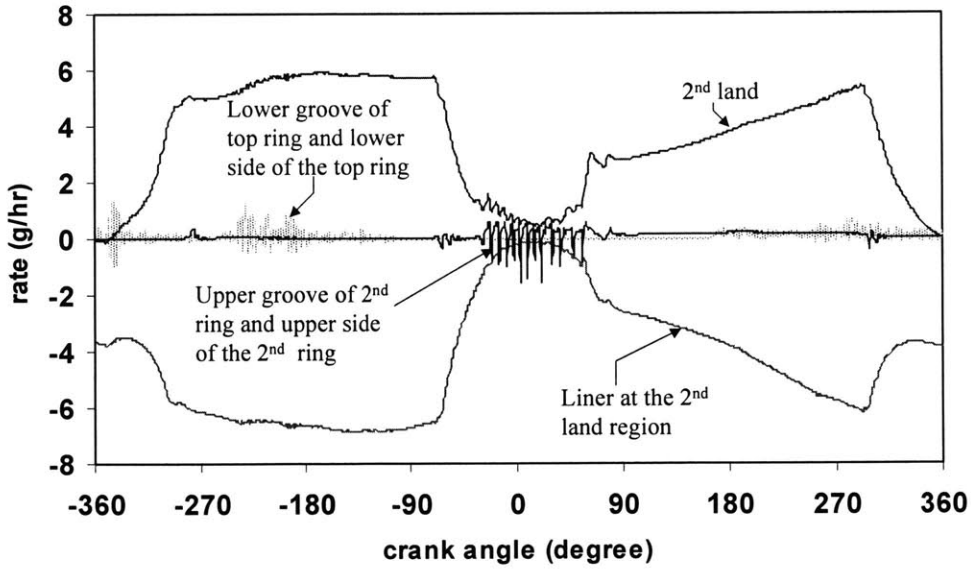

(b) Vaporization rate near 2nd land

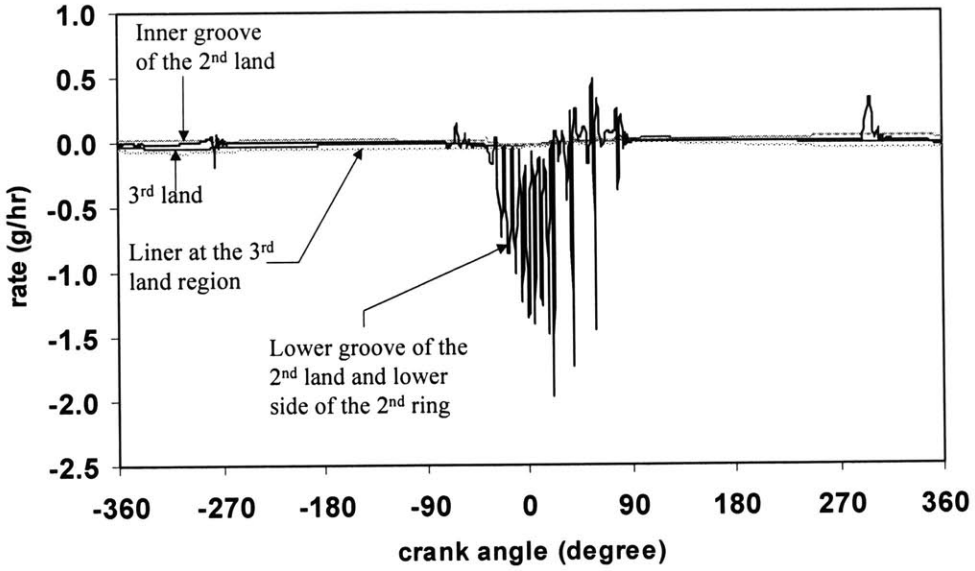

(c) Vaporization rate near 3rd land

Figure 3-5. Vaporization rate in the piston ring pack at fully wetted lubrication condition with infinite oil supply (This result is the vaporization rate of the lightest oil component whose boiling point is about 307 $°C$ and mass fraction in the liquid oil is about 1%)

The relative magnitude of vaporization rate among different piston parts (For example, crown land vaporization rate in **Figure 3-5(a)**, 2nd land vaporization in **Figure 3-5(b)**, and 3rd land vaporization in **Figure 3-5(c)**) is the result of differences in temperature, which determines the amount of oil vapor on the oil film surface, or differences in the vapor pressure which is strongly dependent on the temperature. (**Section 2.1. Engine Oil Modeling**) Low temperature conditions of the cylinder liner almost always result in condensation (**Figure 3-5(a), 3-5(b), and 3-5(c)**).

The overall large value of the vaporization rate on the crown land (**Figure 3-5(a)**) is a result of the high temperatures, combined with the infinite oil supply assumption. The vaporization rate is suppressed near combustion TDC due to the high combustion chamber pressure (**Section 2.1.Engine Oil Modeling**). Furthermore, the high oil vapor

density near combustion TDC acts as an obstacle to vaporization from the oil film surface. (**Figure 3-5(a)**)

For other regions, similar logic can be applied. The vaporization rate almost always follows the pressure behavior, but in the opposite direction. In **Figure 3-5(b)** and **3-5(c)**, the fluctuating pressures due to 2nd ring and oil control ring flutter are reflected in the vaporization rates.

For other oil components, depending on the molecular weight of the oil components, the relative magnitudes of vaporization rate change, or condensation occurs instead of vaporization.

3.2.3. Transport of the Oil Vapor in the Piston Ring Pack

In **Figure 3-6**, the average oil vapor transport rate at full lubrication condition is shown, along with the vaporization and condensation rates.

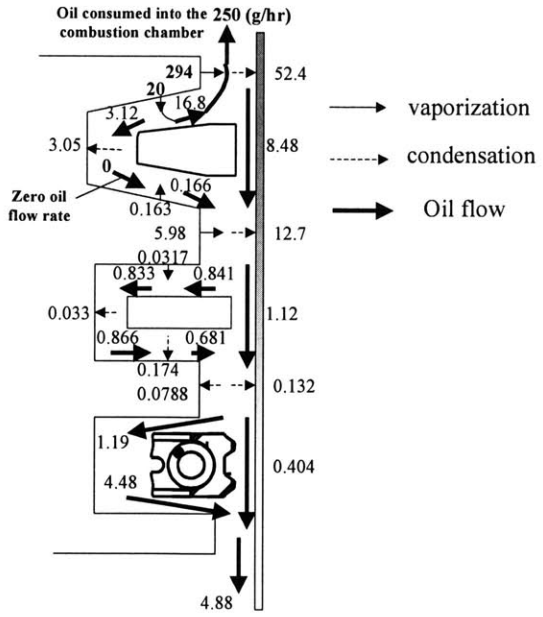

Figure 3-6. Total oil vapor transport rate and vaporization/condensation rate at fully wetted lubrication condition with infinite oil supply (unit: g/hr)

These results are the sum of all the oil components. The flow rates of the oils carried by the gas flows are denoted by thick arrows and the vaporization/condensation rates are denoted by straight-line arrows and dashed arrows respectively. Directions of these arrows represent the oil vapor transport directions.

It can be seen that the amount of oil vapor transported to the combustion chamber is about two orders of magnitude higher than the typical oil consumption value(~5g/hr) for this engine. This result indicates that the assumption of the infinite oil supply to the hot regions (Crown land and upper top ring groove) greatly overestimates the available fresh oil in these hot regions. Therefore, in reality, the wetted area and the composition of the liquid oil in the hot piston regions are substantially different from the ones based on the infinite oil supply assumption. Oil supply to the hot regions and liquid oil composition change, as does their relationship with oil vaporization, which will be discussed in the following sections.

3.2.4. Lubrication Conditions and Vaporized Oil Consumption

Once an oil component vaporizes from the oil film surface, the vaporized oil component is entrained into the gas stream in the piston ring pack. The amount of oil vapor consumed into the combustion chamber is determined by the vaporization rate and removal rate of the oil vapor by gas stream into the combustion chamber. For the same piston design, the pattern of gas stream is almost always constant per cycle. Therefore, lubrication condition on which vaporization depends is a dominant factor to determine vapor-phase oil consumption into the combustion chamber.

Different lubrication conditions and corresponding oil consumption rates into the combustion chamber are shown in **Figure 3-7.** Oil consumption into the combustion chamber is determined by the nearest oil source to the crown land. Here, the nearest oil source means the oil source that has a potential to vaporize oil with a high enough temperature. The different oil consumption sources are denoted by dashed line for each case in **Figure 3-7**.

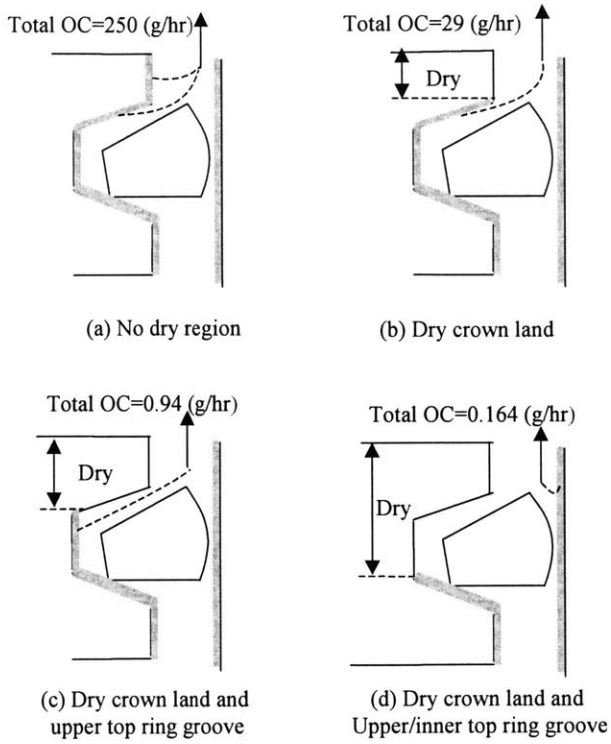

Figure 3-7. Different lubrication conditions and corresponding oil consumption rates with infinite oil supply

Conditions (a) and (b), shown in **Figure 3-7**, result in too much oil consumption, indicating that it is not realistic to cover the crown land or the upper flank of the top ring groove with fresh oil. The inner wall of the top ring groove has a substantial temperature drop ($100\,°C$ in the piston studied) compared to upper regions because it is near the oil gallery inside the piston. As a result, even though fresh oil resides inside the top ring groove, the vaporization rate is much less than the typical oil consumption rate for this engine (Condition (c) in **Figure 3-7**). Large amounts of carbon deposit are usually seen inside the top ring groove. Once the oil is trapped inside the top ring groove, it is difficult to move out in liquid form since there is no direct driving mechanism. The results here further suggest that at the temperatures used in this study, vaporization does not significantly contribute to the removal of oil from inside the top ring groove. Consequently, nearly all the oil that moves into the top ring groove eventually forms a carbon deposit. In condition (d) in **Figure 3-7**, oil consumption is soley due to the

vaporization from the part of the liner that interfaces with the crown land. For all of the conditions shown in **Figure 3-7**, there is vaporization in the 2nd land and below. However, there is zero reverse gas flow from the 2nd land, and therefore, the 2nd land vaporization does not contribute to the oil consumption in this case. The detailed oil transport direction and magnitude with oil vaporization and condensation rate for the condition (b), condition (c), and condition (d) in **Figure 3-7** are shown in **Appendix J.**

3.3. Finite Oil Supply Analysis

The analysis conducted in the previous section implies that, in the engine studied, the vaporization rate in the hot regions, namely crown land and the upper flank of the top ring groove, is limited by the liquid oil supply rate. Consequently, the composition of the remaining liquid oil in the hot regions should be substantially different from that of the fresh oil. This was supported by the result in **Figure 3-8** which shows the oil consumption rate when assuming that the oil is composed of a single heavy component.

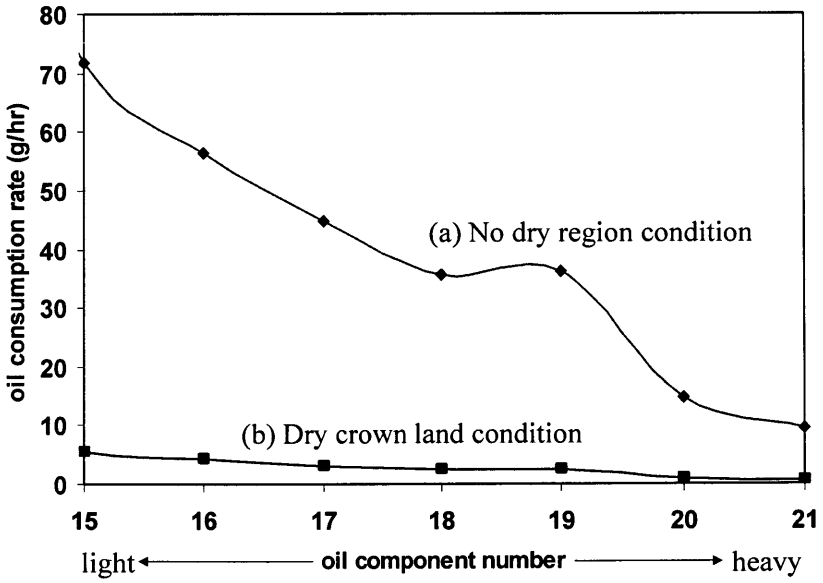

Figure 3-8. Oil consumption rates when assuming the oil is composed of single component with lubrication conditions (a) and (b) in Figure 3-7 with infinite oil supply (Oil component #21 is the heaviest oil component)

A typical oil consumption rate can be obtained only by the heaviest component for the lubrication condition **(a)** in **Figure 3-8** and a heavy component (#15) for the lubrication condition **(b)** in **Figure 3-8**.

Therefore, in order to understand the oil vaporization rate and liquid oil composition change in the hot regions, which are important for analyzing oil consumption and carbon-deposit formation, the liquid oil transport, oil vaporization, and oil vapor transport in the hot regions of the piston need to be coupled. At the present time, liquid oil transport on the top ring groove flank is not fully modeled and therefore will not be discussed further. In the following, liquid oil transport, oil vaporization, oil composition change, and oil residence time will be discussed for the crown land where a model for liquid oil transport exists, developed by Thirouard ([12][16]).

3.3.1. Overall Scenario

In this study, it is assumed that fresh oil flows to the crown land from the liner due to top ring scraping, and the oil flow rate into the crown land is assumed to be a constant of the same order of magnitude as the typical oil consumption rate (~5g/hr) for this engine. This assumption comes from the result of the infinite oil supply analysis as done in **Figure 3-7**. Particularly, condition (d) can be one of the plausible lubrication conditions. For this condition, the most probable oil supply mechanism to the crown land is top ring oil scraping. In calculation, it is assumed that the fresh oil is supplied to the lowest region of the crown land at the beginning of each engine cycle. The oil is spread upwards by the inertial force, and the oil spreading distance in the axial direction is determined by the oil puddle volume. In turn, the oil spreading distance determines the surface area from which the liquid oil can vaporize. At the beginning of the calculation, the crown land is assumed to be completely dry. As the number of the engine cycles increases, the volume and the spreading distance of the liquid oil puddle, as well as the composition of the oil puddle, evolve as a result of the competition between liquid oil supply and vaporization until a steady state is reached.

Under specified conditions, two types of steady state can exist as shown in **Figure 3-9**.

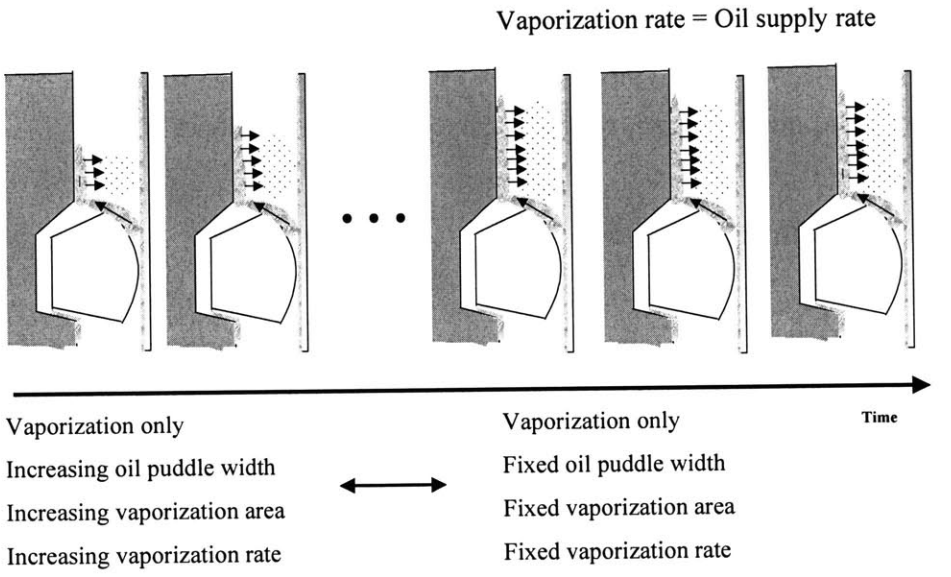

(a) Vaporization-only steady state

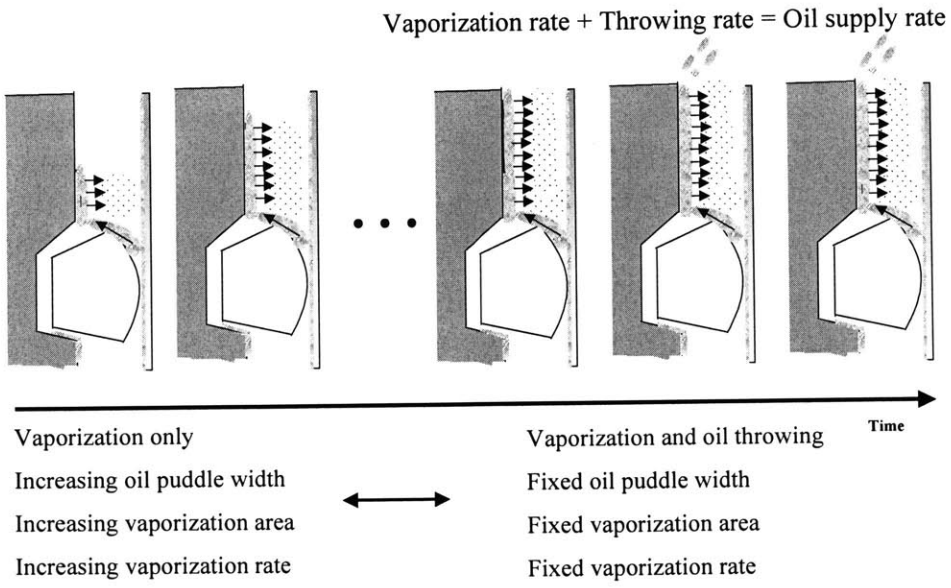

(b) Vaporization & Throwing steady state

Figure 3-9. Steady state scenarios: oil vaporization on the crown land and its relation to oil consumption and liquid oil transport

The first one is that the oil puddle stops spreading upward further before it reaches the top of the crown land because the liquid oil supply and vaporization reaches a perfect balance. In the second steady state, the oil puddle reaches the top of the crown land and the liquid oil supply from the bottom of the crown land is perfectly balanced with the vaporization and liquid oil thrown-off from the top of the crown land.

3.3.2. Dispersion of the Oil Puddle

During engine operation, the oil puddle on the piston land moves up and down due to the changing inertial force. The dispersion width $S(m)$ of the puddle depends on the maximum piston speed $V_{p,\max}(m/s)$, the cross sectional area of the oil puddle $A_{oil}(m^2)$, and the kinematic viscosity of the oil $\nu(m^2/s)$, as shown in **Figure 3-10**.

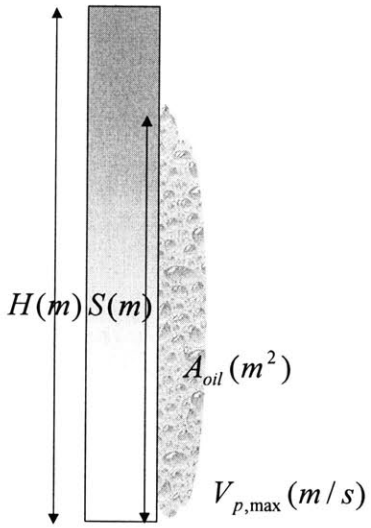

Figure 3-10. Relation between the oil puddle width, the maximum piston speed and the oil puddle volume

The oil kinematic viscosity was determined from the temperature, using the Vogel equation [11]:

$$\nu(m^2/s) = 0.0831 \times \exp\left(\frac{1043.8}{114 + T_{oil\_film}(°C)}\right) \times 10^{-6} \quad \textbf{(3.1)}$$

where,

$\nu(m^2/s)$: Kinematic viscosity of the oil

$T_{oil\_film}(°C)$: The oil film temperature

For the crown land analysis, although the oil temperature is over $300\,°C$, and the oil composition is different from the fresh oil, the same parameters in the Vogel equation **(3.1)** as for the fresh oil were used. The kinematic viscosities from this equation are 0.8958 (cSt) for $325\,°C$, and 0.9469 (cSt) for $315\,°C$, respectively. These values are reliable from the comparison of the dynamic viscosity analysis as done in [15] using the constant oil density 882 kg/m^3.

The relationship between oil puddle width $S(m)$, oil puddle volume or cross section area $A_{oil}(m^2)$ in the circumferential direction, oil kinematic viscosity $\nu(m^2/s)$, and the maximum piston speed $V_{p,\max}(m/s)$ is as follows as done in [12] and [16]:

$$\frac{S}{\sqrt{A_{oil}}} = 1.1883 \times \left(\frac{V_{p,\max}\sqrt{A_{oil}}}{\nu}\right)^{0.394} \quad \textbf{(3.2)}$$

To calculate the cycle-averaged oil puddle width $S(m)$ in **(3.2),** the oil puddle volume or mass must first be calculated.

Case 1 : Vaporization-Only Steady State

At the start of the first cycle, $Q_0(g/cycle)$ of oil is supplied to the crown land, and for each oil component, $Q_1(i) = Q_0 \times mfl_1(i)$ ($i = 1,\cdots,21$) is supplied, where $mfl_0(i) = mfl_1(i)$ is the original mass fraction of oil component i in the liquid oil.

At the end of the first cycle, $V_1(i)(g/cycle)$ of oil for the oil component i is vaporized. The remained oil $R_1(i)(g/cycle)$ is given by:

$$R_1(i) = 0 \text{ if } V_1(i) \geq Q_1(i) \tag{3.3}$$

$$R_1(i) = Q_1(i) - V_1(i) \text{ if } V_1(i) \leq Q_1(i) \tag{3.4}$$

For the second cycle, oil supply for the oil component i is

$$Q_2(i) = R_1(i) + Q_0 \times mfl_0(i)$$

The mass fraction of the oil component i, for the second cycle, is

$$mfl_2(i) = \frac{Q_2(i)}{\sum_{i=1}^{21} Q_2(i)} = \frac{R_1(i) + Q_0 \times mfl_0(i)}{\sum_{i=1}^{21} [R_1(i) + Q_0 \times mfl_0(i)]} = \frac{R_1(i) + Q_0 \times mfl_0(i)}{Q_0 + \sum_{i=1}^{21} [R_1(i)]} \tag{3.5}$$

The vaporization of a component i is determined by this updated mass fraction in the liquid $mfl_2(i)$.

For the next cycle, this procedure is then repeated.

Case 2: Vaporization & Throwing Steady State

For the case of where oil throwing occurs, the oil puddle was assumed to be large enough for the throwing at k th cycle. In this situation, the oil puddle can't hold any more oil calculated by equation **(3.2)** and all excessive oil is thrown off.

If the remaining amount of an oil component i from the k th cycle is denoted as $R_k(i)$, the new oil supply at the start of $(k+1)$ th cycle is given by:

$$Q_{k+1}(i) = R_k(i) + Q_0 \times mfl_0(i) \tag{3.6}$$

The total amount of oil $\sum_{i=1}^{21} Q_{k+1}(i)$ at the start of the cycle will be the same as the total amount of the oil at the end of the cycle, since the sum of vaporized oil amount $\sum_{i=1}^{21} V_{k+1}(i)$ and thrown-off oil amount $\sum_{i=1}^{21} T_{k+1}(i)$ will be equal to the original oil supply Q_0.

The mass fraction of an oil component i, for the next $(k+2)$ th cycle, is then given by:

$$mfl_{k+2}(i) = \frac{Q_{k+1}(i) - V_{k+1}(i) - T_{k+1}(i) + Q_0 \times mfl_0(i)}{\sum_{i=1}^{21}[Q_{k+1}(i) - V_{k+1}(i) - T_{k+1}(i) + Q_0 \times mfl_0(i)]} \tag{3.7}$$

It is then assumed that the thrown-off liquid oil composition is almost the same as the oil composition in the remaining liquid oil on the crown land.

$$\frac{Q_{k+1}(i) - V_{k+1}(i) - T_{k+1}(i) + Q_0 \times mfl_0(i)}{\sum_{i=1}^{21}[Q_{k+1}(i) - V_{k+1}(i) - T_{k+1}(i) + Q_0 \times mfl_0(i)]} \approx \frac{T_{k+1}(i)}{\sum_{i=1}^{21} T_{k+1}(i)} \tag{3.8}$$

Therefore, from equations **(3.7)** and **(3.8)**:

$$mfl_{k+2}(i) \approx \frac{Q_{k+1}(i) - V_{k+1}(i) + Q_0 \times mfl_0(i)}{\sum_{i=1}^{21}[Q_{k+1}(i) - V_{k+1}(i) + Q_0 \times mfl_0(i)]} \quad \textbf{(3.9)}$$

Using the equations **(3.1)** and **(3.9)**, the variation in puddle width of the liquid oil on the crown land was calculated for each cycle. The infinite oil supply assumption was still used as the lubrication condition below the 2nd land and on the liner side. However, as seen in section **3.2.4**, the vaporization below the 2nd land cannot affect the vaporization rate above the 2nd land due to the characteristic ring dynamics of this engine, and furthermore, the ring side acts as an oil sink where a small amount of condensation occurs. Therefore, the infinite oil supply assumption below the 2nd land has little effect on the finite oil supply analysis.

3.3.3. Vaporization-Only Steady State

The variation in puddle width of the liquid oil on the crown land was calculated for each cycle. **Figure 3-11** shows the results for the case of 5 and 10 g/hr fresh liquid oil supplied to the bottom of the crown land.

This oil supply was assumed to be uniformly spread along the circumference of the piston. However, this assumption is unnecessary if the real oil distribution is available. It can be seen that initially the oil puddle width and correspondingly the liquid oil volume are increasing because the oil supply rate is greater than the oil vaporization rate, which is limited by the small available vaporization area. Then, an increase of oil puddle volume and width results in an increase of oil vaporization rate.

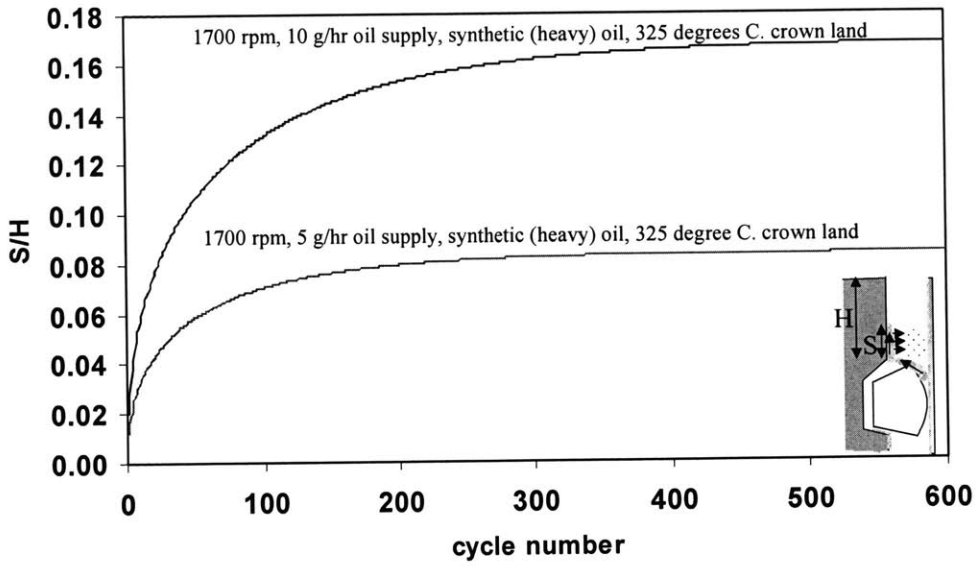

Figure 3-11. The ratio between oil puddle width and crown land height with ongoing vaporization process

At the end of 400 cycles in case of 5g/hr oil supply condition, the vaporization and the oil supply are essentially fully balanced, and steady state is reached. In this calculation, the upper/inner groove flank was assumed to be dry (condition (d) in **Figure 3-7**), which is one of the plausible lubrication conditions from the infinite oil supply analysis.

3.3.3.1. Oil Composition Change in the Oil Puddle

The mass fraction of light oil components decreases while the mass fractions of heavy oil components increases with finite oil supply during the vaporization process. (**Figure 3-12(a)**). The oil components are denoted as #1, #2, …, #21 from the lightest oil component to the heaviest oil component.

In **Figure 3-12(b)**, the initial mass fraction and steady state mass fraction of liquid oil are compared. A comparison between their average molecular weights is also shown in the same figure. The liquid oil remaining on the crown land becomes substantially heavier than the fresh oil.

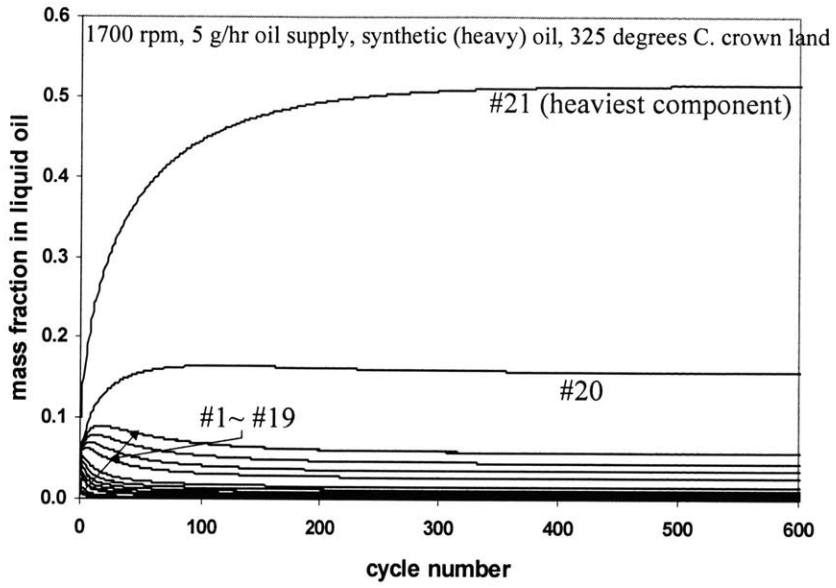

(a) Mass fraction of liquid oil calculated at the start of every cycle

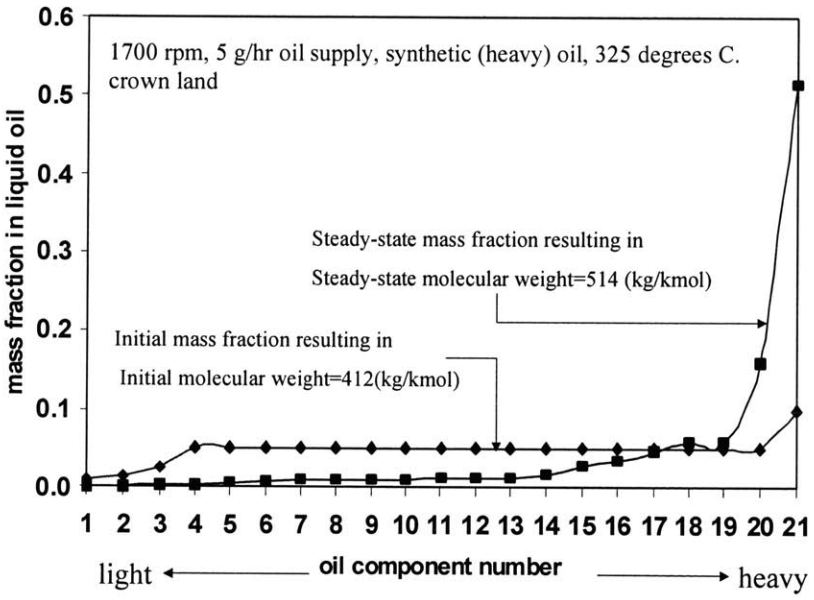

(b) Comparison between initial mass fraction and steady state mass fraction

Figure 3-12. Mass fractions of oil components in the liquid oil

3.3.3.2. Vaporization Rates from the Oil Puddle

Figure 3-13(a) and **3-13(b)** show the average vaporization rates for each cycle, for each of the twenty-one oil components, and the summation of all the components, respectively.

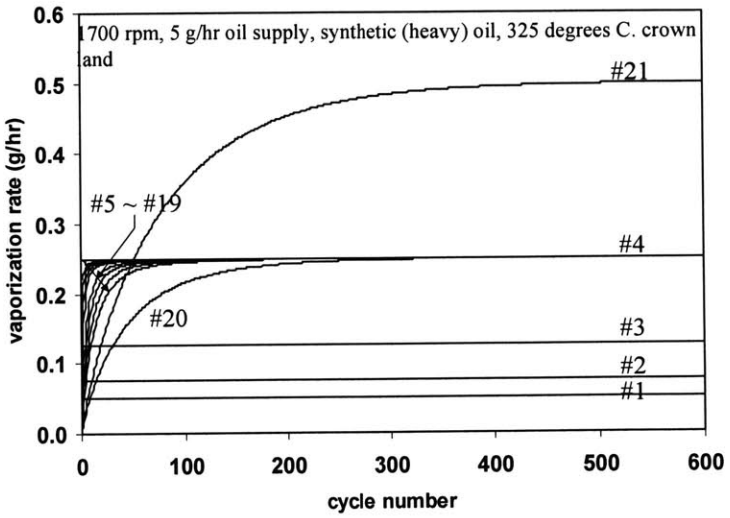

(a) Vaporization rates of oil components with limiting oil supply rate

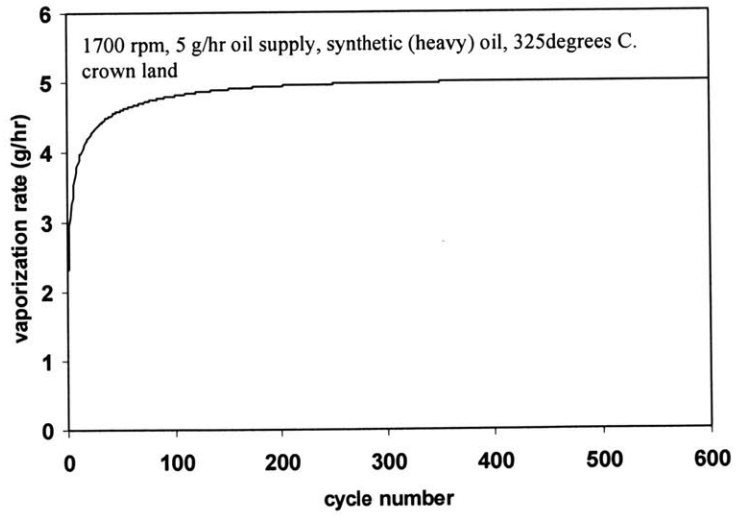

(b)Vaporization rate of oil from the crown land

Figure 3-13. Vaporization rate of each oil component and vaporization rate of oil from the crown land

The vaporization rate of an oil component is limited by the oil supply rate of that component. In this modeling work, the finite oil supply rate to the crown land due to top ring scraping is 5 g/hr. Therefore, the minimum oil supply rate of each oil component at every cycle is calculated as follows.

Minimum oil supply rate for the oil component #.i
$= 5 \times$ (Mass fraction in the fresh oil of component i)
$(i = 1,2,\cdots,21)$

The vaporization rates of the first three light oil components are greater than the minimum oil supply rates of the corresponding oil components. Therefore, the first three oil components are always fully vaporized before the end of each cycle, which is supported by the results in **Figure 3-12(b)** where the steady state mass fractions of the first three oil components are zero. While the first three oil components disappear completely, the remaining seventeen heavy oil components will accumulate in the oil puddle.

Furthermore, as the cycle number reaches four hundred (400) and beyond, the vaporization rates of all components approach steady-state values that are the same as their corresponding supply rates. The vaporization rates of heavy oil components can match their supply rates at steady state because of an increase in their mass fractions. (**Figure 3-13**)

3.3.3.3. Residence Times of Oil Components at Steady State

At steady state, the oil transport on to the crown land can be interpreted in the following way. The fresh liquid oil is supplied from the lower part of the crown land, and then well mixed with the liquid oil already residing on the crown land. Part of the newly supplied oil then vaporizes, and the rest stays on the crown land in liquid form. After a certain number of cycles, most of the fresh oil is almost fully vaporized. (**Figure 3-14**)

In **Figure 3-14**, an illustration of the residence time of oil component i, at steady state is shown. At steady state, the total oil puddle volume on the crown land is almost constant, as is the mass fraction of each oil component. The residence time of oil component i, entering the oil puddle at the first cycle after steady state has been reached, can be interpreted as the time during which all the oil components i entering the oil puddle at the first cycle disappear completely by vaporization process.

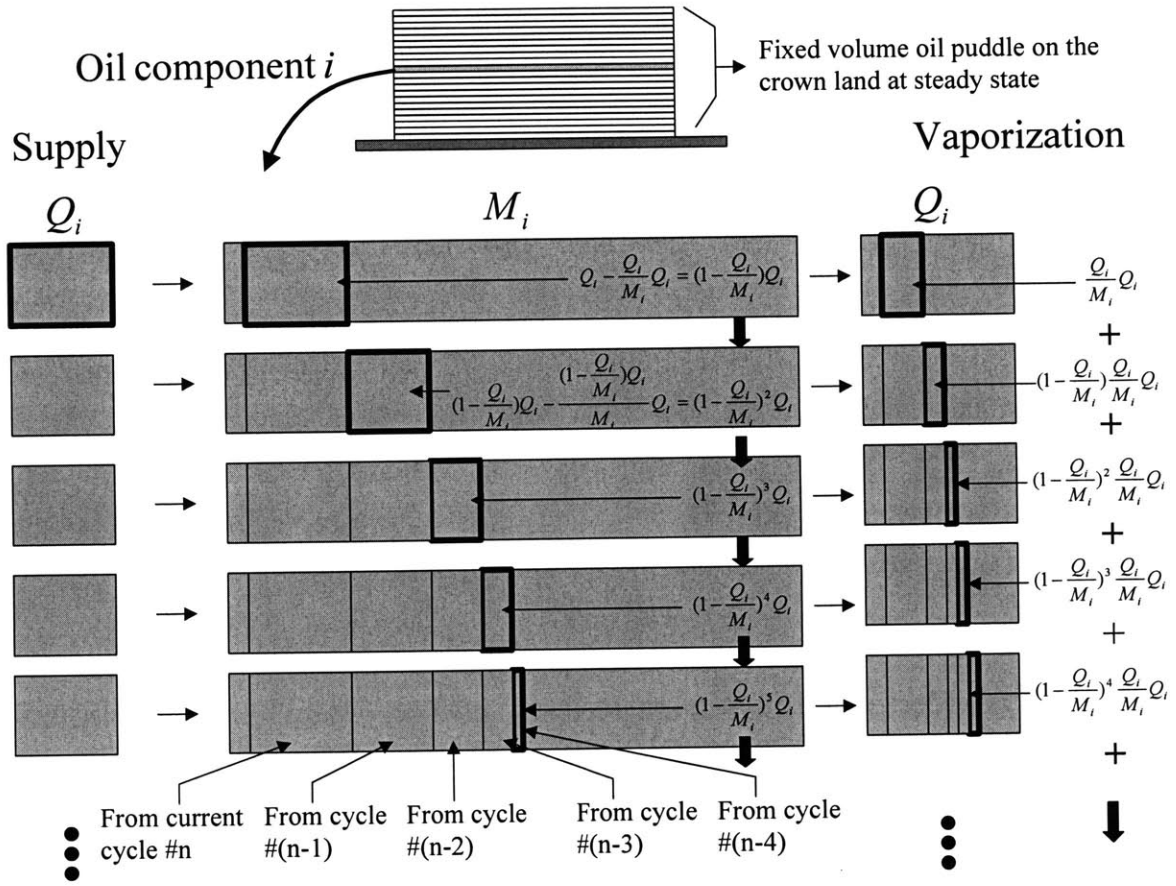

Figure 3-14. Illustration of the residence time of oil component i, at steady state, at which time the oil supply rate equals oil vaporization rate (The oil component i from cycle # (n-4) is being tracked)

Residence Time Calculation in terms of Vaporized Oil Amount

Therefore, if the oil supply per cycle of the oil component i is denoted as Q_i, and the steady state oil puddle mass of oil component i is denoted as M_i, then the amount of vaporized oil component i during the first cycle after steady state has been reached is:

$$\frac{Q_i}{M_i} Q_i \tag{3.10}$$

Here, all the oil components entering the oil puddle are assumed to be mixed homogeneously such that the ratio of that component in the vaporized oil is almost the same as the ratio in the liquid.

At the next cycle, the amount of vaporized oil from the first cycle, for component i, is given by:

$$(1-\frac{Q_i}{M_i})\frac{Q_i}{M_i} Q_i \tag{3.11}$$

The amount of vaporized oil from oil component i, during the n-th cycle after steady state has been reached is:

$$(1-\frac{Q_i}{M_i})^{n-1}\frac{Q_i}{M_i} Q_i \tag{3.12}$$

From equation **(3.12)**, the sum of all of the vaporized oil components i, starting from the first cycle after steady state has been reached, is:

$$\sum_{k=1}^{n}(1-\frac{Q_i}{M_i})^{k-1}\frac{Q_i}{M_i}Q_i = \frac{Q_i}{M_i}Q_i\frac{1-(1-\frac{Q_i}{M_i})^n}{1-(1-\frac{Q_i}{M_i})} = Q_i[1-(1-\frac{Q_i}{M_i})^n] = Q_i[1-(1-\frac{1}{T_r})^n] \quad \textbf{(3.13)}$$

where, $T_r(cycle) \equiv \dfrac{M_i(g)}{Q_i(g/cycle)}$ **(3.14)**

The sum in equation **(3.13)** becomes close to Q_i as $T_r \to 1$, but approaches zero as T_r increases. In other words, if T_r is large for a certain oil component, this oil component is more likely to reside in the oil puddle than other oil components with a small value of T_r. Therefore, the magnitude of T_r is indicative of the residence time of an oil component.

Furthermore, when n in equation **(3.13)** equals T_r in **(3.14)**, equation **(3.13)** becomes:

$$Q_i[1-(1-\frac{1}{T_r})^{T_r}] \quad \textbf{(3.15)}$$

When T_r is large, which is the case for a heavy oil component, the value of **(3.15)** can be 63.2% of Q_i, i.e.,

$$\lim_{T_r\to\infty} Q_i[1-(1-\frac{1}{T_r})^{T_r}] = Q_i(1-e^{-1}) \approx 0.632Q_i \quad \textbf{(3.16)}$$

When T_r is close to unity, which is the case for a light oil component, the value of **(3.13)** is close to Q_i with much smaller value of n.

Therefore, the cycle number n which makes the value of **(3.13)** close to Q_i is smaller than T_r for a light oil component, and is larger than T_r for a heavy oil component. However, in that T_r can represent the approximate residence time for both light and

heavy oil components, the use of T_r defined in this section as an indicator for the residence time can be justified.

Figure 3-15 shows the residence time for the twenty-one oil components after a steady state has been established. For example, from **Figure 3-15**, component #21 remains in the oil for about 80 cycles after the steady state.

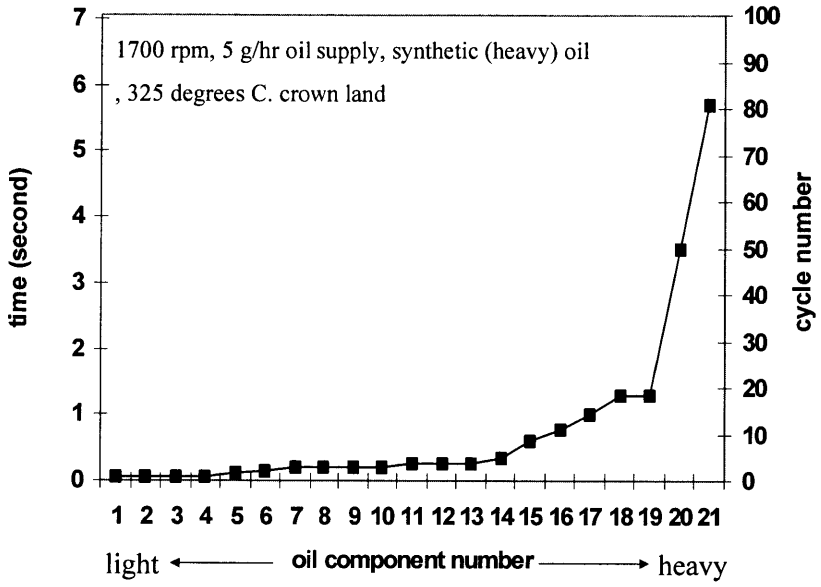

Figure 3-15. Residence time of each oil component

The heavier the oil components are, the longer they stay on the crown land before being vaporized. In this example, for most of the components, the residence time is less than 1 second, and only for the heaviest it is a few seconds.

Residence Time Calculation in terms of Remaining Oil Amount

The amount of remaining oil after the first cycle past steady state has been reached is:

$$(1-\frac{Q_i}{M_i})Q_i \qquad \textbf{(3.17)}$$

The amount of remaining oil after the second cycle past steady state has been reached is:

$$(1-\frac{Q_i}{M_i})^2 Q_i \tag{3.18}$$

The amount of remaining oil after the n-th cycle past steady state has been reached is

$$(1-\frac{Q_i}{M_i})^n Q_i \tag{3.19}$$

The same residence time $T_r(cycle) \equiv \frac{M_i(g)}{Q_i(g/cycle)}$ can be defined same as in equation **(3.14),** i.e., equation **(3.19)** can be represented as follows:

$$(1-\frac{1}{T_r})^n Q_i \tag{3.20}$$

The amount of remaining oil after the n-th cycle past steady state approaches zero as $T_r \to 1$ (as light oil components) and increases as T_r increases (as for heavy oil components). Therefore, T_r can be defined as residence time with physical meaning. In addition, the equivalence of T_r in equations **(3.13)** and **(3.20)** can be shown as follows:

After the first cycle past steady state, the sum of vaporized oil amount in equation **(3.10)** and remaining oil amount in equation **(3.17)** is initial supply Q_i:

$$\frac{Q_i}{M_i} Q_i + (1-\frac{Q_i}{M_i}) Q_i = Q_i \tag{3.21}$$

After the 2nd cycle past steady state, the sum of vaporized oil amounts in equations **(3.11) & (3.12)** and remaining oil amount in equation **(3.18)** is initial supply Q_i:

$$[\frac{Q_i}{M_i}Q_i + (1-\frac{Q_i}{M_i})\frac{Q_i}{M_i}Q_i] + (1-\frac{Q_i}{M_i})^2 Q_i$$
$$\frac{Q_i}{M_i}Q_i[1 + (1-\frac{Q_i}{M_i})] + (1-\frac{Q_i}{M_i})^2 Q_i = Q_i \quad \textbf{(3.22)}$$

In the similar way, after the n-th cycle past steady state, the sum of vaporized oil amounts and remaining oil amount is initial supply Q_i:

$$\frac{Q_i}{M_i}Q_i[1 + (1-\frac{Q_i}{M_i}) + (1-\frac{Q_i}{M_i})^2 + \cdots + (1-\frac{Q_i}{M_i})^{n-1}] + (1-\frac{Q_i}{M_i})^n Q_i$$
$$= \frac{Q_i}{M_i}Q_i \frac{1-(1-\frac{Q_i}{M_i})^n}{1-(1-\frac{Q_i}{M_i})} + (1-\frac{Q_i}{M_i})^n Q_i = Q_i \quad \textbf{(3.23)}$$

3.3.3.4. Comparison of Vaporization Rates

In **Figure 3-16(a), 3-16(b),** and **3-16(c)**, vaporization rates, the puddle widths and residence times for a range of different oils and crown land temperatures are shown.

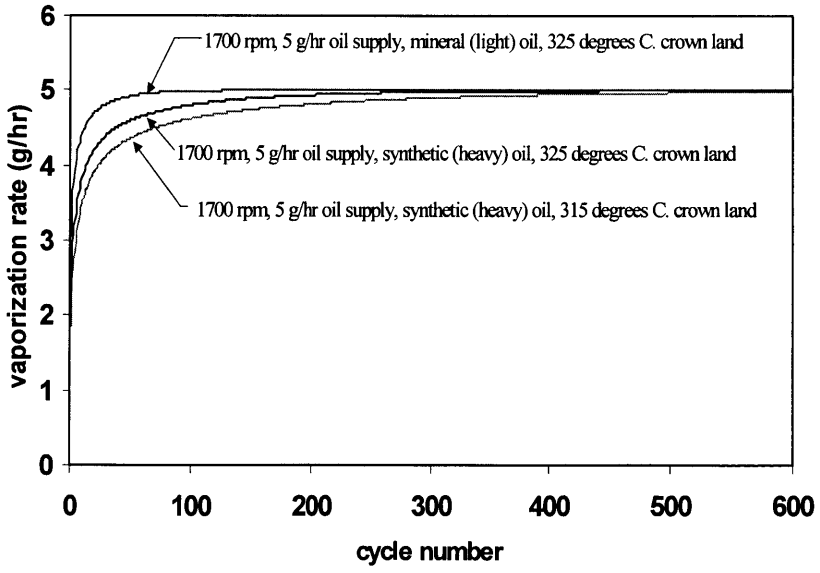

(a) Vaporization rate

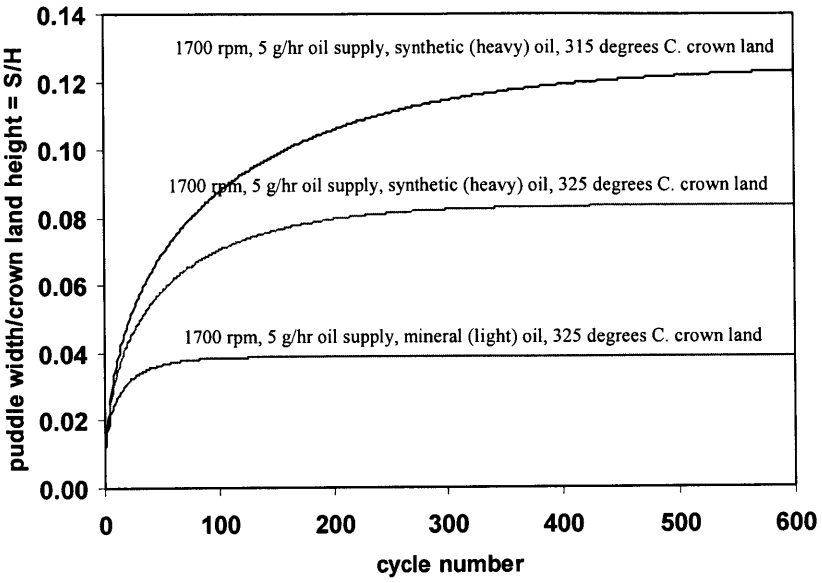

(b) Puddle width to crown land height ratio

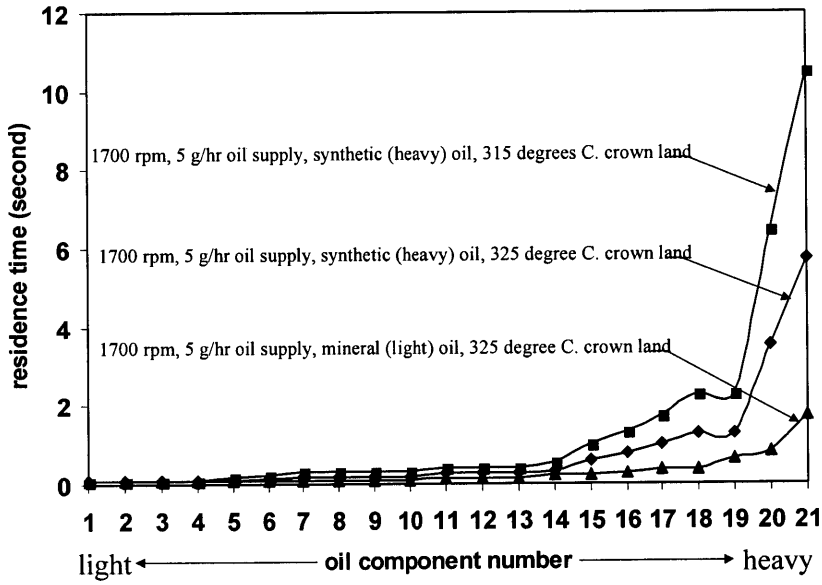

(c) Residence time (For the same oil component number, mineral oil is lighter than the synthetic oil component)

Figure 3-16. Comparison of vaporization rate, S/H (puddle width to crown land height ratio), and residence time

As expected, heavier oil and lower crown land temperatures both result in larger puddle widths, and thus larger volumes residing on the crown land, as well as longer oil residence times on the crown land after steady state is reached

3.3.4. Vaporization & Throwing Steady State

3.3.4.1. Effect of Clustering of the Oil Puddle

The results in the previous section sections **3.3.3** show that the oil can only spread to a small portion of the crown land in the axial direction, if the oil puddle is assumed to be uniformly distributed along the circumferential direction. Realistically, carbon deposits (due to oil) are usually found to cover the entire axial height of the crown land after this engine was run for hundreds of hours, suggesting that the liquid oil may be able to reach higher regions of the crown land than predicted by the current model (vaporization-only steady state). Therefore, the assumption that the oil puddle is always uniform along the circumference may not be accurate.

As observed from experiment by Thirouard [16], the oil on the piston lands usually exhibits a wavy form in the circumferential direction as shown in **Figure 3-17**.

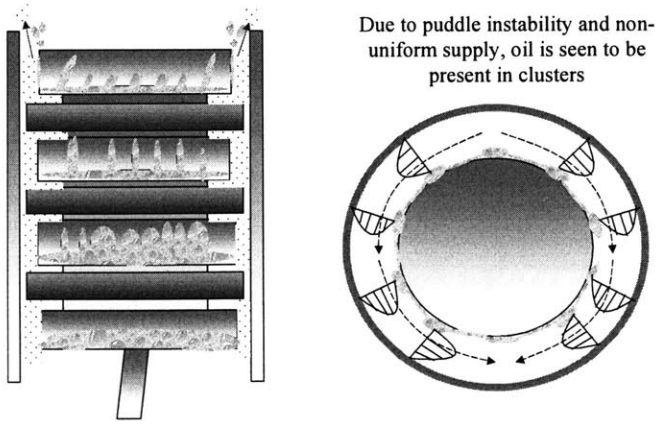

Figure 3-17. Cluster of oil puddle

This wavy form is caused by a combination of the instability in the inertia driven oil flow on the piston and the stabilizing force of the oil surface tension. In other words, oil may cluster with thick oil puddles separated by thin oil films in the circumferential direction, even if oil is supplied uniformly along the circumference.

Furthermore, the oil supply to the crown land may be localized. Localization of the oil puddle on the crown land can reduce vaporization area and increase oil film thickness so that the vaporization is reduced and oil axial spreading speed is increased. As a result, the oil puddle may be able to reach higher regions on the crown land. This effect of oil clustering can be seen in **Figure 3-18** where the oil puddle was assumed to only occupy 10° of the total circumference (360°), and within this10°, the oil puddle is uniform in the circumferential direction. It can be seen that after 300 cycles, the oil puddle reaches the top of the crown land. At this moment, steady state is reached such that the vaporization rate is slightly less than the oil supply rate, and the difference will be thrown off in liquid form into the combustion chamber.

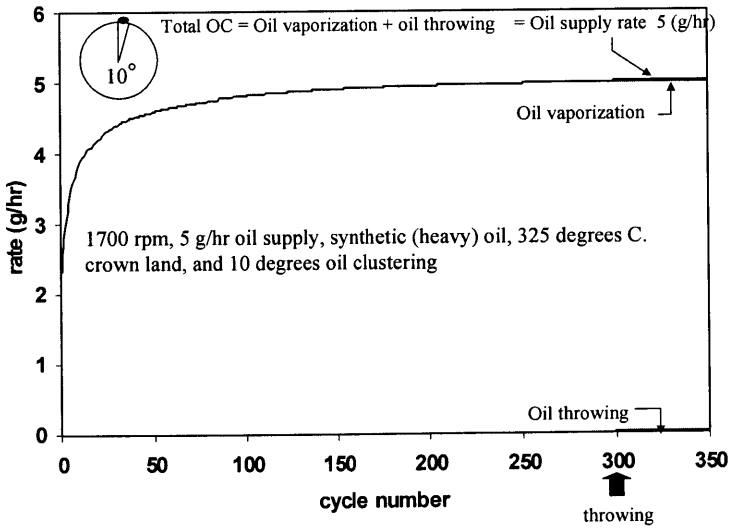

(a) Oil throwing rate, oil vaporization rate and oil supply rate

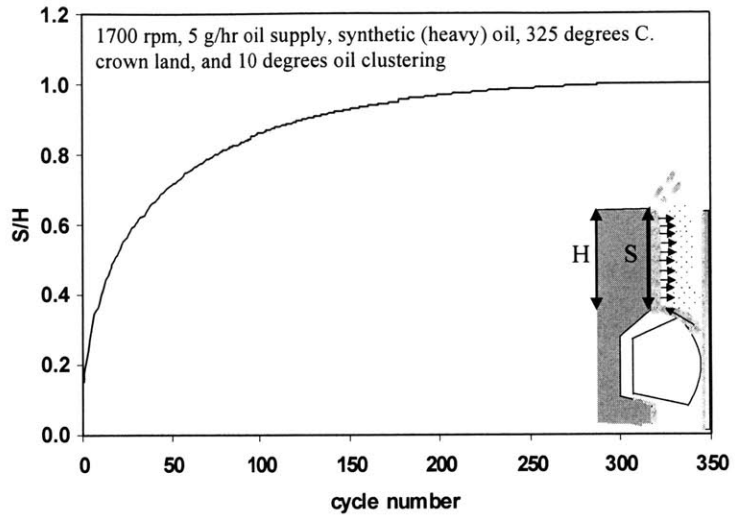

(b) Oil puddle width to crown land height ratio

Figure 3-18. The relationship between oil throwing, oil vaporization and oil supply, and the corresponding oil puddle width

In Figure **3-19**, the low temperature crown land condition is shown to result in the same type of steady state.

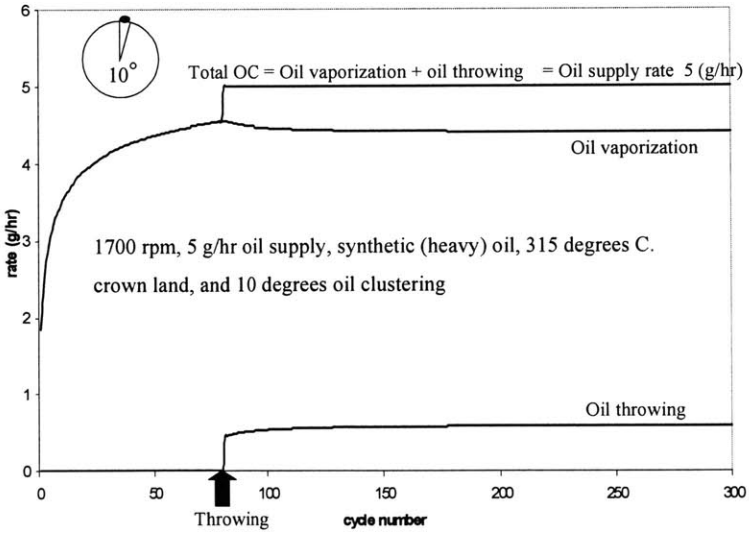

Figure 3-19. The relationship between oil throwing, oil vaporization and oil supply at low temperature crown land

Due to large oil volume, which is the result of low vaporization loss, the oil puddle quickly reaches the top of the crown land. Once a steady state is reached, the vaporization area is fixed. Therefore, a slight decrease in oil vaporization rate is shown from the loss of highly volatile light oil components. In this low temperature condition, oil throwing contribution to total oil consumption increases.

(This page was intentionally left blank)

4. Conclusions

The vaporization of engine oil in the piston ring pack of internal combustion engines was modeled. Engine oil was modeled as a mixture of paraffin hydrocarbons of varying mass fractions. The piston ring pack was subdivided into nine regions with unknown oil vapor densities during engine operation. The model was then applied to a heavy-duty diesel engine at the rated power operating conditions.

- In terms of engine operating characteristics, the most important parameters affecting engine oil vaporization are the temperatures of the surfaces on which the oil is residing, and the oil supply rate to the hot regions of the piston.

The infinite oil supply analysis, without consideration of the liquid oil supply and transport mechanisms, was conducted. Under this infinite oil supply assumption, with fully wetted lubrication condition of the hot piston regions (the upper flank of the top ring groove and the crown land), it was found that

- The oil vapor near hot, top ring groove regions is the primary contributor to oil vaporization.

- High surrounding pressure suppresses the vaporization rate when equilibrium state is assumed in the piston ring pack.

- The hot piston regions result in excessive oil consumption compared to the current measured oil consumption of a test engine.

- Therefore, the hot piston regions cannot be fully wetted with fresh oil, but instead may be wetted with only a few of the heaviest oil components in the oil under the infinite oil supply assumption for the hot piston regions.

From the results of the infinite oil supply analysis, partial lubrication conditions on the hot piston regions, particularly on the crown land, were suggested in order to achieve a realistic oil consumption value. The oil on the crown land with partial lubrication condition was then analyzed by coupling the liquid oil supply to the crown land, oil vaporization process, transport of the oil vapor and an established liquid oil transport model on the crown land.

- Two types of steady states are possible. One is vaporization-only steady state and the other is vaporization & throwing steady state.

- The amount of fresh liquid oil supplied from the oil scraping, the amount of vaporized oil, and the amount of transported oil vapor in the crown land region due to gas flow determine the oil composition change (mass fraction change) in the liquid oil. The liquid oil transport on the crown land determines vaporization area (lubrication condition).

- The results initially show a gradual increase in the mass fraction of the heavy oil components in the liquid oil on the crown land, and in the liquid oil puddle width (vaporization area) over time, until a steady state is reached such that the removal rate of each oil component (mainly through vaporization) matches its supply rate.

- Estimation of the oil residence time at steady state shows that the residence time of the heaviest oil component, which has the potential to form carbon deposit, is of the order of a few seconds.

The vaporization rate is the vaporization rate per unit area multiplied by the vaporization area. Both of these factors are highly affected by oil temperature and oil volatility.

- High oil temperature and more volatile oil increase vaporization rate per unit area, but reduce the vaporization area.

- Low oil temperature and less volatile oil increase vaporization area but reduce vaporization rate per unit area

- The relative contribution of oil vaporization and oil throwing depends on the volatility and the oil temperature.

This work is the first step toward understanding oil residence time, oil degradation, and carbon deposit formation in hot piston regions. It can also be used to determine whether fully wetted lubrication conditions (possible excessive oil consumption) or partial lubrication conditions (lowering oil consumption), are more appropriate when designing a particular engine.

(This page was intentionally left blank)

References

1. Caines, A. J. and Haycock, R. F., Automotive Lubricants Reference Book, SAE, 1996.

2. Nattrass, S. R., Thompson, D. M., and McCann, H., "First In-Situ Measurement of Lubrication Degradation in the Ring Pack of a Running Engine", SAE paper 942026, 1994.

3. Okada, S. et al, "Measurement of Trace Metal Composition in Diesel Engine Particulate and its Potential for Determining Oil Consumption: ICPMS (Inductively Coupled Plasma Mass Spectrometer) and ATOFMS (Aerosol Time of Flight Mass Spectrometer) Measurements", SAE paper 2003-01-0076, 2003.

4. Burnett, P. J. "Relationship Between Oil Consumption, Deposit Formation and Piston Ring Motion for Single-Cylinder Diesel Engines", SAE paper 920089, 1992.

5. Wahiduzzaman, S., Keribar, R., Dursunkaya, Z., and Kelley, F. A., "A Model for Evaporative Consumption of Lubricating Oil in Reciprocating Engines", SAE paper 922202, 1992.

6. Audette III, W. E., and Wong, V. W., "A Model for Estimating Oil Vaporization from the Cylinder Liner as a Contributing Mechanism to Engine Oil Consumption", SAE paper 1999-01-1520, 1999.

7. Yilmaz, E., Tian, T., Wong, V. W., and Heywood, J. B., "An Experimental and Theoretical Study of the Contribution of Oil Evaporation to Oil Consumption", SAE paper 2002-01-2684, 2002.

8. Zwolinski, B. J. and Wilhoit, R. C., "Handbook of Vapor Pressure and Heats of Vaporization of Hydrocarbons and Related Compounds", College Station: Thermodynamics Research Center, Dept. of Chemistry, Texas A&M University, 1971.

9. Mills, A. F., Heat and Mass Transfer, Irwin, 1995.

10. Tosun, I., Modeling in Transport Phenomena: a Conceptual Approach, Elsevier, 2002.

11. Tian, T., "Modeling the Performance of the Piston Ring Pack in Internal Combustion Engines", Ph.D. thesis, Department of Mechanical Engineering, Massachusetts Institute of Technology, June 1997.

12. Thirouard B. and Tian, T., "Oil Transport in the Piston Ring Pack (Part I): Identification and Characterization of the Main Oil Transport Routes and Mechanisms", JSAE paper 20030345, SAE paper 2003-01-1952, 2003.

13. Reid, R. C., Prausnitz, J. M., and Sherwood, T. K., The Properties of Gases and Liquids, 3rd ed., McGraw-Hill, 1977.

14. Tian, T., "Dynamic Behaviors of Piston Rings and Their Practical Impact. Part 1: Ring Flutter and Ring Collapse and Their Effects on Gas Flow and Oil Transport", Proc. Instn Mech. Engrs, Vol. 216 Part J, Journal of Engineering Tribology, pp.209-227.

15. Yilmaz E., "Sources and Characterization of Oil Consumption in a Spark-Ignition Engine", Ph.D. thesis, Department of Mechanical Engineering, Massachusetts Institute of Technology, September 2003.

16. Thirouard, B., "Characterization and Modeling of the Fundamental Aspects of Oil Transport in the Piston Ring Pack of Internal Combustion Engines", Ph.D. thesis, Department of Mechanical Engineering, Massachusetts Institute of Technology, June 2001.

17. Bender, C. M. and Orszag, S. A., Advanced Mathematical Methods for Scientists and Engineers: Asymptotic Methods and Perturbation Theory, Springer, 1999.

18. Rohsenow, W. M., Hartnett, J. P., and Cho, Y. I., Handbook of Heat Transfer, 3rd ed., McGraw-Hill, 1998.

Appendices

Appendix A. Structures of Base Stocks and Additives in the Engine Oil [1]

A.1 Base Stocks

Hydrocarbons

Each angle shown in **Figure A.1** represents a carbon (C) atom.

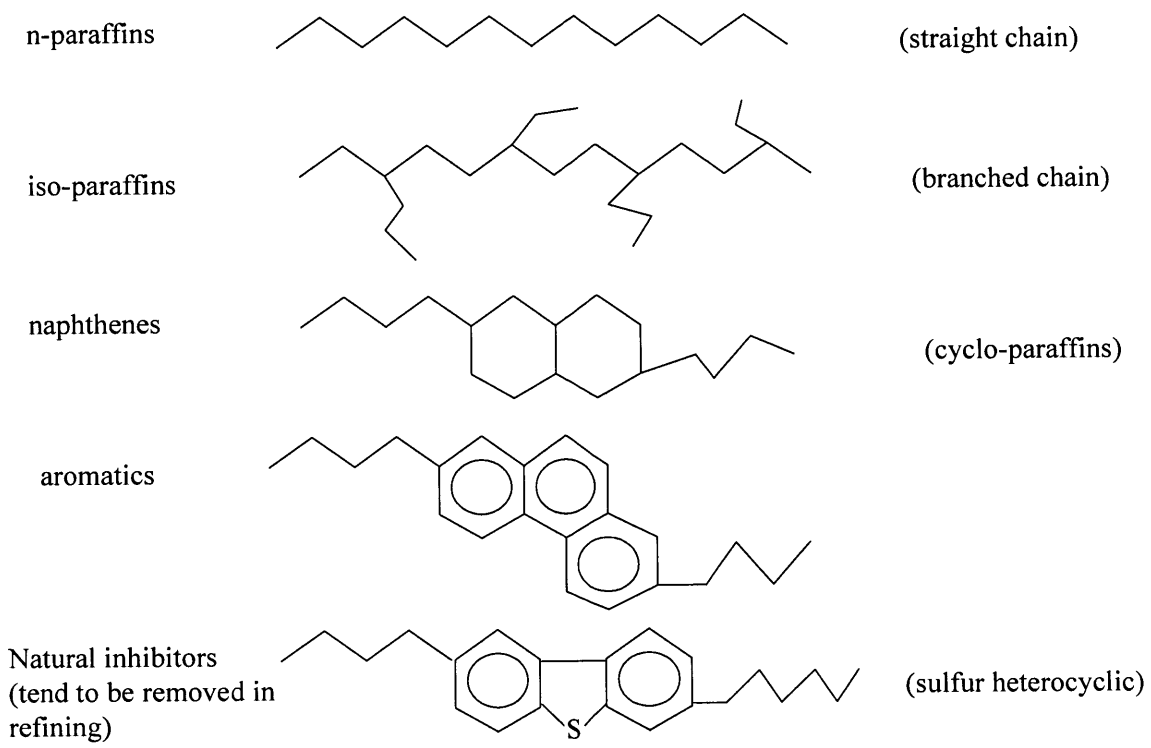

Figure A.1 Principal hydrocarbon types in lubricants

Olefin oligomers

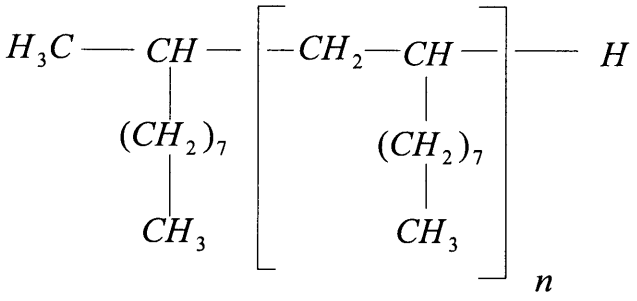

Figure A.2 Structure of a polyalphaolefin

Alkylated aromatics

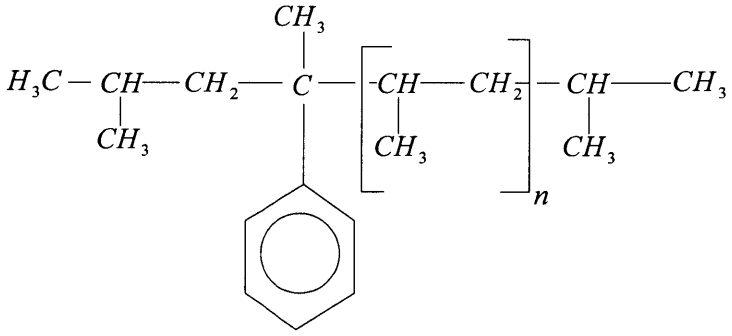

Figure A.3 An alkyl benzene, derived from polypropylene

Organic esters

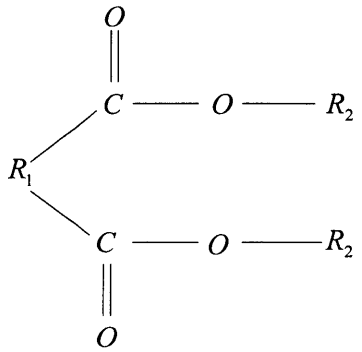

Figure A.4 The diester $R_1(COOH)_2$ and R_2OH

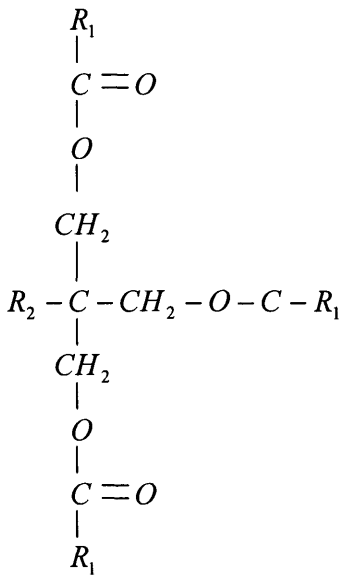

Figure A.5 Structure of a neopentyl ester

Polyglycols

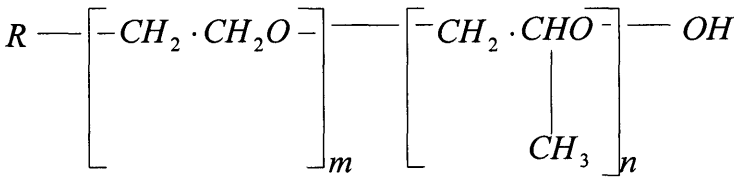

Figure A.6 A polyglycol based on ethylene and propylene oxides

A.2 Additives

Viscosity modifiers

Polymer type	structure	monomers
Olefin co-polymers	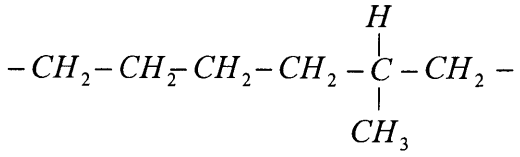	Ethylene Propylene butylene
polymethacrylates	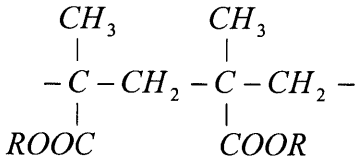	Methacrylic Acid alcohols
Styrene-butadiene co-polymers	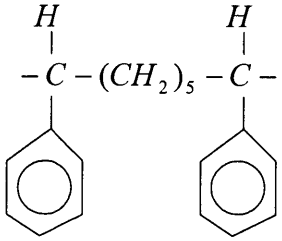	Styrene butadiene
Hydrogenated polyisoprene	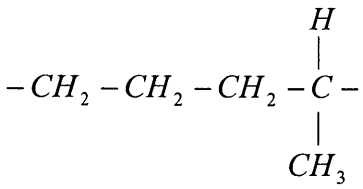	isoprene

Figure A.7 Structure of some viscosity modifier polymers

Detergents

(a) metal phenate

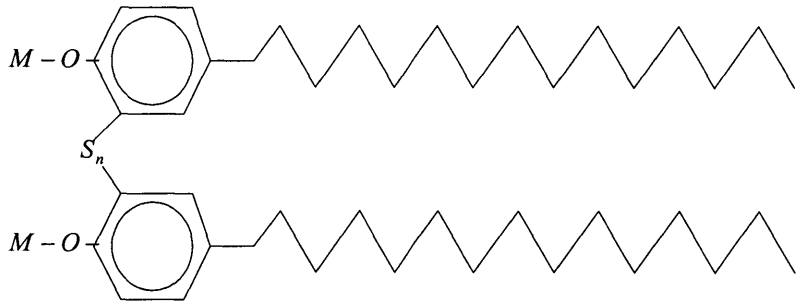

(b) sulfurized phenate

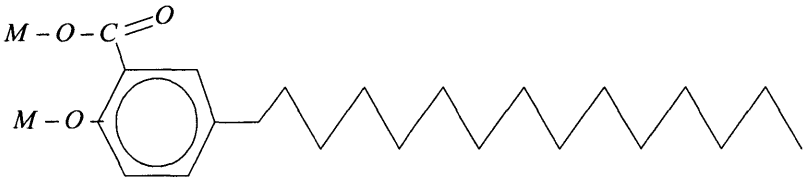

(c) metal salicylate

(d) metal sulfonate

Figure A.8 Structures of some detergents

Anti-wear additives

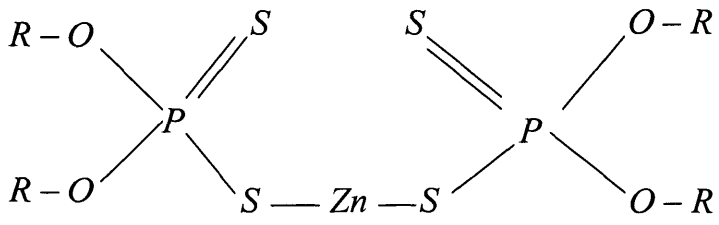

Figure A.9 Structure of ZDDP (zinc dialkyldithiophosphates)

Rust inhibitors

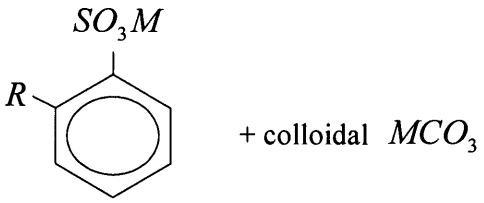

(a) overbased sulfonates

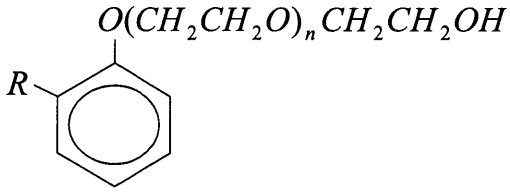

(b) ethoxylated phenols

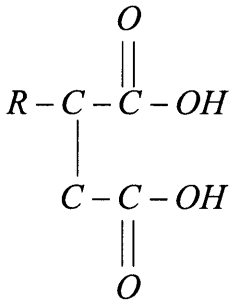

(c) substituted succinic acids

Figure A.10 Structures of some rust inhibitors

Appendix B. Derivation of Equation (2.31) - Series Solution

Under the velocity field in equation **(2.26)**

$$u(y) = 6u_{avg}\frac{y}{a}\left(1-\frac{y}{a}\right) \tag{B.1}$$

The partial differential equation **(2.27)**

$$u\frac{\partial \rho}{\partial x} = D_{12}\frac{\partial^2 \rho}{\partial y^2} \tag{B.2}$$

With boundary conditions **(2.28) ~(2.30)**,

$$\rho(x, y = 0) = \rho_s \tag{B.3}$$

$$\frac{\partial \rho}{\partial y} = 0 \text{ at y = a} \tag{B.4}$$

$$\rho(x = 0, y = a) = \rho_0 \tag{B.5}$$

First to make use of homogeneous boundary condition,

$$\tilde{\rho}(x, y) \equiv \rho(x, y) - \rho_s \tag{B.6}$$

Then, the given partial differential equation **(B.2)** and boundary conditions **(B.3)** and **(B.4)** becomes

$$u(y)\frac{\partial \tilde{\rho}}{\partial x} = D_{12}\frac{\partial^2 \tilde{\rho}}{\partial y^2} \tag{B.7}$$

With boundary conditions

$$\tilde{\rho} = 0 \quad \text{at y} = 0 \tag{B.8}$$

$$\frac{\partial \tilde{\rho}}{\partial y} = 0 \quad \text{at y} = \text{a} \tag{B.9}$$

By introducing separation of variables

$$\tilde{\rho}(x, y) = X(x) \cdot Y(y) \tag{B.10}$$

(B.7) becomes

$$\frac{1}{X}\frac{dX}{dx} = \frac{D_{12}}{u(y)}\frac{1}{Y}\frac{d^2Y}{dy^2} = -k^2 < 0 \tag{B.11}$$

$$\frac{dX(x)}{dx} + k^2 \cdot X(x) = 0 \quad \text{and} \quad \frac{d^2Y(y)}{dy^2} = \frac{Y(y) \cdot u(y)}{D_{12}}(-k^2) \tag{B.12}$$

x – equation

$$X(x) = C_1 \cdot \exp(-k^2 \cdot x) \tag{B.13}$$

y – equation

The y-equation in **(B.12)** has no singular point. Therefore, the solution can have the form

$$Y(y) = \sum_{n=0}^{\infty} a_n \cdot y^n \tag{B.14}$$

With boundary conditions from **(B.8)** and **(B.9)**

$$Y = 0 \quad \text{at y} = 0 \tag{B.15}$$

$$\frac{dY(y)}{dy} = 0 \quad \text{at y} = \text{a} \tag{B.16}$$

First from **(B.14)** and **(B.15)**

$$Y(y=0) = a_0 + a_1 \cdot 0 + a_2 \cdot 0^2 + \cdots = a_0 = 0 \tag{B.17}$$

And from equation **(B.14)**,

$$\frac{d^2Y(y)}{dy^2} = \sum_{n=2}^{\infty} a_n \cdot n(n-1)y^{n-2} \tag{B.18}$$

Substituting **(B.14)** and **(B.18)** into the y-equation in **(B.12)** gives

$$\sum_{n=2}^{\infty} a_n \cdot n(n-1)y^{n-2} = \sum_{n=0}^{\infty} a_n \cdot y^n \cdot 6 \cdot u_{avg} \frac{y}{a}(1-\frac{y}{a}) \cdot \frac{-k^2}{D_{12}} \tag{B.19}$$

$$\sum_{n=2}^{\infty} a_n \cdot n(n-1)y^{n-2} = \frac{6 \cdot u_{avg} \cdot (-k^2)}{D_{12} \cdot a^2} \sum_{n=0}^{\infty} a_n \cdot (a \cdot y^{n+1} - y^{n+2}) \tag{B.20}$$

Comparison term by term up to the order of y^3,

$$y^0 : 2a_2 = 0 \rightarrow a_2 = 0 \tag{B.21}$$

$$y^1 : 6a_3 = \frac{6 \cdot u_{avg} \cdot (-k^2)}{D_{12} \cdot a^2} \cdot a_0 \cdot a \rightarrow a_3 = 0 \tag{B.22}$$

$$y^2 : 12a_4 = \frac{6 \cdot u_{avg} \cdot (-k^2)}{D_{12} \cdot a^2} \cdot (a_1 \cdot a - a_0) \rightarrow a_4 = \frac{u_{avg} \cdot (-k^2)}{2D_{12} \cdot a} a_1 \quad \textbf{(B.23)}$$

$$y^3 : 20a_5 = \frac{6 \cdot u_{avg} \cdot (-k^2)}{D_{12} \cdot a^2} \cdot (a_2 \cdot a - a_1) \rightarrow a_5 = -\frac{3}{10} \frac{u_{avg} \cdot (-k^2)}{D_{12} \cdot a^2} a_1 \quad \textbf{(B.24)}$$

From these results, the $g(y)$ becomes

$$Y(y) = a_1 y + \frac{u_{avg}(-k^2)}{2D_{12}} \frac{a_1}{a} y^4 - \frac{3}{10} \frac{u_{avg}(-k^2)}{D_{12}} \frac{a_1}{a^2} y^5 \quad \textbf{(B.25)}$$

From boundary condition **(B.16)** at y=a, k^2 can be obtained as follows.

$$a_1 (1 + 2 \frac{u_{avg}(-k^2)}{D_{12}} a^2 - \frac{3}{2} \frac{u_{avg}(-k^2)}{D_{12}} a^2) = 0 \rightarrow k^2 = \frac{2D_{12}}{u_{avg} a^2} > 0 \quad \textbf{(B.26)}$$

Therefore, **(B.13)** becomes

$$X(x) = C_1 \cdot \exp(-k^2 \cdot x) = C_1 \cdot \exp(-\frac{2D_{12}}{u_{avg} a^2} \cdot x) = C_1 \cdot \exp(-\frac{4}{\mathrm{Re} \cdot Sc} \cdot \frac{x}{a}) \quad \textbf{(B.27)}$$

Here,

$\mathrm{Re} \equiv \frac{u_{avg}(2a)}{\nu}$, $Sc \equiv \frac{\nu}{D_{12}}$, and ν is a kinematic viscosity of the air stream in the piston ring pack.

From **(B.25)** and **(B.26)**,

$$Y(y) = a_1 y + \frac{1}{2}(-\frac{2}{a^2})\frac{a_1}{a} y^4 - \frac{3}{10}(-\frac{2}{a^2})\frac{a_1}{a^2} y^5 = a_1 y(1 - \frac{y^3}{a^3} + \frac{3}{5}\frac{y^4}{a^4}) \quad \textbf{(B.28)}$$

From **(B.27)** and **(B.28)**,

$$\rho(x,y) - \rho_s = \tilde{\rho}(x,y) = X(x)Y(y) = (C_1 \cdot a_1) y(1 - \frac{y^3}{a^3} + \frac{3}{5}\frac{y^4}{a^4}) \cdot \exp(-\frac{4}{\mathrm{Re} \cdot Sc}\frac{x}{a}) \quad \textbf{(B.29)}$$

From boundary condition **(B.5)**,

$$\rho_0 - \rho_s = (C_1 \cdot a_1) a(1 - 1 + \frac{3}{5}) \rightarrow C_1 \cdot a_1 = \frac{\rho_0 - \rho_s}{3a/5} \quad \textbf{(B.30)}$$

Finally, the oil vapor density profile **(2.31)** is proved to be

$$\rho(x,y) = \rho_s + \frac{\rho_0 - \rho_s}{3a/5} y(1 - \frac{y^3}{a^3} + \frac{3}{5}\frac{y^4}{a^4}) \cdot \exp(-\frac{4}{\mathrm{Re} \cdot Sc}\frac{x}{a}) \quad \textbf{(B.31)}$$

Appendix C. Derivation of Equation (2.34) – Equivalent Diffusion Length using the Series Solution from Appendix B

The bulk oil vapor density $\rho_m(x)$ was defined as below,

$$\rho_m(x) = \frac{1}{u_{avg} a} \int_0^a \rho(x,y) \cdot u(y) \cdot dy \tag{C.1}$$

And was calculated using **(B.1)** and **(B.31)**,

$$\rho_m(x) = \rho_s + (\rho_0 - \rho_s)\left(\frac{59}{84}\right) \cdot e^{-\frac{4}{\mathrm{Re}\,Sc}\left(\frac{x}{a}\right)} \tag{C.2}$$

The $\rho_m(x)$ satisfies the fully developed condition mass transfer, i.e.,

$$\frac{\partial}{\partial x}\left[\frac{\rho_s - \rho(x,y)}{\rho_s - \rho_m(x)}\right] = 0 \tag{C.3}$$

To get the average equivalent diffusion length $\delta_{diffsuion}$, the vaporized oil vapor flux was considered along the half circumference of the surface in a specified ring pack region.

$$\int_0^{\frac{\pi B}{2}} -\left.\frac{\partial \rho}{\partial y}\right|_{y=0} dx = \frac{\pi B}{2} \cdot \frac{\rho_s - \overline{\rho}_m}{\delta_{diffusion}} \tag{C.4}$$

$$\text{Where, } \overline{\rho}_m \equiv \frac{2}{\pi B} \int_0^{\frac{\pi B}{2}} \rho_m(x) dx = \rho_s + \frac{2}{\pi B}(\rho_0 - \rho_s)\frac{59}{84 \times 4}\mathrm{Re}\,Sc \cdot a \cdot (e^{-\frac{2B\pi}{\mathrm{Re}\,Sc \cdot a}} - 1) \tag{C.5}$$

The left hand side in **(C.4)** is

$$\int_0^{\frac{\pi B}{2}} -\left.\frac{\partial \rho}{\partial y}\right|_{y=0} dx = \int_0^{\frac{\pi B}{2}} \frac{5}{3a}(\rho_0 - \rho_s)\cdot e^{-\frac{4}{\mathrm{Re}\,Sc\,a}x} dx = \frac{5}{12}(\rho_0 - \rho_s)\,\mathrm{Re}\,Sc(e^{-\frac{2B\pi}{\mathrm{Re}\,Sc\cdot a}} - 1) \qquad \textbf{(C.6)}$$

The right hand side in **(C.4)** is

$$\frac{\pi B}{2}\cdot\frac{\rho_s - \overline{\rho}_m}{\delta_{diffusion}} = \frac{1}{\delta_{diffusion}}(\rho_0 - \rho_s)\frac{59}{84\times 4}\mathrm{Re}\,Sc\cdot a\cdot(e^{-\frac{2B\pi}{\mathrm{Re}\,Sc\cdot a}} - 1) \qquad \textbf{(C.7)}$$

From the equality of **(C.6)** and **(C.7)**, equation **(2.34)** can be proved to be

$$\delta_{diffusion} = \frac{12\times 59}{84\times 4\times 5}a = 0.42\cdot a \qquad \textbf{(C.8)}$$

Appendix D. Exact Solution of Partial Differential Equation (2.27) with Boundary Conditions (2.28)~(2.30)

To solve the same partial differential equation dealt in **Appendix B** exactly, independent variables x and y are non-dimensionalized for the mathematical convenience as follows.

$$\frac{x}{a} = \tilde{x} \text{ and } \frac{y}{a} = \tilde{y} \tag{D.1}$$

Then, using the separation of variables $\tilde{\rho}(\tilde{x},\tilde{y}) = \rho(\tilde{x},\tilde{y}) - \rho_s = X(\tilde{x})Y(\tilde{y})$, the given partial differential equation becomes

$$\frac{6u_{avg}a}{D_{12}}\frac{X'}{X} = \frac{1}{\tilde{y}-\tilde{y}^2}\frac{Y''}{Y} = -k^2 \tag{D.2}$$

Here, k is an arbitrary constant to be determined.

With homogeneous boundary conditions

$$\tilde{\rho} = 0 \text{ at } \tilde{y} = 0 \tag{D.3}$$

$$\tilde{\rho} = \rho_0 - \rho_s \quad \text{at } \tilde{x} = 0 \text{ and } \tilde{y} = 1 \tag{D.4}$$

$$\frac{\partial\tilde{\rho}}{\partial y} = 0 \text{ at } \tilde{y} = 1 \tag{D.5}$$

X equation

$$X' + \frac{k^2 D_{12}}{6u_{avg}a}X = 0 \tag{D.6}$$

$$\rightarrow X(\tilde{x}) = C_0 \exp(-\frac{k^2 D_{12}}{6u_{avg} a}\tilde{x}) \qquad \textbf{(D.7)}$$

Y equation

$$Y'' + k^2(\tilde{y} - \tilde{y}^2)Y = 0 \qquad \textbf{(D.8)}$$

$$Y'' + k^2(\frac{1}{4} - (\tilde{y} - \frac{1}{2})^2)Y = 0 \qquad \textbf{(D.9)}$$

Let $\tilde{y} - \frac{1}{2} = z$, then

$$Y'' + k^2(\frac{1}{4} - z^2)Y = 0 \qquad \textbf{(D.10)}$$

To erase k, let $t = m \cdot z$

$$m^2 \frac{d^2Y}{dt^2} + k^2(\frac{1}{4} - \frac{t^2}{m^2})Y = 0 \qquad \textbf{(D.11)}$$

$$\rightarrow \frac{d^2Y}{dt^2} + (\frac{k^2}{m^2}\frac{1}{4} - \frac{k^2 t^2}{m^4})Y = 0 \qquad \textbf{(D.12)}$$

Comparing **(D.12)** with a **parabolic cylinder equation**

$$Y'' + (v + \frac{1}{2} - \frac{t^2}{4})Y = 0 \qquad \textbf{(D.13)}$$

results in

$$v + \frac{1}{2} = \frac{k^2}{4m^2} \quad \text{and} \quad \frac{m^4}{k^2} = 4 \qquad \textbf{(D.14)}$$

$$\rightarrow m^2 = 2k > 0 \text{ and } \nu = \frac{k}{8} - \frac{1}{2} \tag{D.15}$$

Therefore, the solution of **Y equation** is

$$Y(t) = C_1 \cdot D_\nu(t) + C_2 \cdot D_\nu(-t) \tag{D.16}$$

or

$$Y(\tilde{y}) = C_1 \cdot D_{\frac{k}{8}-\frac{1}{2}}(\sqrt{2k}(\tilde{y} - \frac{1}{2})) + C_2 \cdot D_{\frac{k}{8}-\frac{1}{2}}(-\sqrt{2k}(\tilde{y} - \frac{1}{2})) \tag{D.17}$$

Here, $D_\nu(t)$ is a **parabolic cylinder function,** which is a solution of a **parabolic differential equation** $Y'' + (\nu + \frac{1}{2} - \frac{t^2}{4})Y = 0$ and whose Taylor series is

$$D_\nu(t) = \frac{\sqrt{\pi} \cdot 2^{\nu/2}}{\Gamma(\frac{1}{2} - \frac{1}{2}\nu)} \sum_{n=0}^{\infty} \frac{a_{2n} t^{2n}}{(2n)!} - \frac{\sqrt{\pi} \cdot 2^{(\nu+1)/2}}{\Gamma(-\frac{1}{2}\nu)} \sum_{n=0}^{\infty} \frac{a_{2n+1} t^{2n+1}}{(2n+1)!} \tag{D.18}$$

Where $a_0 = a_1 = 1$ and $a_{n+2} = -(\nu + \frac{1}{2})a_n + \frac{1}{4}n(n-1)a_{n-2}$ [17]

$$\Gamma(z) = \int_0^\infty t^{z-1} e^{-t} dt, \ \mathrm{Re}\, z > 0 \tag{D.19}$$

Therefore, with equation **(D.7)** and **(D.17)**, the general solution is

$$\tilde{\rho}(\tilde{x}, \tilde{y}) = C_0 \exp(-\frac{k^2 D_{12}}{6u_{avg} a}\tilde{x})[C_1 \cdot D_{\frac{k}{8}-\frac{1}{2}}(\sqrt{2k}(\tilde{y} - \frac{1}{2})) + C_2 \cdot D_{\frac{k}{8}-\frac{1}{2}}(-\sqrt{2k}(\tilde{y} - \frac{1}{2}))] \tag{D.20}$$

Or by letting $K_1 \equiv C_0 C_1$ and $K_2 \equiv C_0 C_2$

$$\tilde{\rho}(\tilde{x},\tilde{y}) = \exp(-\frac{k^2 D_{12}}{6u_{avg}a}\tilde{x})[K_1 \cdot D_{\frac{k}{8}-\frac{1}{2}}(\sqrt{2k}(\tilde{y}-\frac{1}{2})) + K_2 \cdot D_{\frac{k}{8}-\frac{1}{2}}(-\sqrt{2k}(\tilde{y}-\frac{1}{2}))] \qquad \textbf{(D.21)}$$

From boundary condition **(D.3)**,

$$K_1 \cdot D_{\frac{k}{8}-\frac{1}{2}}\left(-\sqrt{\frac{k}{2}}\right) + K_2 \cdot D_{\frac{k}{8}-\frac{1}{2}}\left(\sqrt{\frac{k}{2}}\right) = 0 \qquad \textbf{(D.22)}$$

From boundary condition **(D.5)**,

$$K_1 \cdot D'_{\frac{k}{8}-\frac{1}{2}}\left(\sqrt{\frac{k}{2}}\right) - K_2 \cdot D'_{\frac{k}{8}-\frac{1}{2}}\left(-\sqrt{\frac{k}{2}}\right) = 0 \qquad \textbf{(D.23)}$$

Here, prime (') means derivative with respect to x.

From **(D.22)** and **(D.23)**,

$$\begin{bmatrix} D_{\frac{k}{8}-\frac{1}{2}}\left(-\sqrt{\frac{k}{2}}\right) & D_{\frac{k}{8}-\frac{1}{2}}\left(\sqrt{\frac{k}{2}}\right) \\ D'_{\frac{k}{8}-\frac{1}{2}}\left(-\sqrt{\frac{k}{2}}\right) & -D'_{\frac{k}{8}-\frac{1}{2}}\left(\sqrt{\frac{k}{2}}\right) \end{bmatrix} \begin{bmatrix} K_1 \\ K_2 \end{bmatrix} = \begin{bmatrix} 0 \\ 0 \end{bmatrix} \qquad \textbf{(D.24)}$$

For the simultaneous equation set in **(D.24)** to have nontrivial solution K_1 and K_2, the determinant of 2 by 2 matrix in **(D.24)** should be zero, i.e.,

$$D_{\frac{k}{8}-\frac{1}{2}}\left(\sqrt{\frac{k}{2}}\right) D'_{\frac{k}{8}-\frac{1}{2}}\left(-\sqrt{\frac{k}{2}}\right) + D_{\frac{k}{8}-\frac{1}{2}}\left(-\sqrt{\frac{k}{2}}\right) D'_{\frac{k}{8}-\frac{1}{2}}\left(\sqrt{\frac{k}{2}}\right) = 0 \qquad \textbf{(D.25)}$$

Therefore, the unknown k can be calculated by numerical calculation of **(D.25)** with the help of following difference equation [17].

$$D_\nu'(x) = -\frac{1}{2}xD_\nu(x) + (\nu + \frac{1}{2})D_{\nu-1}(x) \tag{D.26}$$

Also, from **(D.22)**,

$$K_2 = -\frac{D_{\frac{k}{8}-\frac{1}{2}}\left(-\sqrt{\frac{k}{2}}\right)}{D_{\frac{k}{8}-\frac{1}{2}}\left(\sqrt{\frac{k}{2}}\right)}K_1 \tag{D.27}$$

Therefore, the remaining unknown is now K_1. From the remaining boundary condition **(D.4)** and **(D.21)**, the K_1 can be determined.

$$K_1 \cdot D_{\frac{k}{8}-\frac{1}{2}}\left(\sqrt{\frac{k}{2}}\right) + K_2 \cdot D_{\frac{k}{8}-\frac{1}{2}}\left(-\sqrt{\frac{k}{2}}\right) = \rho_0 - \rho_s \tag{D.28}$$

From **(D.27)** and **(D.28)** with already determined k in **(D.25)**,

$$K_1 = \frac{D_{\frac{k}{8}-\frac{1}{2}}\left(\sqrt{\frac{k}{2}}\right)}{\left[D_{\frac{k}{8}-\frac{1}{2}}\left(\sqrt{\frac{k}{2}}\right)\right]^2 - \left[D_{\frac{k}{8}-\frac{1}{2}}\left(-\sqrt{\frac{k}{2}}\right)\right]^2}(\rho_0 - \rho_s) \tag{D.29}$$

$$K_2 = -\frac{D_{\frac{k}{8}-\frac{1}{2}}\left(-\sqrt{\frac{k}{2}}\right)}{\left[D_{\frac{k}{8}-\frac{1}{2}}\left(\sqrt{\frac{k}{2}}\right)\right]^2 - \left[D_{\frac{k}{8}-\frac{1}{2}}\left(-\sqrt{\frac{k}{2}}\right)\right]^2}(\rho_0 - \rho_s) \tag{D.30}$$

Finally, the exact solution is

$$\rho(\mathrm{x},\mathrm{y}) = \rho_s + \frac{\exp(-\frac{k^2 D_{12}}{6u_{avg}a^2}x)\cdot(\rho_0-\rho_s)}{\left[D_{\frac{k}{8}-\frac{1}{2}}\left(\sqrt{\frac{k}{2}}\right)\right]^2 - \left[D_{\frac{k}{8}-\frac{1}{2}}\left(-\sqrt{\frac{k}{2}}\right)\right]^2}\times$$
$$[D_{\frac{k}{8}-\frac{1}{2}}\left(\sqrt{\frac{k}{2}}\right)\cdot D_{\frac{k}{8}-\frac{1}{2}}(\sqrt{2k}(\frac{y}{a}-\frac{1}{2})) - D_{\frac{k}{8}-\frac{1}{2}}\left(-\sqrt{\frac{k}{2}}\right)\cdot D_{\frac{k}{8}-\frac{1}{2}}(-\sqrt{2k}(\frac{y}{a}-\frac{1}{2}))] \quad \textbf{(D.31)}$$

Or

$$\rho(\mathrm{x},\mathrm{y}) = \rho_s + \frac{\exp(-\frac{k^2}{3\mathrm{Re}\,Sc}\frac{x}{a})\cdot(\rho_0-\rho_s)}{\left[D_{\frac{k}{8}-\frac{1}{2}}\left(\sqrt{\frac{k}{2}}\right)\right]^2 - \left[D_{\frac{k}{8}-\frac{1}{2}}\left(-\sqrt{\frac{k}{2}}\right)\right]^2}\times$$
$$[D_{\frac{k}{8}-\frac{1}{2}}\left(\sqrt{\frac{k}{2}}\right)\cdot D_{\frac{k}{8}-\frac{1}{2}}(\sqrt{2k}(\frac{y}{a}-\frac{1}{2})) - D_{\frac{k}{8}-\frac{1}{2}}\left(-\sqrt{\frac{k}{2}}\right)\cdot D_{\frac{k}{8}-\frac{1}{2}}(-\sqrt{2k}(\frac{y}{a}-\frac{1}{2}))] \quad \textbf{(D.32)}$$

This exact solution is not practical in use compared to approximate series solution **(B.31)**. Therefore, the results from **(B.31)** were used exclusively in this work.

Appendix E. Derivation of Equation (2.36) – Mass Transfer Entrance Length

To estimate the mass transfer entrance length, the density profile in the mass transfer boundary layer was determined first. If the non-dimensional oil vapor density is represented as follows,

$$\frac{\rho(x,y)-\rho_s}{\rho_0-\rho_s} \equiv \theta(x,y) \qquad \textbf{(E.1)}$$

Here, ρ_s and ρ_0 were defined in **(B.3)** and in **(B.5)** respectively. $\theta(x,y)$ is the non-dimensional oil vapor density with variation of mass transfer boundary layer.

Since mass transfer boundary layer δ_m grows with x, i.e. along the circumference, the non-dimensional oil vapor density $\theta(x,y)$ can be seen as a function of $\delta_m(x)$ and y (piston axial direction). Particularly, if $\theta(x,y)$ is a function of $\frac{y}{\delta_m(x)}$ considering the similarity between varying density profiles in the mass transfer boundary layer,

$$\theta(\eta=\frac{y}{\delta_m(x)}) = A+B\cdot\eta+C\cdot\eta^2+D\cdot\eta^3 \qquad \textbf{(E.2)}$$

With boundary conditions on θ

At $y=0$, $\theta=0$ and $\theta''=0$ **(E.3)**

At $y=\delta_m$, $\theta=1$ and $\theta'=0$ **(E.4)**

Therefore, from **(E.2)~(E.4)**,

$$\theta(\eta) = \frac{3}{2}\eta - \frac{1}{2}\eta^3 \qquad \textbf{(E.5)}$$

Applying integral methods to the original partial differential equation **(B.2)**,

$$\frac{d}{dx}\int_0^{\delta_m} \rho \cdot u \cdot dy + D_{12} \cdot \left.\frac{\partial \rho}{\partial y}\right|_{y=0} = 0 \qquad \textbf{(E.6)}$$

From equation **(E.1)**,

$$\frac{\partial \rho}{\partial y} = (\rho_0 - \rho_s)\frac{\partial \theta}{\partial y} \qquad \textbf{(E.7)}$$

Therefore, equation **(E.6)** becomes

$$\frac{d}{dx}\int_0^{\delta_m} [\rho_s + (\rho_0 - \rho_s)\cdot\theta]\cdot u \cdot dy + D_{12} \cdot (\rho_0 - \rho_s)\left.\frac{\partial \theta}{\partial y}\right|_{y=0} = 0 \qquad \textbf{(E.8)}$$

For the mathematical convenience, $\rho_0 \equiv 0$, then **(E.8)** becomes

$$\frac{d}{dx}\int_0^{\delta_m} (\theta - 1)\cdot u \cdot dy + D_{12} \cdot \left.\frac{\partial \theta}{\partial y}\right|_{y=0} = 0 \qquad \textbf{(E.9)}$$

Substituting **(B.1)** and **(E.5)** into **(E.9)** results in

$$\frac{d}{dx}\int_0^{\delta_m} 6\cdot\frac{y}{a}\cdot\left(1-\frac{y}{a}\right)\cdot\left[\frac{3}{2}\frac{y}{\delta_m} - \frac{1}{2}\left(\frac{y}{\delta_m}\right)^2 - 1\right]\cdot dy + \frac{D_{12}}{u_{avg}}\cdot\frac{3}{2}\cdot\frac{1}{\delta_m} = 0 \qquad \textbf{(E.10)}$$

After simplifying the integral term,

$$\delta_m \frac{d}{dx}[-\frac{\delta_m{}^2}{10 \cdot a} + \frac{\delta_m{}^3}{18 \cdot a^2}] + \frac{D_{12}}{4u_{avg}} = 0 \qquad \textbf{(E.11)}$$

If $\frac{\delta_m}{a} \equiv \zeta$, then **(E.11)** becomes

$$\zeta \frac{d}{dx}[\frac{\zeta^3}{18} - \frac{\zeta^2}{10}] + \frac{D_{12}}{4u_{avg}a^2} = 0 \qquad \textbf{(E.12)}$$

Integrating from $x = 0$ to $x = x_{m,e}$ (mass transfer entrance length),

$$\frac{\zeta^4}{24} - \frac{\zeta^3}{15} + \frac{D_{12}x_{m,e}}{4u_{avg}a^2} = 0 \qquad \textbf{(E.13)}$$

Substituting $\delta_m \approx \frac{a}{2}$ at $x = x_{m,e}$ into **(E.13)** results in

$$x_{m,e} = \frac{11}{480}\frac{u_{avg}a}{D_{12}} \qquad \textbf{(E.14)}$$

By introducing $\mathrm{Re} = \frac{u_{avg}(2a)}{\nu_{air}}$ and $Sc = \frac{\nu_{air}}{D_{12}}$, **(E.14)** can be represented as

$$\frac{x_{m,e}}{a} = \frac{11}{960}\mathrm{Re}\,Sc \qquad \textbf{(E.15)}$$

Appendix F. Sample Calculation of Entrance Length in the 2nd Land Region in the Piston Ring Pack

In the 2nd land region of the piston ring pack tested in this work,

T(temperature) ~ $426.4(K)$, μ(viscosity) ~ $23.53\times10^{-6}(kg/m\cdot s)$,

ν(kinematic viscosity) ~ $28.6\times10^{-6}(m^2/s)$, Pr(Prnadtl number) ~ 0.69,

$\dot{V}$(volume flow rate) ~ $20(l/\min)$, $a(clearance)$ ~ $5\times10^{-5}(m)$,

L(2nd land height) ~ $7\times10^{-3}(m)$, D_{12}(diffusion coefficient) ~ $6.24\times10^{-6}(m^2/s)$,

B(bore) ~ $0.13101(m)$, Sc(Scmidt number) ~ 4.58, Re(Reynolds number) ~ 1591

The length of half circumference of the 2nd land ~ 20 (cm)

Hydrodynamic entrance length

From [18], the hydrodynamic entrance length $x_{h,e}$ in the developing region for the laminar flow is

$$x_{h,e} = D_h(0.011\cdot \mathrm{Re} + \frac{0.315}{1+0.0175\cdot \mathrm{Re}})$$

Here $D_h = 2a$ is the hydraulic diameter for the flow between parallel plates.

$$x_{h,e} = 2(5\times10^{-5})(0.011\times1591 + \frac{0.315}{1+0.0175\times1591}) = 0.0018(m) = 1.8(mm) << 20(cm)$$

Thermal entrance length

From analogy between heat transfer and mass transfer, the thermal entrance length $x_{t,e}$ can be calculated as follows.

$$x_{t,e} = \frac{11}{960} \cdot \mathrm{Re} \cdot \mathrm{Pr} \cdot a = \frac{11}{960}(1591)(0.69)(5 \times 10^{-5}) = 6.3 \times 10^{-4}(m) = 0.63(mm) << 20(cm)$$

Mass transfer entrance length

From **(E.15)**, the mass transfer entrance length $x_{m,e}$ is

$$x_{m,e} = \frac{11}{960} \cdot \mathrm{Re} \cdot Sc \cdot a = \frac{11}{960}(1591)(4.58)(5 \times 10^{-5}) = 0.0042(m) = 4.2(mm) << 20(cm)$$

Appendix G. Lennard-Jones 6-12 Model

Characteristic Lennard-Jones length

The characteristic Lennard-Jones length or the collision diameter σ used in equation **(2.46)** is based on the Lennard-Jones 6-12 model that explains the forces acting between a pair of molecules during a collision by a potential energy of interaction ϕ [9]. (**Figure G.1**)

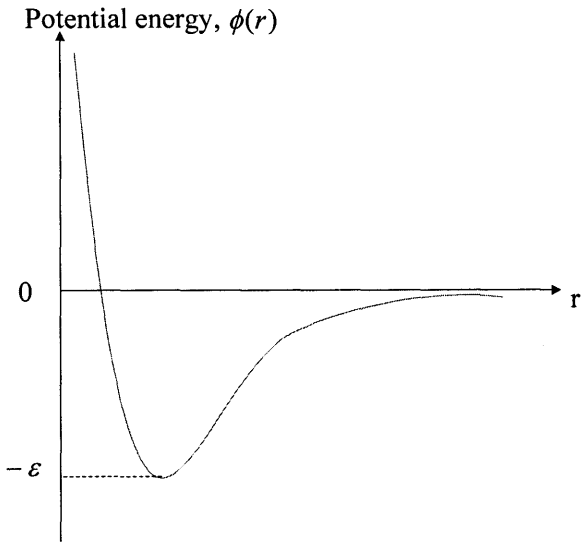

Figure G.1. Potential energy for interaction as given by the Lennard-Jones 6-12 Model

$$\phi(r) = 4\varepsilon\left[\left(\frac{\sigma}{r}\right)^{12} - \left(\frac{\sigma}{r}\right)^{6}\right] \qquad \textbf{(G.1)}$$

Where, the collision diameter σ is the value of r for which $\phi(r) = 0$, ε is the maximum energy of attraction between a pair of molecules. The model exhibits weak attraction, due to London dispersion forces at large separation (r^{-6}), and strong repulsion due to electron cloud overlapping, at small separation (r^{-12}).

Le Bas volume [13]

For a pure oil component

$$\sigma_{oil} = 1.18 \cdot V_b^{\frac{1}{3}} (\mathring{A}) \qquad \textbf{(G.2)}$$

And the Le Bas volume is

$$V_b = 14.8 \times (\text{Number of C}) + 3.7 \times (\text{Number of H}) \qquad \textbf{(G.3)}$$

For the air,

$$\sigma_{air} = 3.711 (\mathring{A}) \qquad \textbf{(G.4)}$$

For the air-oil vapor mixture,

$$\sigma_{oil,air} = \frac{\sigma_{oil} + \sigma_{air}}{2} \qquad \textbf{(G.5)}$$

Diffusion Collision Integral [13]

The diffusion collision integral Ω_D used in equation **(2.46)** is

$$\Omega_D = \frac{A}{T^{*B}} + \frac{C}{e^{DT^*}} + \frac{E}{e^{FT^*}} + \frac{G}{e^{HT^*}} \qquad \textbf{(G.6)}$$

Where,

$A = 1.06036, B = 0.15610, C = 0.19300, D = 0.47635$
$E = 1.03587, F = 1.52966, G = 1.76474, H = 3.89411$

$$T^* = \frac{kT}{\varepsilon_{oil,air}} = \frac{T}{(\varepsilon/k)_{oil,air}} \qquad \textbf{(G.7)}$$

where,

T : The air-oil vapor mixture temperature (K)

k : Boltzman constant = $1.381 \times 10^{-23} (J/K)$

$$\varepsilon_{oil,air} = \sqrt{\varepsilon_{oil}\varepsilon_{air}}(J) \text{ or } (\varepsilon/k)_{oil,air} = \sqrt{(\varepsilon/k)_{oil}(\varepsilon/k)_{air}}(J) \qquad \textbf{(G.8)}$$

$$(\varepsilon/k)_{oil} = 1.15T_b(K) \text{ and } (\varepsilon/k)_{air} = 78.6(K) \qquad \textbf{(G.9)}$$

Here, $T_b(K)$ is the boiling point of the oil component considered.

Appendix H. Required Pre-Evaluation (I)

Volume of each region

$V_1, V_{1\_2}, V_2, V_{2\_3}, V_3, V_{3\_4}, V_4, V_{4\_5}, V_5$

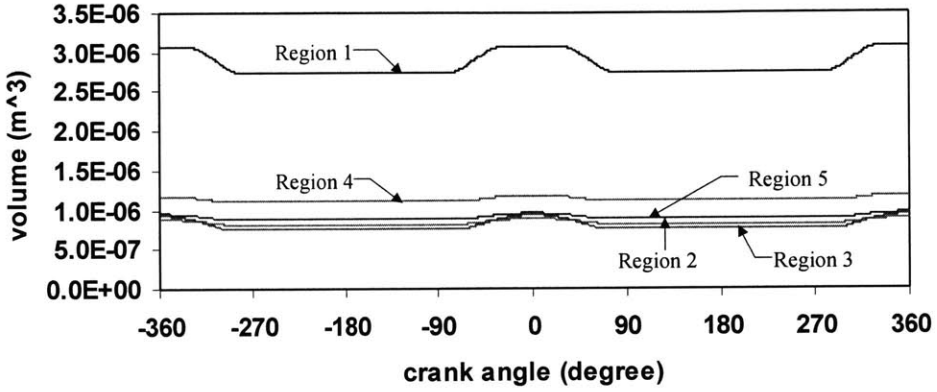

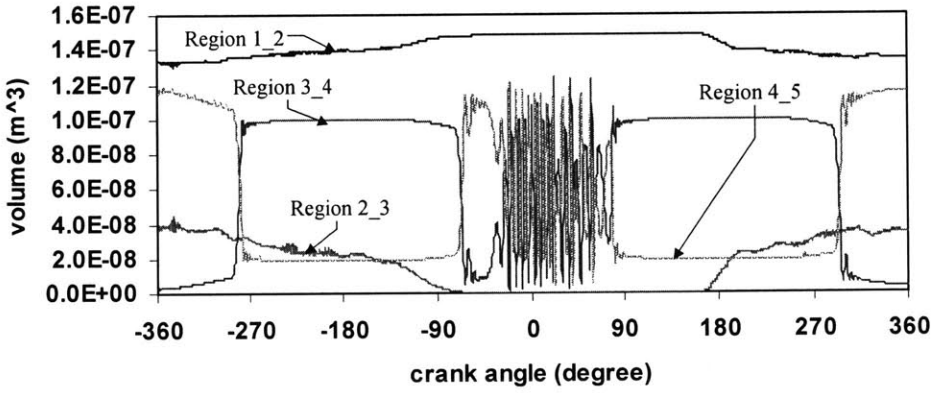

Figure H.1. Volume of each region in the piston ring pack during engine operation

Volume change of each region

$\dot{V}_1, \dot{V}_{1\_2}, \dot{V}_2, \dot{V}_{2\_3}, \dot{V}_3, \dot{V}_{3\_4}, \dot{V}_4, \dot{V}_{4\_5}, \dot{V}_5$ where, dot denotes $\frac{d}{d\hat{t}}$

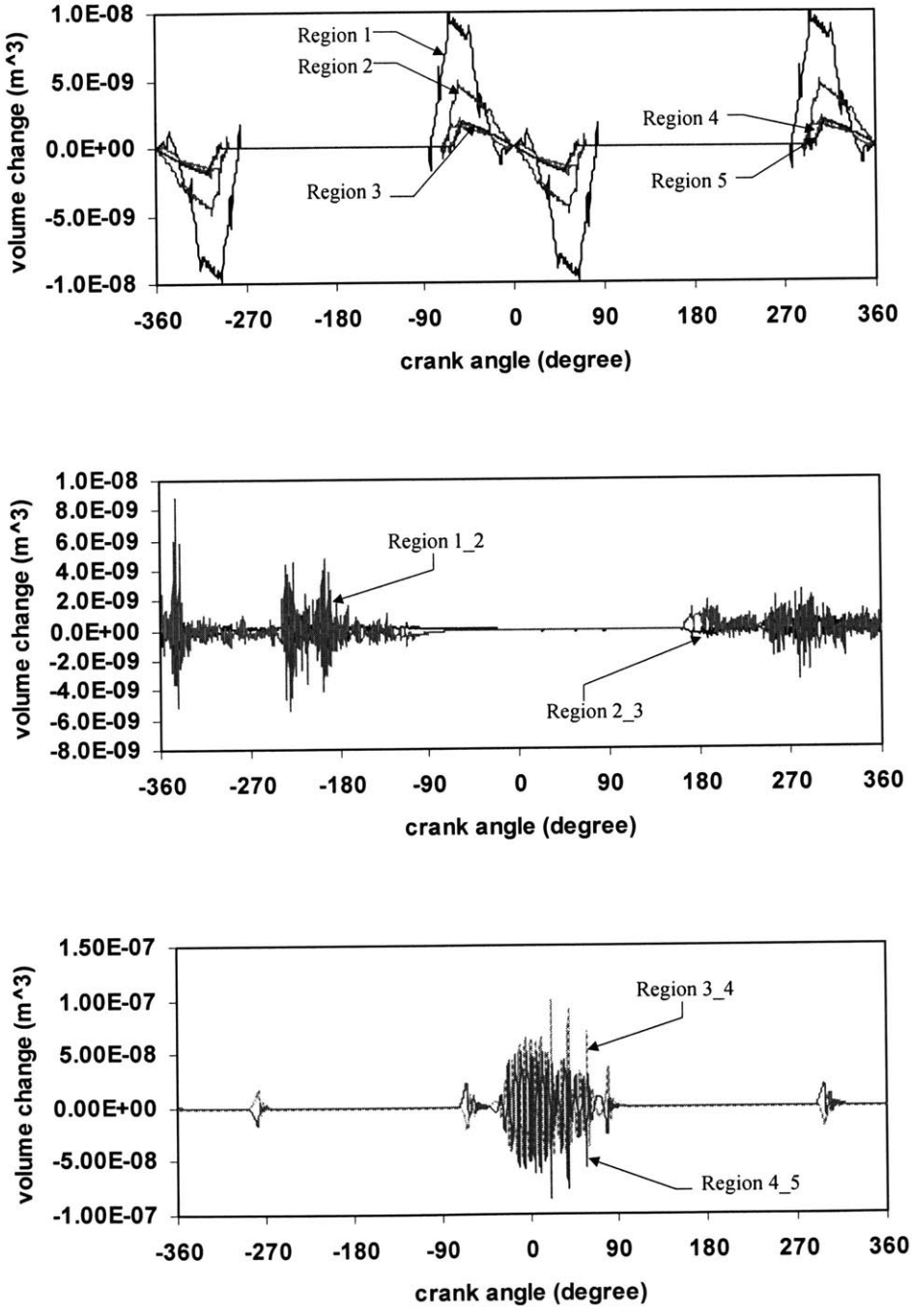

Figure H.2. Volume change of each region in the piston ring pack during engine operation

Pressure-driven volume flow rate of gas

$$\dot{V}_{0\to1}, \dot{V}_{1\to1\_2}, \dot{V}_{1\to3}, \dot{V}_{1\_2\to2}, \dot{V}_{2\to2\_3}, \dot{V}_{2\_3\to3}, \dot{V}_{3\to3\_4}, \dot{V}_{3\to5}, \dot{V}_{3\_4\to4}, \dot{V}_{4\to4\_5}, \dot{V}_{4\_5\to5}, \dot{V}_{5\to6}, \dot{V}_{5\to7}, \dot{V}_{6\to7}$$

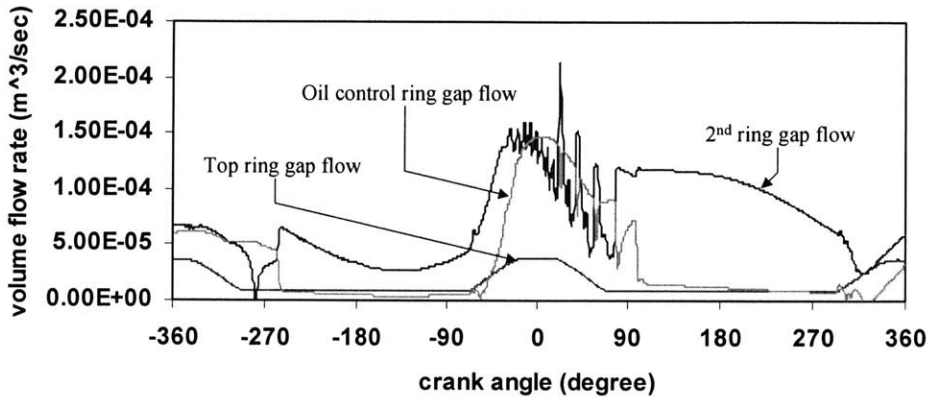

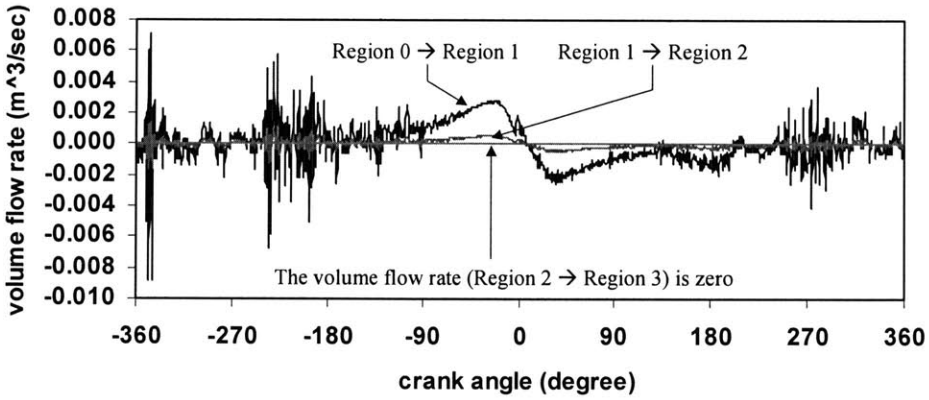

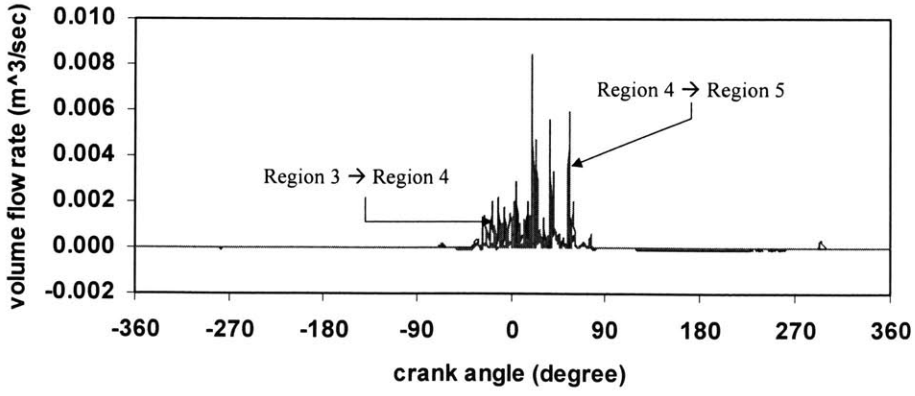

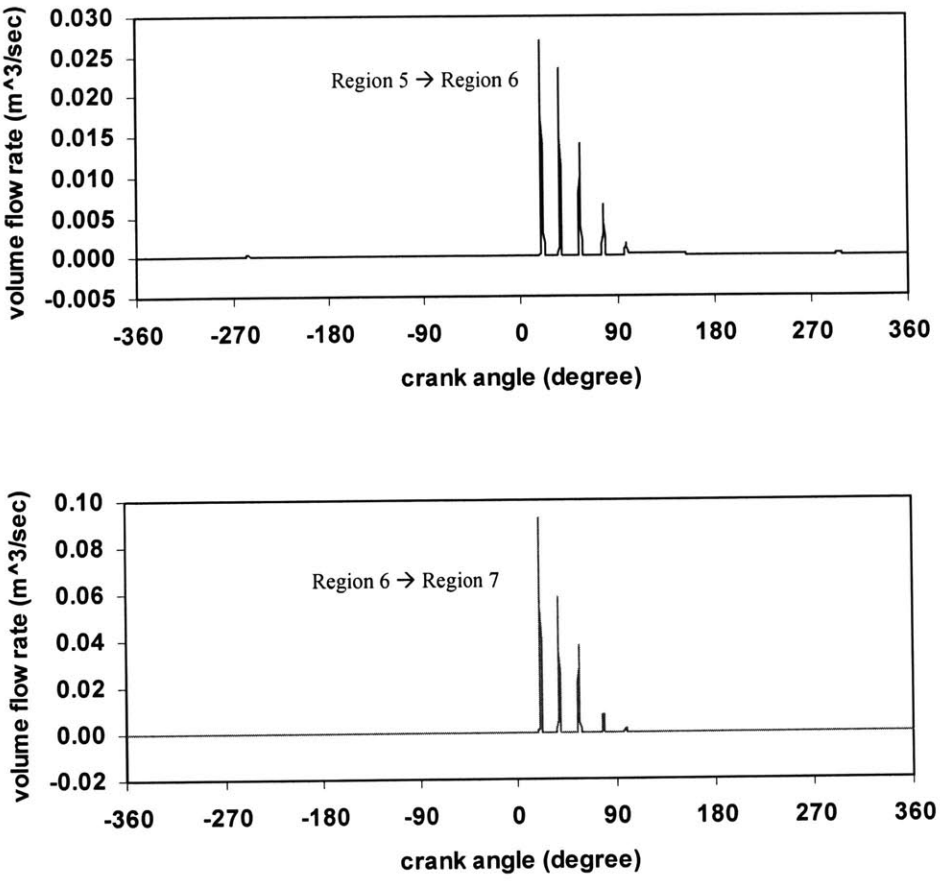

Figure H.3. Pressure-driven volume flow rate in the piston ring pack during engine operation

Pumping-driven volume flow rate

$$\dot{V}_{1\to1\_2,pump}, \dot{V}_{2\to1\_2,pump}, \dot{V}_{2\to2\_3,pump}, \dot{V}_{3\to2\_3,pump}, \dot{V}_{3\to3\_4,pump}, \dot{V}_{4\to3\_4,pump}, \dot{V}_{4\to4\_5,pump}, \dot{V}_{5\to4\_5,pump}$$

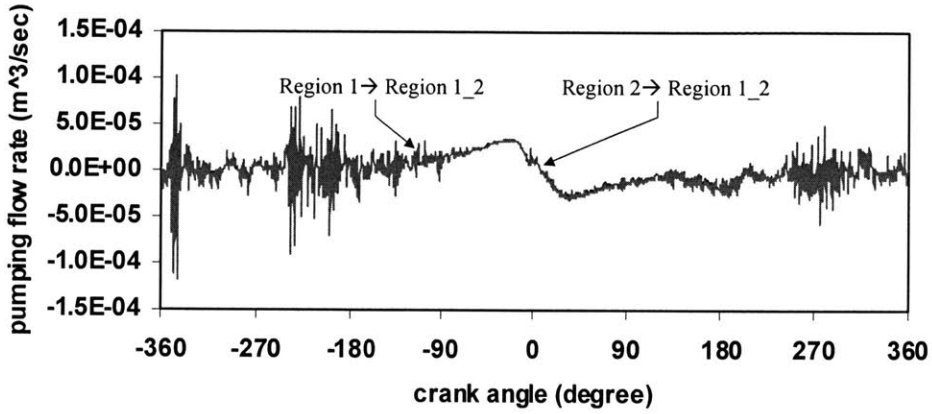

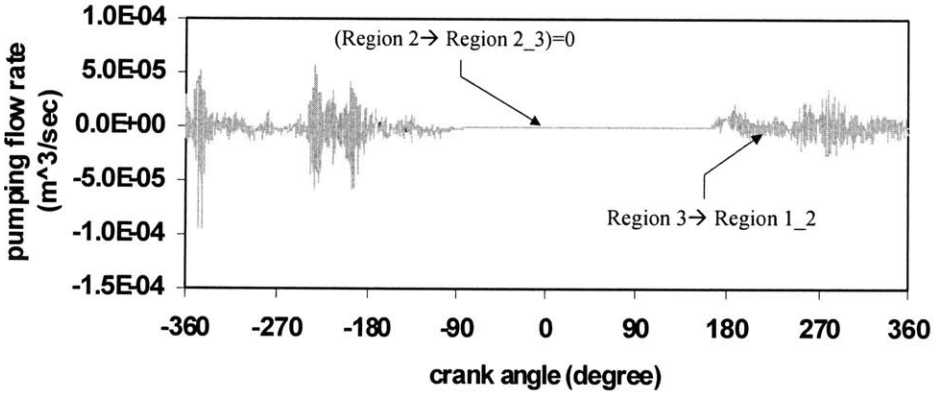

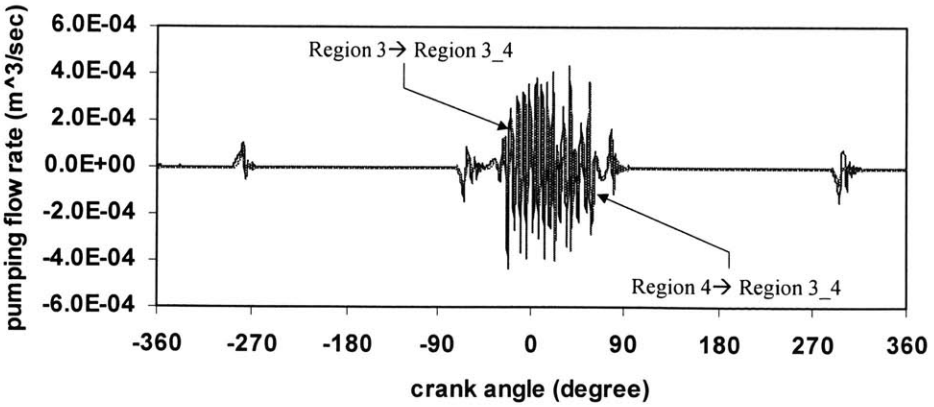

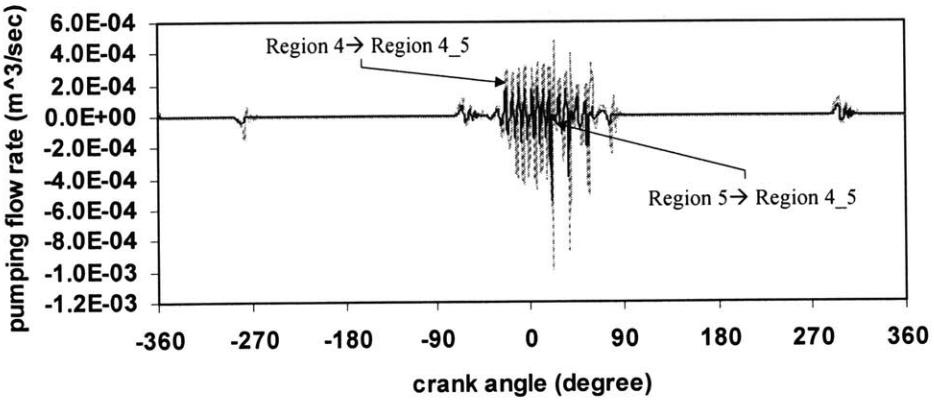

Figure H.4. Pumping-driven volume flow rate in the piston ring pack during engine operation

Pressure change

$P_1, P_{1\_2}, P_2, P_{2\_3}, P_3, P_{3\_4}, P_4, P_{4\_5}, P_5$

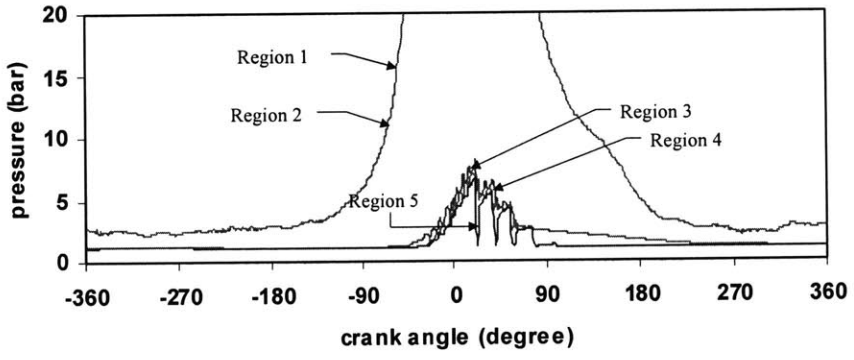

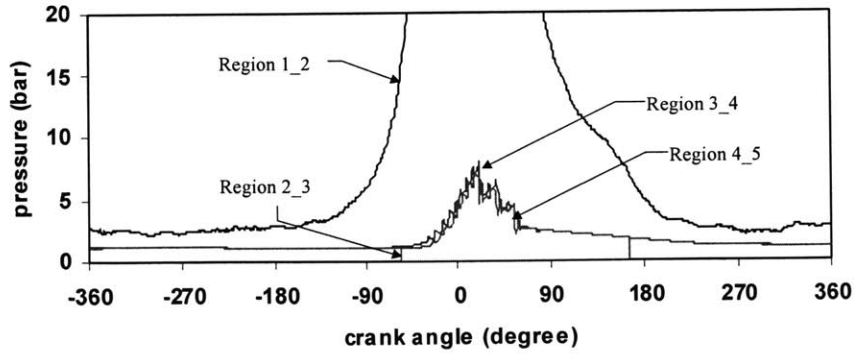

Figure H.5. Pressure change in the piston ring pack during engine operation

Appendix I. Required Pre-Evaluation (II)

Equivalent diffusion length

$L_{1,land}, L_{1,liner}, L_{1\_2}, L_2, L_{2\_3}, L_{3,land}, L_{3,liner}, L_{3\_4}, L_4, L_{4\_5}, L_{5,land}, L_{5,liner}$

where, $L_{1,land} = L_{1,liner}, L_{3,land} = L_{3,liner}, L_{5,land} = L_{5,liner}$

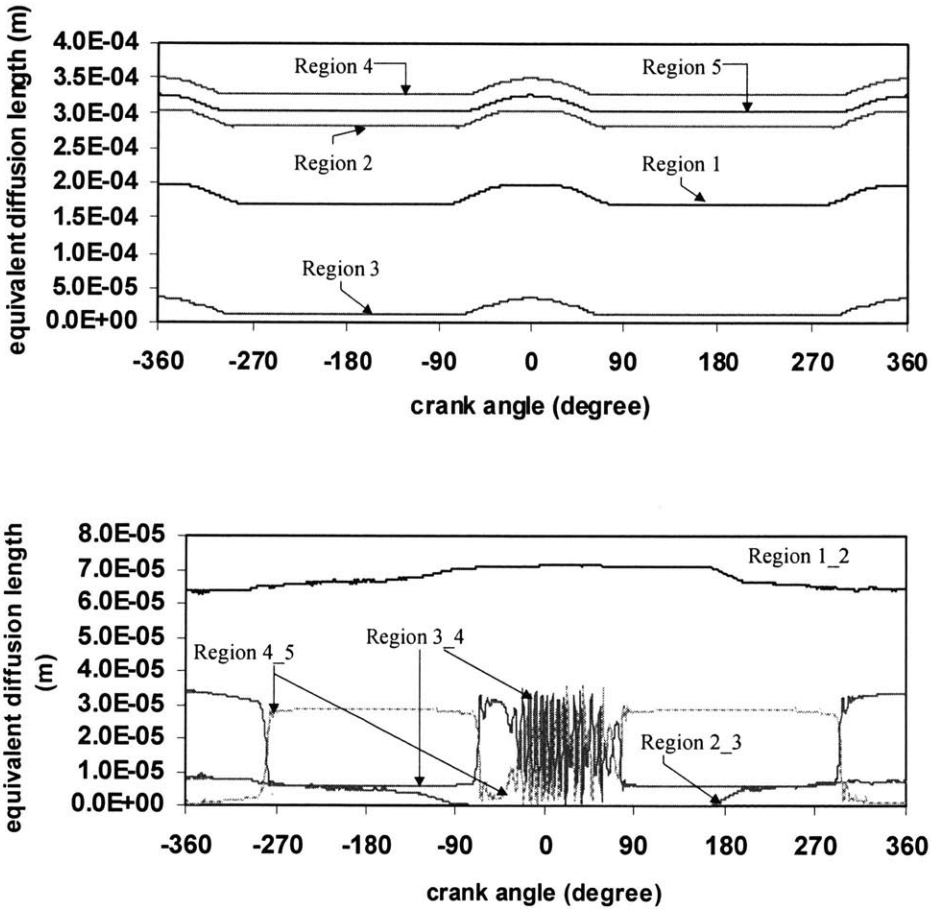

Figure I.1. Equivalent diffusion length in the piston ring pack during engine operation

Vaporization area

$A_{1,land}$, $A_{1,liner}$, A_{1_2}, A_2, A_{2_3}, $A_{3,land}$, $A_{3,liner}$, A_{3_4}, A_4, A_{4_5}, $A_{5,land}$, $A_{5,liner}$

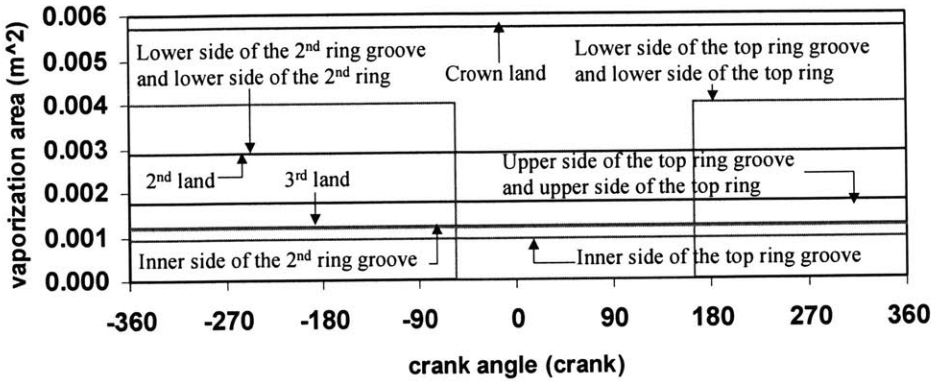

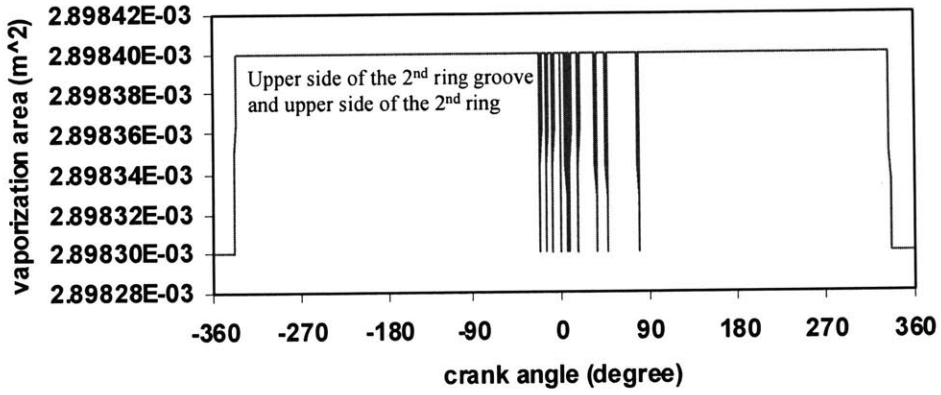

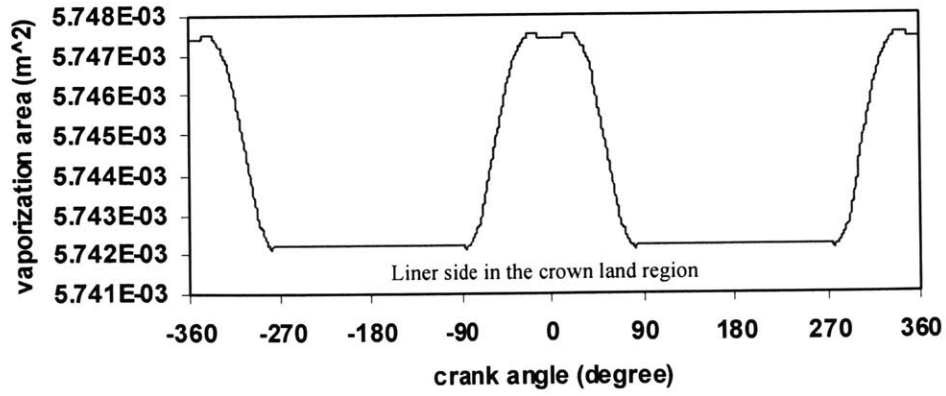

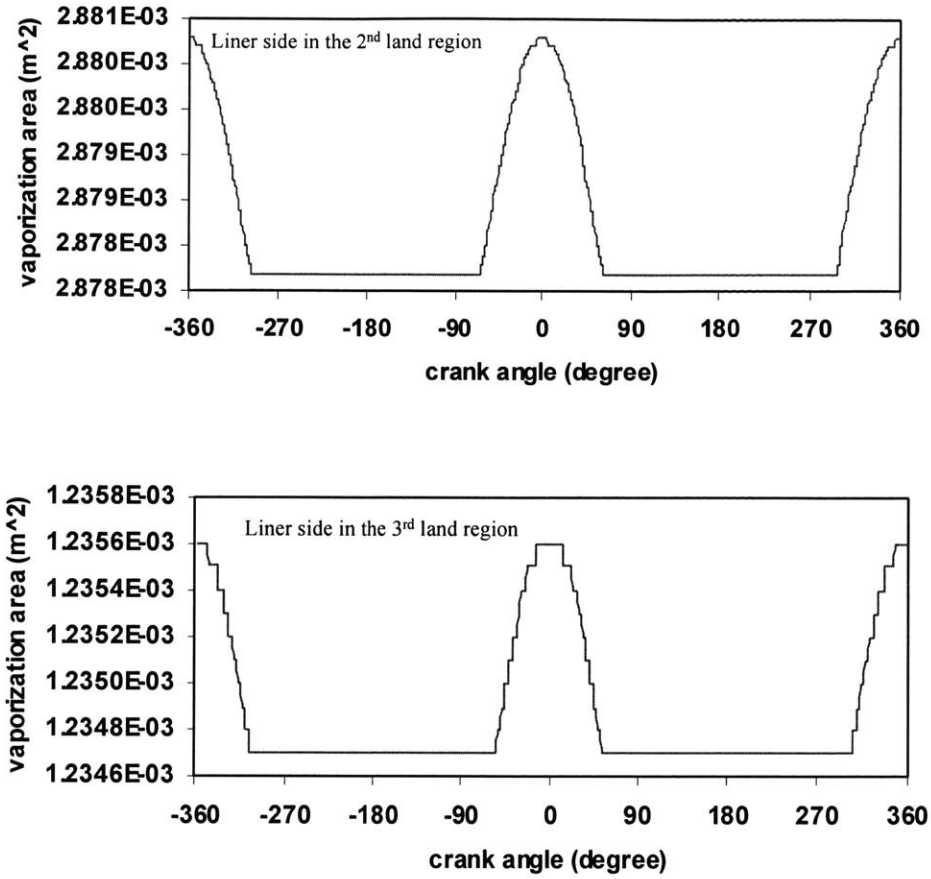

Figure I.2. Vaporization area in the piston ring pack during engine operation

Equivalent diffusion coefficient

$(D_{oil,air})_1, (D_{oil,air})_{1\_2}, (D_{oil,air})_2, (D_{oil,air})_{2\_3}, (D_{oil,air})_3, (D_{oil,air})_{3\_4}, (D_{oil,air})_4, (D_{oil,air})_{4\_5}$, $(D_{oil,air})_5$

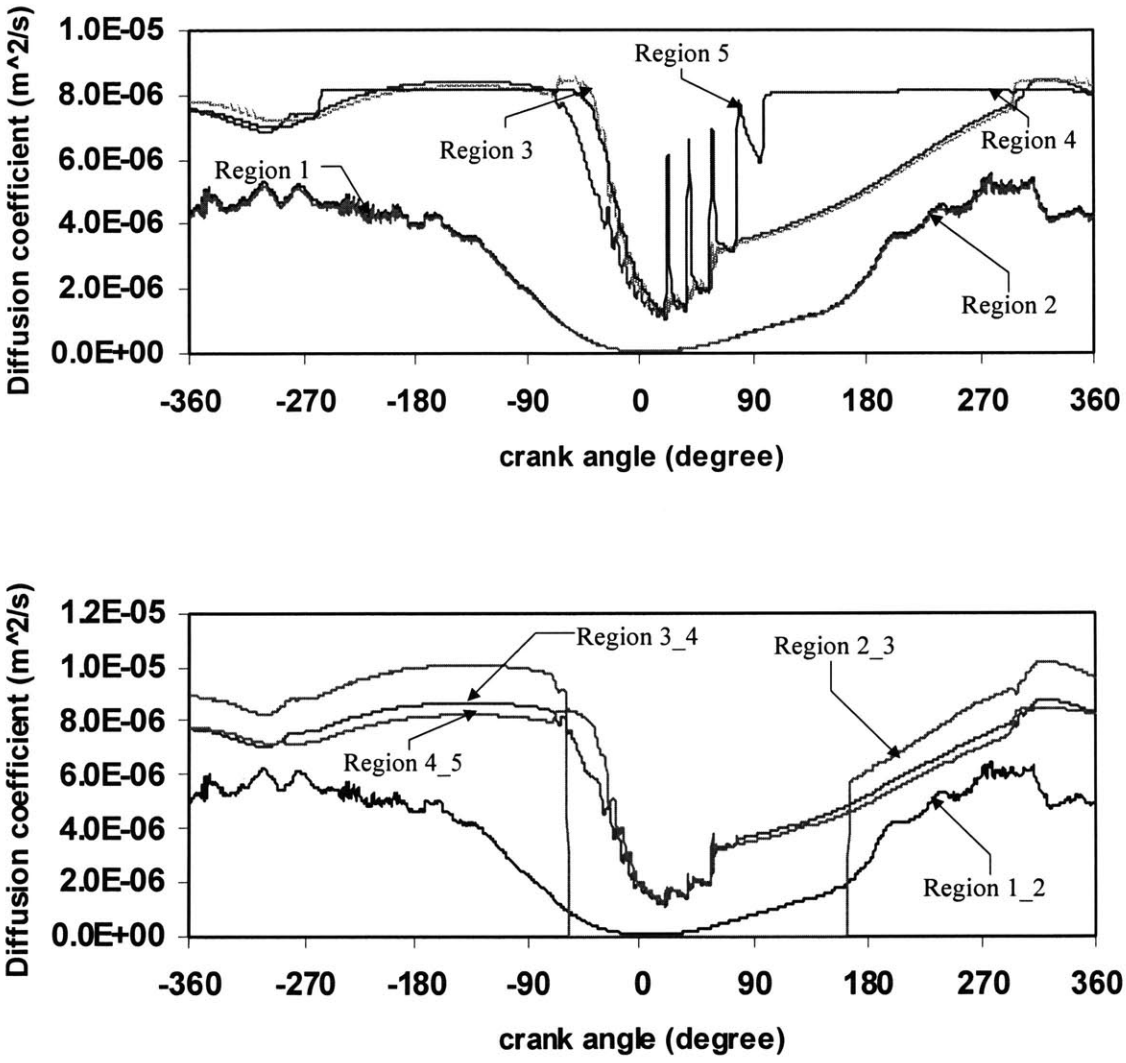

Figure I.3. Equivalent diffusion coefficient in the piston ring pack during engine operation

Mass fraction of an oil component on the oil film surface

$(mf_{oil,surface})_{1,land}$, $(mf_{oil,surface})_{1,liner}$, $(mf_{oil,surface})_{1\_2}$, $(mf_{oil,surface})_{2}$, $(mf_{oil,surface})_{2\_3}$, $(mf_{oil,surface})_{3,land}$, $(mf_{oil,surface})_{3,liner}$, $(mf_{oil,surface})_{3\_4}$, $(mf_{oil,surface})_{4}$, $(mf_{oil,surface})_{4\_5}$, $(mf_{oil,surface})_{5,land}$, $(mf_{oil,surface})_{5,liner}$

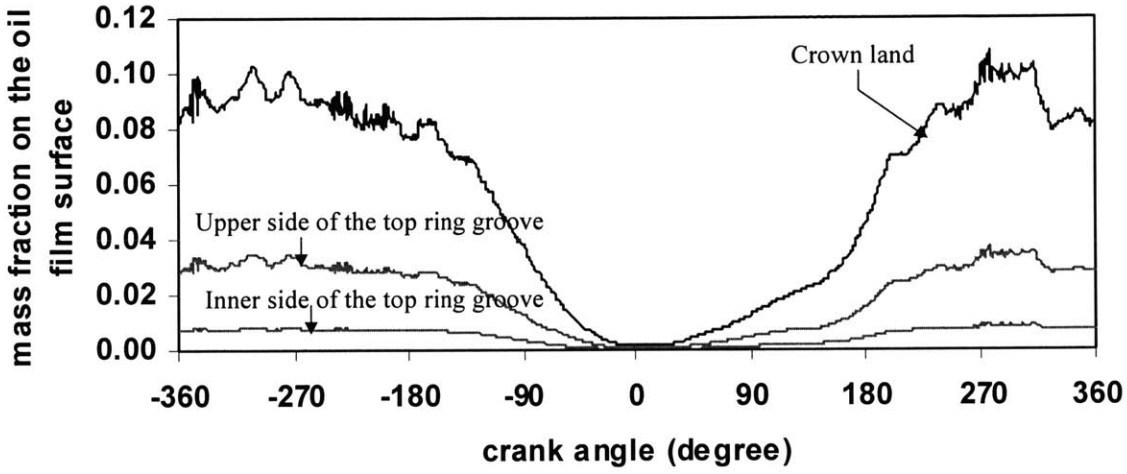

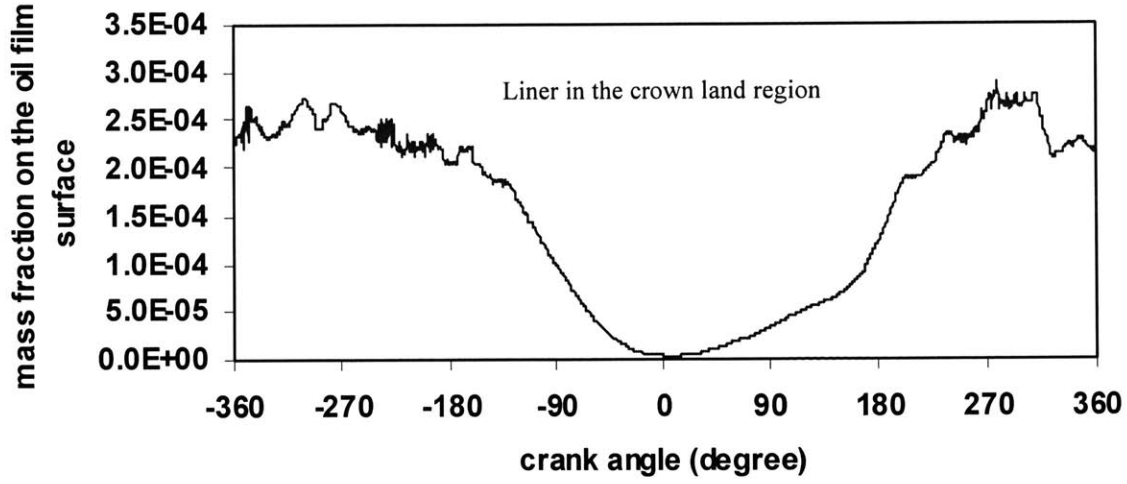

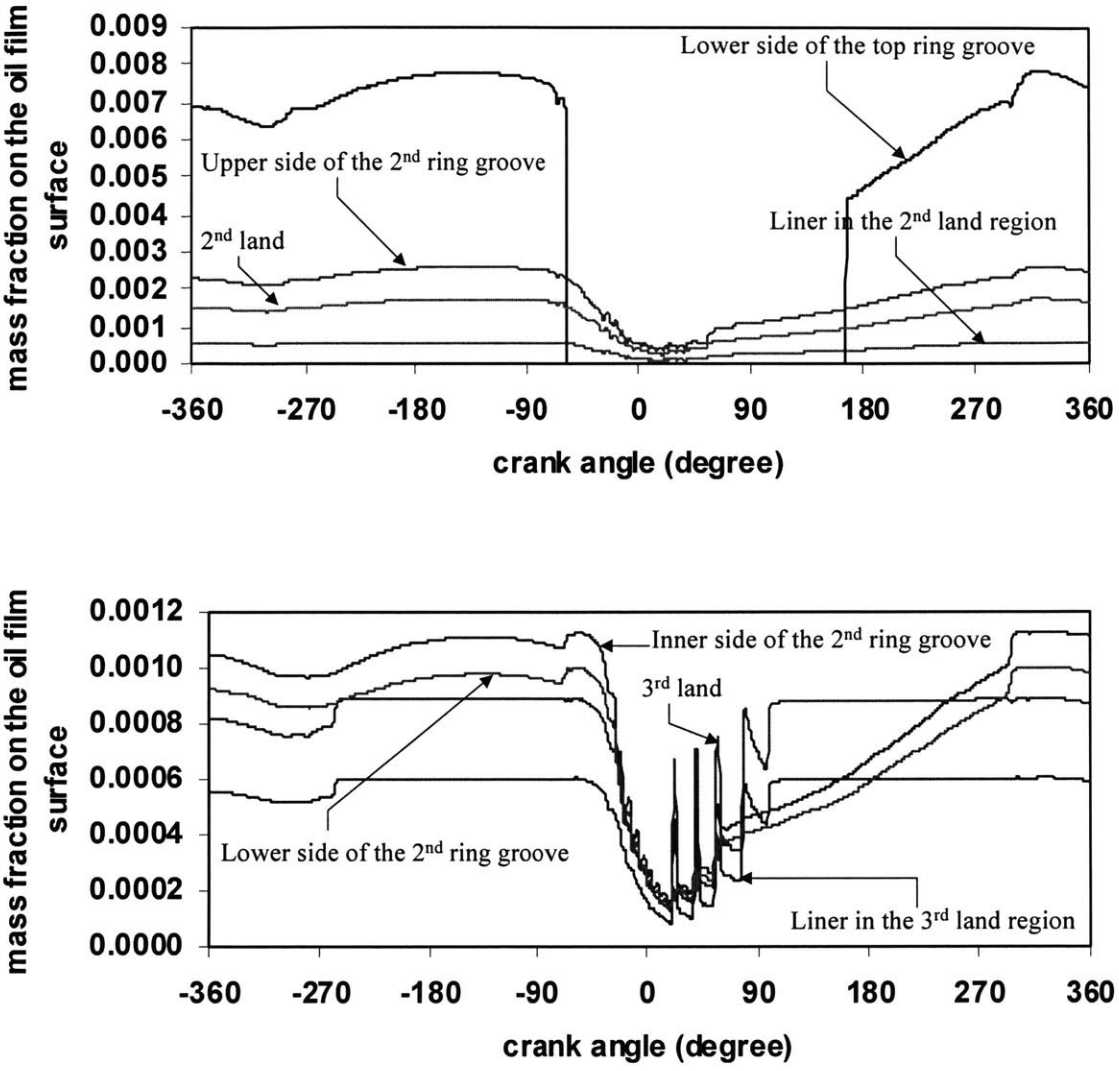

Figure I.4. Mass fraction of the lightest oil component on the oil film surface in the piston ring pack during engine operation

Air density

$\rho_{air,1}, \rho_{air,1\_2}, \rho_{air,2}, \rho_{air,2\_3}, \rho_{air,3}, \rho_{air,3\_4}, \rho_{air,4}, \rho_{air,4\_5}, \rho_{air,5}$

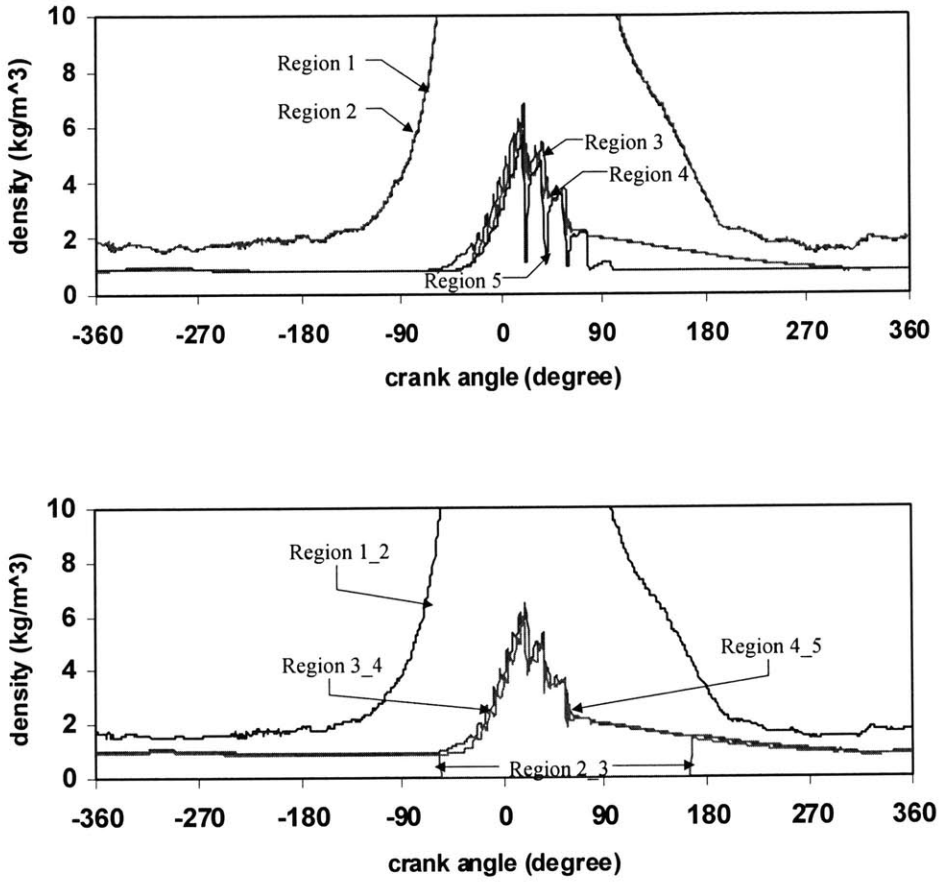

Figure I.5. Air densities in the piston ring pack during the engine operation

Appendix J. Total Oil Vapor Transport Rate and Vaporization/Condensation Rate at Fully-Wetted Lubrication Condition with Infinite Oil Supply for the Conditions (b), (c), and (d) in Figure 3-7

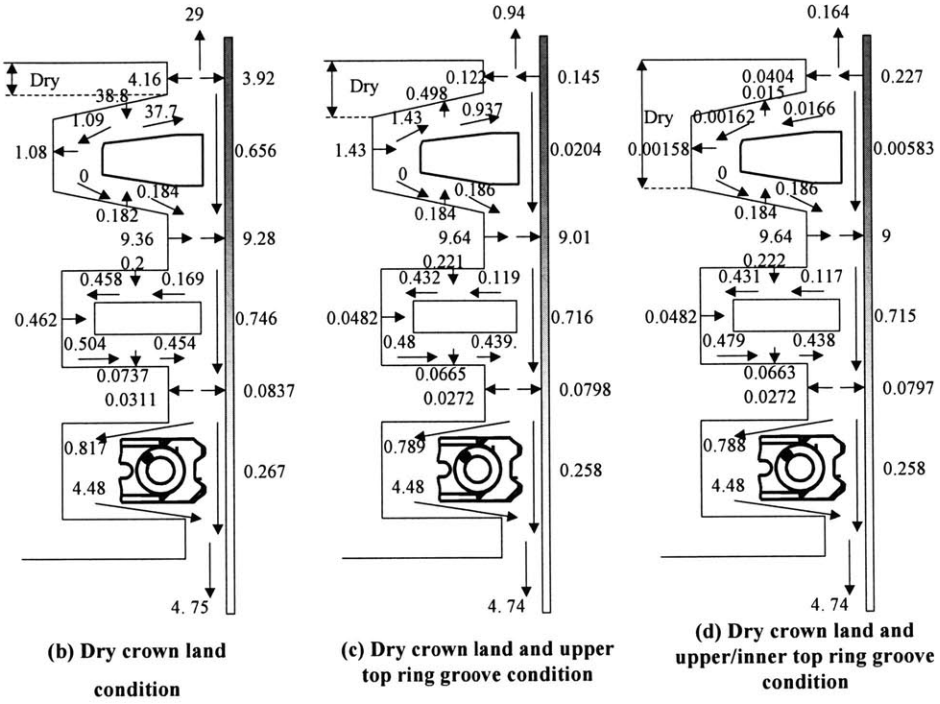

(b) Dry crown land condition

(c) Dry crown land and upper top ring groove condition

(d) Dry crown land and upper/inner top ring groove condition

Figure J.1. Total oil vapor transport rate and vaporization/condensation rate at fully-wetted lubrication condition with infinite oil supply for the conditions (b), (c), and (d) in Figure 3-7